Title
BYPASS FLOW AND TISSUE PERFUSION: A DUAL TRACER DETERMINATION

Authors
Goris, Michael L.
Dobson, Ernest L.
Schmidt, Charles T.
et al.

Publication Date
1972-09-01

LBL-1303

BYPASS FLOW AND TISSUE PERFUSION: A DUAL TRACER DETERMINATION

Michael L. Goris,* Ernest L. Dobson,
Charles T. Schmidt and Howard G. Parker

DONNER LABORATORY

September 1972

AEC Contract No. W-7405-eng-48

*Filed as a Ph. D. Thesis

LBL-1303

DISCLAIMER

Bypass Flow and Tissue Perfusion:

A dual tracer determination*

Michael L. Goris,** Ernest L. Dobson,

Charles T. Schmidt and Howard G. Parker

*Doctoral Dissertation submitted by M. L. Goris

**"Aspirant" of the Belgian National Foundation for Scientific Investigation

TABLE OF CONTENTS

To my son, Steven, for whom, if it exists, heaven was made.

Michael L. Goris

BYPASS FLOW AND TISSUE PERFUSION: A DUAL TRACER DETERMINATION

Michael L. Goris

University of California
Berkeley, California

ABSTRACT

The density function of transit times of a tracer through a vascular or perfusion system contains information about the flow of carrier and the distribution volumes of the tracer.

To derive the density function of transit times from observational data, one has to correct the latter for recirculation.

This is done by independently estimating the effect of recirculation on a known density function of transit times (in this case a delta function).

It is shown how the tissue perfusion of an organ can be estimated from the density function of transit times of a diffusable tracer injected into the organ, and how an error in this estimation results if bypass or shunting is not accounted for.

The physiological significance of this shunting is reviewed, and it is shown how the shunting fraction of the flow can be estimated from the simultaneous analysis of the density functions of transit times of a diffusable and a non-diffusable tracer.

The method is applied to the hind limb of a dog. The

tracers are colloid (^{99m}Tc labeled) and Xenon (^{133}Xe). The results are consistent with observations on the bypass flow made by other means.

INTRODUCTION

We intend to present a method allowing one to determine the bypass, or functional shunt flow, and the tissue perfusion of peripheral organs.

We will show how external detection of radioactive tracers can be used in such a manner that counting geometry does not introduce an error, and how the first passage of the tracer through the organ can be determined by correcting for recirculation.

A. The Density Function of Transit Times: The First Pass Determination

The relation between the function describing the first passage through an organ (or vascular bed) and the tissue perfusion (or blood or plasma flow), will be discussed extensively in the next chapters. At this point it is sufficient to state that we will show how the average time spent within the system (or the mean transit time $\bar{t}$) by a true flow tracer is related to the virtual distribution volume (V) of the tracer, and the flow of carrier (F), as

$$\bar{t} = V/F$$

The function describing the first passage through the system, h(t), is the density function of transit times and has dimension time^{-1}. The function h(t) is defined as follows:

The system (which is an organ, or some tissue) is assumed to be stationary as far as flow (F) and volume (V) are

concerned. For the tracer used there are no infinite pools (or metabolization), often referred to as "sinks", within the system. There is a single input artery, and a single output vein.

If a quantity Q of the tracer is injected at time = 0 in the system through the input artery, the amount of tracer leaving the system per unit of time, at time t, through the output vein is

$$Fc(t),$$

where F is the carrier flow, and c(t) the concentration of the tracer in the carrier at the output, at time t.

In the absence of recirculation h(t) is defined as

$$h(t) = \frac{Fc(t)}{Q}$$

and represents the fraction of the injected amount (Q) leaving at time t, per unit of time, or alternatively, the fraction of the tracer having a transit time t.

From the preceding (the absence of infinite pools) it follows that

$$\int_0^\infty h(t)dt = 1$$

Furthermore, by definition the mean transit time is given by

$$\bar{t} = \int_0^\infty t\, h(t)\, dt = V/F$$

In the presence of recirculation h(t) cannot be determined directly.

B. The Experimental Determination of h(t)

1. External detection

The defining equation for h(t) can be rewritten as

$$Qh(t) = Fc(t)$$

and since the flow is constant, and there are no infinite pools

$$Q = F\int_0^\infty c(t)dt$$

Therefore, h(t) can be determined from the venous concentration of the tracer (c(t)) as follows

$$h(t) = \frac{c(t)}{\int_0^\infty c(t)dt}$$

The venous concentration c(t) could be determined directly by blood sampling, but fast and accurate blood sampling presents its own difficulties, even if in the final analysis it leads to more accurate counting.

External detection is more convenient. In general external detection is used topically: the detector is so placed that the organ is in its field. The detected value is therefore not Fc(t), but q(t), which is the amount remaining in the organ.

If one defines H(t) as:

$$H(t) = \int_0^t h(\tau)d\tau$$

then, barring recirculation, q(t) is necessarily defined as

$$q(t) = (1-H(t)).Q$$

However, the detecting system yields count rates cr(t) which are only proportional to q(t)

$$cr(t) = y.q(t)$$

where y is the yield, or counting efficiency. The counter efficiency depends on the inherent characteristics of the counter, which are invariant in time, but also on the geometrical relation between the tracer and the counter, and the absorbing medium between them. Those last factors may change as the tracer flows through the organ, unless the counting efficiency is uniform for tracer elements localized at different points in the organ, or if the tracer distribution is homogeneous at all times. If not, we have the relation

$$cr(t) = y(t).q(t)$$

but since no localization information is independently given, y(t) is unknown. Topical external detection is nevertheless frequently used.

Although nobody claims a uniform efficiency of counting for tracer elements localized in different points of the system, many people assume that the claim to homogeneity can be satisfied to some extent. The basis for it is dichotomous. First, they do restrict the system to that part of organ or tissue that the detector effectively sees, normalizing the injected dose by using the zero intercept. Secondly, they assume that - in compartmental terms - the compartments are geometrically intermixed, so that globally no compartment is better seen than any other. Hence, since q(t) is a linear

combination of the amounts $q_i(t)$ in the different compartments, it is assumed that

$$cr(t) = yq(t) = \sum_{i=1}^{n} y\, q_i(t)$$

Indeed, since the counting efficiency is assumed to be the samefor all compartments, y becomes invariant in time, since the tracer can only go from one compartment to another.

The first assumption is fair only if it can be shown that a large fraction of the tracer detected is not tracer going to - and coming back from - a distal part of the organ not seen by the detector.

As for the second, sound as it may appear, it implicitly restricts all the information to the visible part of the organ, since one cannot by any stretch of the imagination accept that any other region of the same organ has exactly the same compartments in exactly the same proportion.

From C. T. Schmidt's microsphere experiments (1972) the lack of homogeneity of the hind limb of a dog is undeniable. We also believe that some of the lack of correlation between clinical status and Xenon washout after intramuscular injection derives from the lack of representability of the "visualized" region, besides the fact that the volume injected influences the washout.

In short, the homogeneity assumption is not without problems, and therefore external detection of the injected region has some objections. Immediately it should be pointed out that detecting systems with more homogeneous response

as a function of geometry can be considered, and that therefore the remarks we made may prove to be relevant only in a strict technical sense.

We will use external detection to determine the output function, by measuring the count rates over the efferent vein. The homogeneity problem is resolved in this way, but the problem of recirculation remains. Indeed, if the external detector "sees" the output vein, the count rate detected is proportional to the activity in the vein, or

$$cr(t) = y.Fc(t)$$

Since the vein has a unique location, and since within the vein the concentration can be considered homogeneous, y is time invariant. However, the relation between Fc(t) and h(t) is direct only if there is no recirculation.

2. The Recirculation

If the output function of a tracer can be used to derive some important physiological parameters (and this still remains to be proven), the determination itself depends in nearly all cases on the absence of recirculation, or some computational means to account for recirculation.

Dobson introduced the correction for recirculation from the data collected over the non-injected paired organ. This method can be used only if such an organ exists. Even for organs which obviously seem paired, like limbs, the presence of pathology is a problem since the pathology often is not symmetrical.

The alternative approach is the separate evaluation of

the recirculation. The theory will be discussed in Chapter I, Section 3, the application in Chapter III.

It is sufficient to say that if blood sampling is the method used, recirculation can be taken into account with a single injection if there is a single input artery, and a single output vein, by sampling both. As we shall show, there is a way to detect externally the activity in the vein, but the anatomical structure of blood supply does not allow separate external detection of venous and arterial blood concentration so that a double injection technique will be needed.

3. The Noise

At this point we have not yet discussed in what way the output functions (corrected for recirculation) will be analyzed, and what parameters are going to be determined. The only suggestion has been that the bypass flow and the turnover of tracer diffused into the tissue are the values of importance.

Noise is inherent in external detection, as in any experimental data. Besides the randomness of radioactive decay, one has to cope with small instrument drift, mobility of the subject, cosmic rays or background noise, all to varying degrees. The different corrections applied to the raw data (cpm) for background and recirculation all tend to enlarge the relative noise.

It is the noise, then, that will partly determine the level of sophistication that can be reached in the analysis

of the data, but not exclusively the noise. Obviously the fitting is dependent on the model. The combination of noise and model bias are the final restricting factors. It is for this reason that we will discuss different models, with varying degrees of sophistication.

C. The Distribution Volumes and h(t)

The function h(t), like $\bar{t}$, is determined by the flow of carrier and the virtual distribution volume of the tracer. Two tracers having the same distribution volume in blood and plasma, may have a different distribution volume in the extravascular space. Both Na^+ and colloidal particles are plasma tracers, but the colloidal tracer does not diffuse to the interstitial space, Na^+ does. Hence, although for both tracers F is the same, V is not, and their mean transit times, as well as their density function of transit times, will be different.

However, if there is a vascular bed where anatomical or structural factors prevent Na^+ from diffusing from the plasma to the interstitial space, the distribution volume of Na^+, within that vascular system, is per force reduced to the plasma volume, and hence, for that vascular bed, the density function of transit times of Na^+ would be identical to that of the colloid.

We will show that in this case the same applies to any tracer, even if its distribution volume is blood (instead of plasma), to the extent that there is no significant difference between blood and plasma linear velocity.

We will define $n(t)$ as the density function of transit times for a tracer without extravascular distribution volume (a non-diffusable tracer) and $d(t)$ as the density function of transit times for a tracer with an extravascular distribution volume (the diffusable tracer). Furthermore, we will consider a case where the flow of carrier F is divided along two pathways: $(1-\alpha)F$ goes through a vascular network where diffusion, even for the diffusable tracer, is impossible: $(1-\alpha)F$ is bypass flow; αF is tissue perfusion ($0 \leq \alpha \leq 1$).

In general then, since the tracer is divided as the flow, one has

$$h(t) = (1-\alpha)h_1(t) + \alpha\, h_2(t)$$

where $h_1(t)$ is the density function of transit times through the bypass pathway, $h_2(t)$ through the perfusion pathway.

In the same way for our two tracers we have

$$n(t) = (1-\alpha)n_1(t) + \alpha\, n_2(t)$$

$$d(t) = (1-\alpha)d_1(t) + \alpha\, d_2(t)$$

where $n_1(t)$ and $d_1(t)$ are analogous to $h_1(t)$, and $n_2(t)$ and $d_2(t)$ are analogous to $h_2(t)$.

However, since in the bypass pathway both tracers have the same (distribution volume/carrier flow) ratio, one can show that $n_1(t) = d_1(t)$. On the other hand, it is not at all obvious to what extent $n_2(t)$ will be reflected in $d_2(t)$. We will show that it is, but that resolution is not possible within the precision limits of our method.

At any rate, if, as we shall see, tissue perfusion is related to extravascular turnover, then $d(t)$ as a whole does

not reflect tissue turnover. Hence, one needs to use a non-diffusable tracer to determine n(t), and so eventually derive $d_2(t)$ from d(t).

D. Physiological Definition of Tissue Perfusion and Bypass Flow

Tissue perfusion, as opposed to blood flow, is defined as the flow of blood to a tissue which effectively contributes to the metabolic needs of the tissue. This definition follows from the realization that a fraction of the blood flow does not contribute to the metabolic needs of the tissue. This fraction is the bypass flow.

The distinction however is not absolute. To be precise the definition needs to be given for each metabolic substance specifically: the flow is bypass flow for a given substance, if at no place between arteriole and venule the substance can diffuse from blood to tissue, or vice versa.

In an attempt to generalize, the concepts of the freely diffusable tracer and the non-permeable membrane are introduced. The membrane is localized between blood and tissue. It is not necessary at this point to assume anything but the following: the vascular wall of the big vessels (arteries and veins) are non-permeable membranes. The capillary walls are permeable. It is possible, but not necessary for our purpose, to allow for the possibility that some specialized vessels responsible for the bypass flow, have non-permeable walls, in the same sense as the big vessel walls are non-permeable. A freely diffusable tracer or substance is a tracer

(or substance) that is not prevented by its nature from diffusing through the so-defined permeable vascular membranes.

In the extravascular space the cell membranes represent the next obstacle. From the preceding it does not follow that a freely diffusable tracer will pass the cell membrane. Depending on whether it does it or not, its extravascular distribution volume is the interstitial space and the intracellular space or the interstitial space alone.

It follows then that in the evaluation of tissue perfusion the value to determine is the extravascular turnover (or washout) of a freely diffusable tracer or substance. Since diffusion and equilibrium concentration are not the same for all substances, a unique tracer would not be sufficient to evaluate to what extent the transport of any diffusable substance is adequate. On the other hand, since from one physiological state to another it is unrealistic to expect changes in diffusion rate or equilibrium concentration rather than flow changes, unless enough time elapsed for gross structural changes, it can generally be stated that short term changes in the turnover of any diffusable tracer reflect changes in the turnover of any diffusable substance, irrespective of all other assumptions, except for tracer specific changes in cell membrane permeability.

The statement becomes even more general if one can assume the behavior of the tracer to be flow-limited and not diffusion limited. The modalities by which a substance is flow limited may differ, but empirically the definition is

unambiguous. When bypass flow is accounted for, if the washout of a tracer or substance is linearly related to the flow, one has a "flow limitation" situation.

In that case, the behavior of a diffusable tracer is indicative of the flow and the volumes perfused, with the understanding that the flow is not separated from the volumes by a barrier which restricts the tracer's diffusion (bypass flow).

This last point must be carefully examined. Indeed, if a large fraction of the flow is separated from the tissues, in the sense that no diffusion is possible, for all practical purposes, a large fraction of a tracer originally in the plasma or blood does not act as a diffusable substance, and therefore the first statement - that the tissue perfusion can be evaluated by determining the turnover rate of the tracer - fails to be true. Since a fraction of the tracer never left the plasma (or blood) its turnover is dependent only on plasma or blood turnover. If the tracer was originally in the tissues, the tracer turnover is independent of the bypass flow.

The possible importance of the bypass fraction of the flow should not be underestimated. Manifestly it contributes to the heart's work, without direct benefit to the extravascular turnover of metabolic substances. This contribution is even more important if the regulation of the bypass flow reflects itself in the peripheral resistance, and hence the pressure the heart has to overcome to open the aortic valves.

Furthermore, we feel that if bypass flow is a process happening in a parallel circuit, it may provide the central circulation with a regulating mechanism dissociated from the autoregulation based on tissue needs, so that the central circulation can be maintained independently of the tissue needs in extreme cases.

It seems, therefore, that the bypass flow may not only be a factor complicating the evaluation of tissue perfusion, but may also be an important parameter of the circulatory status.

It is clear why we do not consider intravascular turnover, as such, of primary importance in the local circulation, since because of the bypass factor, tissue perfusion is to some extent independent of the global intravascular turnover.

There may be some objections to the assumption that the turnover of diffusable tracers like Na and inert gases is flow limited. If the density of the capillaries in any tissue is low, instant equilibration becomes unlikely, and diffusion more important. In that case, if an increase in flow is associated with the opening of more capillaries, one has seemingly a situation of flow limitation (as empirically defined) when in fact the changes are due to a shift from more to less diffusion limitation. It is for this reason that we choose Xenon as the diffusable tracer, since Jones (1950) was able to demonstrate that the turnover of inert gases is not diffusion limited.

CHAPTER I: TISSUE PERFUSION

Section 1. The local blood flow regulation

Since the aim of this study is to develop a method to quantitate local blood flow and tissue perfusion - the latter one being the function limiting exchange of metabolites at the tissular level - a brief discussion of the relationship of local flow and tissue needs is in order. But the local circulation, although it has been studied extensively as such, is not necessarily independent of the global circulation, or central circulation. On the other hand, it seems that for the largest part the central circulation has its proper regulation mechanism: endocrinological, neurogenic and the intrinsic regulation mechanism of the heart (Starling's law). Volume, osmolarity and flow are well controlled through the combined action of baroreceptors, osmoreceptors, the angiotensine-renin system, the central venous filling, the hypophysial and adrenal hormones. To that extent, the central circulation is not exclusively dependent on the combined effect of all the local circulation systems.

As we shall see, local circulation systems have a pronounced autoregulation mechanism. In intact animals it is not possible to demonstrate that the general autoregulation of the central circulation is secondary to the local ones. Teleologically speaking, this is to be expected, since even at a moment where all the metabolic needs of the tissues are satisfied, blood has to flow, and the central vascular system has to remain well filled.

This is not to say that the central circulation is separate from the local ones as far as regulation goes. The arterial pressure is maintained against a peripheral resistance primarily located at the arteriolar and capillary level (Rodbar 1971). In decerebrated, and despinalized dogs, Coleman (1969) and Guyton (1971) have shown that an initial increase in cardiac output leads to autoregulation of flow by an increase of peripheral resistance, leading to a residual hypertension, while subsequently the cardiac output is decreased to near normal levels, due to a decreased venous return. They postulate this to be the mechanism of some types of hypertension. Julius (1971) finds indeed, that if patients with borderline hypertension tend to have an increased cardiac output, the hypertension remains, even when the cardiac output is brought below normal with a combination of atropine and propanolol. That the primary event is an increase in cardiac output, followed by a peripheral autoregulative increase in resistance is not generally accepted. Byrom (1954) found that in hypertensive rats the arterial pattern consists of segments of arteries showing intense vasoconstriction, alternating with overdistended dilated segments, resembling a string of sausages. Hill (1970, 1968) believes that in steroid hypertension the primary lesion, prior to hypertension is a muscular lesion, provoking overextension in passive dilations of the vascular wall. Sodium intoxication of the smooth muscle would be the cause. Hence, there is no direct, unequivocal evidence, that the

local autoregulation mechanisms reflect themselves profoundly in the general circulation.

However, the local circulation seems to be maintained to a very large extent independently of the general circulation. On the local level autoregulation, and adaptation to local metabolic needs, are very well documented.

There are two main schools of thought, but they do not exclude each other. The main difference, on a functional level, lies in the fact that in one case the regulation of the flow is essentially capillar, and depends on tissue pressure vs. intravascular pressure, while in the other case the mechanism is localized at the arteriolar, and to some extent venular level, and the mediator is metabolic. Scott (1968) and Haddy (1968) have extensively reviewed the chemical mediators responsible for reactive (post-occlusion) and active (during contraction) muscle hyperaemia. Oxygen tension, H^+, pCO_2, potassium, adenosine and adenosine nucleotides, have all been mentioned.

pH increase provokes arteriolar constrictions; a decrease causes arteriolar dilation. But the direct effect of the blood pH can be doubted. Indeed, in the muscle of the human forearm, Kontos (1971) finds pCO_2 to be more important than pH, suggesting that an intracellular pH decrease in the smooth muscle of the arteriole is the main factor. However, an Alkaline Amine buffer (tromethamine) inhibits the effect of hypercapnia more in reactive than in active hyperaemia. Thureau (1971) found that in the brain a decrease of blood

pH with ammonium chloride, with a constant pCO_2 does not dilate the arterioles, however direct application of an acid solution to the tissues surrounding the arteriolar walls provokes dilation. He speculates that the mechanism is triggered by intracellular pH decrease, and that the extracellular fluid pH follows the metabolic state of the nerve cells. A definite exception seems to be the kidney, where the basal state seems to be maximal dilation, and pCO_2 increase has no effect. In this organ the regulation of flow is governed by the juxtaglomerular apparatus with the renin-angiotensin system. Furthermore, the changes in arteriolar resistance seem dependent on the glomerular filtrates. He suggests that the macula densa cells transmit information about the composition of the tubular fluid to the juxtaglomerular cells in the walls of the glomerular arterioles. That the kidney appears to be exceptional regarding local regulation, is consistent with the fact that it is part of the primary regulation system of the central circulation. It is interesting to note that in coronary vessels and muscle arterioles, while pCO_2 has a marked effect on the vascular tone, pO_2 decrease has an effect only below 40 mm Hg. Dougherty (1967) considers this as evidence that those substances act on a different system of autoregulation.

Rodbar, in a general discussion of the resistance vessels (1971) pointed out that if the agents of autoregulation are metabolic substances, theoretically one would expect their effect on the distal end of the local vessels. Of

course, this is, to some extent, a semantic misconception, since all microvessels do not run parallel. Interestingly enough however, Duhling (1970, 1971) demonstrated a longitudinal pO_2 gradient in the wall of the arterioles, depending on the tissue consumption of oxygen. He also found the oxygen saturation of hemoglobin to be about 65% at the entry of capillaries, even when the central arterial saturation level was higher than 95%. If necessary, this would, at least for the oxygen, answer Rodbar's objection.

The role of adenosine, and the adenosine nucleotides have been extensively studied. Bern (1971) finds adenosine to be a potent dilator of the coronary resistance vessels, and during cardiac hypoxia, the interstitial adenosine levels are high enough to account for the decrease in resistance. In skeletal muscle during exercise or hypoxia the tissue levels of adenosine increase slightly, but the venous increase is marked. In neither case did he find an increase in ATP, ADP or AMP.

Hilton (1971) could pinpoint the specificity of the action of phosphates even more: The soleus muscle of the cat shows no active hyperaemia, even at very high frequency contraction rates, although its resistance vessels have a good tone and can be dilated. Furthermore, no increase of plasma phosphates can be demonstrated. In fast muscles however, there is active hyperaemia, and an increase in phosphates; finally, if phosphates are perfused through the soleus muscle, there is hyperaemia.

Potassium and magnesium ions have also been associated with the local regulation of blood flow. Kelburn (1966) demonstrated the muscular origin of the elevated potassium levels found in the effluent plasma after exercise. Reduction in extracellular potassium provokes arteriolar constriction, a slight increase provokes dilation, and is antagonistic to the constrictive effect of levarterenol, while a large increase produces contraction of the large arteries (Scott 1968).

Osmolarity in the effluent blood has been found to increase in active but not in reactive hyperaemia (Scott 1970, 1971) but when infused, hyperosmolar solutions have only transient effects on the peripheral resistance (Stainsby 1971). Furthermore, it does not seem that only one agent can possibly be "the" agent. Mellander (1971) proposes that changes in osmolarity have an effect on the pacemaker activity of the smooth muscle cells by changing the membrane ionic concentration gradients. Skinner (1967a-b, 1971) found, with infusion experiments, maximal effect with a combination of hypoxia, osmolarity increase, and hyperkaliaemia, while any of those agents alone has minimal effect.

Obviously no single agent can be considered as principal in the autoregulation. The main point, however, is that there is a chemical mediator, or a combination of chemical mediators, which are found to appear during occlusion hyperaemia, or active hyperaemia. Haddy (1971) and Scott (1965) demonstrated this with a bioassay, where an organ was per-

fused with the effluent from the treated organ. They found that oxygen (within the range they tested), histamine and acetylcholine were not the factors.

But the regulatory mechanism need not be exclusively localized at the arteriolar (or venular) level. The capillary unit itself presents some autoregulatory features. The main feature here is the movement of fluid through the capillary membrane. Guyton (1966) confirmed with direct microscopic measurements that the interstitial fluid pressure affects this movement to a great extent, as predicted by Starling. There are, besides the capillary permeability, four important values: the interstitial pressure, the capillary pressure, the plasma and interstitial colloid pressure. He finds that transcapillary transduction is more influenced by interstitial fluid pressure increase than by an identical venular pressure increase. A very important aspect of Guyton's work (1963) is that he finds the mean interstitial pressure to be negative. To explain this one has to assume that the precapillary arterioles or precapillary sphincters are closed most of the time. Not all authors accept this negative tissue pressure however, and in general, it is found that the autoregulation at the capillary level is due to positive tissue pressure.

Beer (1971) and Rodbar (1971b) propose essentially the same mechanism. The first observation is that most tissues are capsular at the microscopic level and the macroscopic level. They define a capillary unit, the capillaron, as a

capillary (or a few capillaries) connected to an arteriole and a venule, and surrounded by its own tissue, which is contained into a capsule. The capsule has some limited compliance. As the pressure on the arteriolar side is high, fluid passes through the capillary wall into the extravascular space. As the interstitial volume increases, the extravascular pressure becomes larger than the intravascular pressure and the capillary collapses. Distal to the collapse, on the venular end, the pressure is now equal to the venous pressure, and fluid goes from the interstitial space to the venule.

The merit of this model would lie in the fact that it explains post-occlusion hyperaemia (where at the end of the occlusion the interstitial pressure is very low), the lack of reactive hyperaemia after venous occlusion (high interstitial pressure), and the inhibition of postarterial-occlusion hyperaemia when the artery is slowly opened (since there the rise in intravascular pressure is closely followed by a rise in interstitial pressure).

Active hyperaemia is then partially explained by assuming, at least for muscles, that exercise enhances lymph flow and tends to decrease the interstitial mean pressure. It is interesting to note that Hinshaw's (1971) measures of tissue pressure in the kidney during post-occlusion hyperaemia, or autoregulation, are consistent with this hypothesis.

On the other hand, although this model has been vindicated by observation and simulation (Beer 1971), no one

claims that it is the only mechanism, or that it explains everything.

If one considers the fact that by Poiseuille's law that the flow F is proportional to the pressure gradient ΔP and the fourth power of the radius r, while inversely proportional to the length over which the pressure gradient exists, ($F \propto \Delta P r^4/l$) it is apparent that to monitor a constant flow against changes of pressure, a very fine regulation of the vessel's diameter is needed. Furthermore, if the vessel has some compliance, as does the capillary, an increase in pressure would actually increase the radius (until extravascular pressure has equilibrated), while if there is a contractile mechanism in the vessel wall, the changes in lumen diameter will be different from the changes in outside diameter, due to the folding of the endothelial layer. Furthermore, contractile vessels are essentially unstable, and tend to be open or closed. Thus, even if the term "critical" pressure is ill-chosen, since the closing pressure depends on the interstitial pressure also, Olson's (1969) thesis that capillaries are alternately opened and closed, and that thus the autoregulation, the pressure and flow are in fact determined more by the number of open elements, than by their radius, is indeed reasonable.

In this brief discussion of the local regulation of blood flow we did not yet discuss the presence of arteriolar-venous shunts, or bypass vessels. The reason is that bypass is a functional concept, having to do with exchange, and that

the problem can better be evaluated after the introduction of the tracer kinetics methods (next sections). However, assuming that bypass vessels do exist, one expects them to be controlled by general mechanisms. This is indeed what has been observed in muscle, where blood flow, not tissue perfusion, increases in athletes before the exercise (Freedman 1966). It has been shown that during exercise the oxygen need is satisfied by increased blood flow rather than by increased desaturation in venous blood (Kontos 1966).

The whole body of evidence related here indicates that local blood flow is regulated by the status of the perfused tissues. This regulation is very much independent of the general circulatory status. One cannot therefore predict from changes in cardiac output and arterial pressure what the tissue perfusion changes will be. Treatments which are known to influence the central circulatory status may do so with minimal tissue perfusion changes in any organ. Indeed, the global effect detected is the sum total of the peripheral flows and resistances. Part of this may be at the bypass circuit level. Therefore evaluation of a treatment should be done at the local-tissue perfusion level, and should include more than simple flow and pressure evaluation in the big vessels. Furthermore, if one assumes indeed that local flow is autoregulated locally, as a function of tissue metabolism, then subliminar pathology might be reflected in a decrease in local reactivity, long before actual "decompensation" occurs.

This has one very important practical implication, since a first determination of bypass flow and the mean transit times show a large variation between individual animals, but the changes under "treatment" within any single "normal" animal are distinctive and consistent in their general trend.

If specialized shunts do exist, one expects them to be one of the first mechanisms called upon when increased tissue perfusion is needed. There lies the importance of bypass determination. On top of that, to the extent that microscopic flow redistribution is important in autoregulation, exclusive local monitoring may be unrepresentative. This will be discussed in Chapter V, when the results of some experiments are presented.

Section 2. Tracer theory for flow and volume determinations

To evaluate the circulation or the tissue perfusion status of an organ one obviously needs a non-destructive method, at least if subsequent measures after "treatment" are needed, and in any case if the method is to be applied to patient evaluation. It is also obvious that the measure itself should not disturb the system. This may well be the main advantage of tracer kinetics studies. A true tracer, besides the fact that its behavior is in all measured ways identical to that of the traced substance, is also, by definition, introduced into the system in such small amounts, that the mass of the system does not change.

The main problem of tracer kinetics however resides in

the "globality" of the information. It may well be that the measured value is so global that all information about the mechanism leading to the result is lost. However, if a model is postulated, the potential information becomes larger as the complexity of the model increases, while on the other hand model bias becomes eventually harder to detect, the solutions become less unique, and the derived values may be entirely irrelevant to the biological system.

In what follows we will briefly review the different methods of analysis used in the estimation of blood flow and/or tissue perfusion.

Meier and Zierler (1954) defined the general form of Hamilton's (1932) dye dilution theory. Their derivation is certainly the most general, and yields the most global results. The basic assumptions are as follows:

1. Stationarity of flow and volume during the time of the experiment.

2. The flow of particles is representative of the flow of fluid.

3. The system has no stagnant pool.

4. There is no recirculation.

Condition 1 however is not restrictive enough. Later (1961) Zierler points out that the whole system must be stationary. In other words, the behavior of a particle must be entirely independent of its introduction time. This however is not strictly true in general. A periodical opening and closing of precapillary sphincters has been postulated or

described (Guyton 1963; Zweifach, B.W. 1954; Nicoll, P.A. and Webb, R.L. 1955). That this phenomenon excludes the use of Zierler's model is unlikely, and has not been noted. It may however be an argument in favor of continuous infusion techniques (see later).

Condition 2 may be too restrictive. The tracer is always representative of the volume it occupies. Generalization is obtained by introducing the concept of virtual volumes. If at equilibrium the concentration of a tracer in a volume V_1 is found to be c_1, then any unsampled compartment i is defined as having a volume $Vi = Qi/c_1$, where Qi is the amount of tracer in compartment i. This is no more than Kety's (1949) relation between tissue volume and tracer volume, with the difference that Kety considers a single compartment, combining plasma and tissue. Of course, in any biological system condition 4 is essentially never satisfied, and recirculation will probably have to be accounted for (see later).

The main point of the derivation is that if an amount Q of tracer is injected, it has to come out between $t = 0$ (injection time) and $t = \infty$, since there are no stagnant pools. If one groups the tracer elements by their appearance time during each interval $t + dt$, the amount of tracer leaving the system is $Qh(t)dt$. Since flow and volume are stationary, if there is a single output vessel, the concentration, $c(t)$, in that vessel at the output, as a function of time is

$$c(t) = \frac{Qh(t)}{F} \qquad (1.1)$$

Obviously then the following relations hold

$$\int_0^\infty h(t)dt = 1 \tag{1.2}$$

$$F\int_0^\infty c(t)dt = Q \tag{1.3}$$

$$h(t) = \frac{c(t)}{\int_0^\infty c(t)dt} \tag{1.4}$$

The observed value is, if one samples at the single output vein, $yc(t)$, where y is a fraction due to counter efficiency and, eventually, the fact that samples are taken from the output vein. Since in Eq.(1.4) y would appear in both numerator and denominator, it is easy to define h(t).

The next argument is that if one groups the tracer elements leaving at time t + dt, they do represent a volume element given by

$$dV = tFh(t)dt \tag{1.5}$$

Therefore

$$V = \bar{t}F \tag{1.6}$$

Once again we have to emphasize that the volume is virtual, and that up to here the derivation applies regardless of the distribution volume of the tracer. Nothing was said about the shape of h(t), which has been defined by different authors on different grounds (Dobson, 1957; Ingvar, 1962; Bassinghwaight, 1966a-b; Goresky, 1970; Perl 1968).

If the input function is not a delta function (spike injection), but is i(t), then the resulting output function g(t) is defined as

$$g(t) = \int_o^t i(t-\tau)h(\tau)d\tau \tag{1.7}$$

If the infusion is constant I, then

$$Ig(t) = I\int_o^t h(\tau)d\tau \tag{1.8}$$

and the concentration at the output point

$$c(t) = \frac{I}{F}\int_o^t h(\tau)d\tau \tag{1.9}$$

or

$$c(\infty) = I/F$$

The relation between the output function (Meyer 1959; Zierler 1965) in cases of delta function injections, and the amount of tracer remaining in the systems q(t) follows easily

$$q(t) = \left[1 - \int_o^t h(\tau)d\tau\right]Q \tag{1.10}$$

therefore

$$\int_o^\infty q(t)dt = \int_o^\infty \left[1 - \int_o^t h(\tau)d\tau\right]Q \cdot dt$$

$$= \int_o^\infty [1 - H(t)]Q dt$$

$$= \left[t[1 - H(t)]\Big|_o^\infty + \int_o^\infty th(t)dt\right]Q$$

$$= [o + \bar{t}]Q$$

and therefore

$$\frac{\int_o^\infty q(t)dt}{Q} = \bar{t} \tag{1.11}$$

However, and this is a point that the author fails to make,

it is indeed very difficult to count q(t) with a proportionality constant k invariant in time.

This model has been applied with different variations. Zierler (1965) discusses the method where one combines external monitoring to determine q(t) and blood sampling to define c(t). It is obvious that

$$\dot{q}(t) = -Fc(t) \tag{1.12}$$

However, $\dot{q}(t)$ and c(t) are not measured experimentally in the differential sense as implied above. The measured values, since counting takes a finite time, are

$$\Delta q(t) = \int_t^{t+dt} \dot{q}(\tau)d\tau = -F\int_t^{t+dt} c(\tau)d\tau \tag{1.13}$$

If both the arterial $c_A(t)$ and venous $c_v(t)$ concentrations are followed, when the injection is not a delta function injection:

$$\Delta q(t) = F\int_t^{t+dt} (c_A(\tau) - c_v(\tau))d\tau \tag{1.14}$$

which is the equation used by Lewis (1960) to determine blood flow to the brain. The condition of course is that during the time of integration t to t+dt, F be constant.

Whether one uses Eq. (1.13) or (1.14) the problem of counting efficiency is the most difficult. Furthermore, if the integration time is short the error due to the time spent by the tracer between the system and the sampling site becomes important.

For compartmental analysis one supplementary assumption

is made: distribution volumes of the tracer can be distinguished in which the probability for any tracer element to leave the volume is time invariant.

This first order process mode of analysis was first introduced by Kety (1949), and led quite naturally to the expression of flow as ml/100 gm/min. Kety, unlike many people who used his analysis method, did not in fact claim that equilibrium is necessarily reached from time t = 0 on. But if it is reached, then

$$\dot{q}(t) = F(c_A - c_v)$$

assuming that at equilibrium the tissue + plasma mean concentration $c = \lambda c_v$, where λ is the distribution coefficient between blood (or plasma) and tissue. If c_A is zero then

$$\dot{q}(t) = -\frac{F}{\lambda W} q(t) \qquad (1.16)$$

where W is the tissue weight. Since Eq.(1.16) is a first order linear differential equation, q(t) is an exponential function, the slope of which is $F/\lambda W$, a flow per weight if λ is 1. Eq.(1.16) is linear only if λ, F and W are constant. If equilibration is not immediately reached, then

$$\dot{q}(t) = -\frac{F}{W}\frac{1}{\lambda(t)} \cdot q(t) \quad .$$

But equilibration does not have to be reached to express $\bar{t}$ as volume of tissue/flow (Zierler 1965), and therefore although the function $\dot{q}(t)$ cannot easily be defined as an exponential unless equilibration is complete, $\bar{t}$ is always

dependent on the distribution volume.

The so-called mean transit time or integral method is therefore based on a minimum of assumptions, and can be used to determine $\bar{t}$, V/F, or by combination of external monitoring and blood sampling both F and V.

Since from those assumptions one cannot predict the shape of h(t), recirculation if it appears much before h(t) has reached zero is difficult to account for, although (see next section) it can be done to some extent. Furthermore, V as defined is somewhat obscure, V/F is an average value, and not many circulatory systems are well-defined by this restricted number of parameters only.

However the idea that one can distinguish different volumes with different flow rates follows logically from the observation that h(t) can be well-fitted by a sum of exponentials. Using external monitoring, and intraarterial injection of ^{24}Na, Dobson (1957) presented a paper in which h(t) is fitted by a sum of 3 exponentials. The basic assumption here is that although there are three distinct perfused volumes in parallel, anatomically they are so well intermixed that the external detector counts the activity in each of them with the same efficiency. The fitting function he found was

$$q(t) = Q \sum_{i=1}^{3} A_i \, e^{-a_i t} \qquad (1.17)$$

The analysis is based on the following derivation:

Kety's principle applies to each of the compartments in

which we define

$q_i(t)$ = tracer amount in compartment i

F_i = flow through compartment i

V_i' = volume of compartment i

λ_i = equilibration coefficient in compartment i

$C_i(t)$ = venous concentration in compartment i

$Cv_i(t)$ = venous concentration at exit of compartment i

V_i = virtual volume of the tracer in compartment i

We have then

$$\dot{q}_i(t) = -F_i Cv_i \tag{1.18}$$

$$\dot{q}_i(t) = \frac{-F_i}{\lambda} C_i$$

$$\dot{q}_i(t) = \frac{-F_i}{\lambda V_i'} q_i(t)$$

$$\dot{q}_i(t) = \frac{-F_i}{V_i} q_i(t) \tag{1.19}$$

And so if there are 3 compartments in parallel, the fitting function is Eq. (1.17)

$$q(t) = Q \sum_{i=1}^{3} A_i \, e^{-a_i t}$$

where

$$QA_i = q_i(0)$$

$$a_i = F_i/V_i$$

However, the amount in each of the compartments is proportional to the relative flow to that compartment and the injected amount Q, and hence

$$QA_i = \frac{F_i}{\Sigma F_i} \; Q \tag{1.20}$$

To illustrate the fact that this is indeed a more specific case of Zierler's model we derive, using Eq. (1.11)

$$\int_o^\infty q(t)\, dt = Q \int_o^\infty \Sigma A_i e^{-a_i t} \tag{1.21}$$

$$Q\bar{t} = Q\, \Sigma A_i/a_i$$

$$\bar{t} = \sum \frac{F_i}{\Sigma F_i} \cdot \frac{V_i}{F_i}$$

$$\bar{t} = \sum \frac{V_i}{\Sigma F_i} = \frac{\Sigma V_i}{F} = \frac{V}{F} \tag{1.22}$$

If in Zierler's model changes in $\bar{t}$ can be caused by changes either in F or V or both, Dobson's analysis - based on more assumptions than Zierler's - also permits more detailed analysis.

From the preceding we have

$$A_i = F_i/\Sigma F_i \tag{1.20}$$

$$a_i = F_i/V_i \tag{1.19}$$

Therefore

$$\frac{QA_i/a_i}{\sum_j QA_j/a_j} = \frac{F_i}{\Sigma F_j} \cdot \frac{V_i}{F_i} \cdot \frac{\Sigma F_j}{\sum_j V_j}$$

or

$$\frac{QA_i/a_i}{\Sigma QA_j/a_j} = \frac{V_i}{\Sigma V_j} \tag{1.23}$$

This allowed the author to demonstrate that adrenalin not

only increases the flow to some of the compartments, but increased also the relative volume of those compartments. The effect of adrenalin is redistribution of flow, not only increase. This piece of information is not only interesting from a physiological viewpoint, but vindicates in our mind the use of tracers.

On other grounds the model may be hard to defend. Zierler, as we noted (1963), objects to the automatic use of exponentials as fitting functions, and deriving the model on this ground. Dobson points out himself that the number of exponentials used is somewhat arbitrary.

The fact that $QA_i = QF_i/\Sigma F_i$ presents a technical problem. Poorly perfused compartments are hard to detect, since they contain very little tracer. To circumvent this, all compartments can be prefilled to the same concentration with a continuous infusion up to t = 0 (Ingvar 1962). If λ (the equilibration coefficient between blood and tissue) is the same in all compartments we have when the infusion stops, and barring recirculation,

$$\dot{q}_i(t) = -F_i Cv_i$$

and the solution is also

$$Q\Sigma A_i \, e^{-a_i t} \qquad (1.24)$$

However

$$QA_i = CV_i \qquad (1.25)$$

where C is the uniform concentration reached at the end of the infusion

$$a_i = F_i/V_i \qquad (1.26)$$

In this case the information about volumes used by Dobson is obviously lost, but poorly perfused compartments may be better detected. This loading technique was used by Jones (1950) and allowed him to detect the poorly perfused body fat.

Different ways of measuring can be used, and the described derivation can also be applied with blood sampling. Shinohara (1969) uses the same model for the brain, using H_2 as tracer and venous hydrogen detectors. Maseri described in 1966 a technique for continuous monitoring of a dye dilution curve. Bing (1964) also uses external detection, but with a positron annihilation coincidence technique, in a study of cardiac blood flow. In this way some of the problems, such as scatter and collimation, are resolved, but the basic objections against local monitoring remain.

The first order process analysis led in time to a method where the tracer is directly injected in the tissue (Lassen 1964). In this case Eq. (1.19) applies, but one can also use the more general approach and simply compute $\bar{t}$ as in Eq. (1.11) (Holzman 1964). Lassen (1964a-b) assumes good equilibration of the tracer around the injection site, hoping that the dilution volume is indeed the muscle. Warner et al (1953) found however that the washout rate is a function of the injected volume. They found that the time needed for the activity to reach 50% of the initial value can vary from 5 min for 0.01 ml to 25 min for 1.0 ml. This may be explained by diffusion limitation within the injection

bubble, and/or the ratio of volume/area of the bubble. Reproducibility in general is complicated by the fact that the trauma may vary, as will the location of the injection relative to fascia and muscle.

To eliminate trauma, Sejrsen (1969), in cutaneous perfusion studies, preloads the skin by diffusion, but this method has no application beyond superficial tissues. It is interesting that Lassen in general uses values after reactive hyperaemia, when flow is not stationary, in that case

$$\dot{Q}(t) = F(t)\ Cv(t) \qquad (1.27)$$

$$\dot{Q}(t) = F(t)\ \frac{C(t)}{\lambda V}\ V \qquad (1.27)'$$

$$\dot{Q}(t) = \frac{F(t)}{\lambda V}\ Q(t)$$

$$\frac{F(t)}{\lambda V} = (Q'/Q)t \qquad (1.28)$$

and is followed as a function of time. In this manner he compared $(F\lambda_{Na}V_{Na})t$ and $(F/\lambda_{Xe}V_{Xe})t$ where $\lambda_{Na}V_{Na}$ are the distribution coefficient and distribution volume for sodium, while $\lambda_{Xe}V_{Xe}$ are the same values, for Xenon. He found (1964a) that at higher flow rates sodium clearance is relatively smaller than Xenon clearance, indicating a more pronounced diffusion limitation for sodium. We take exception to that argument. If there is indeed any diffusion limitation, Eq. (1.27)' does not hold, and $\dot{Q}/Q$, which is the measured value does not yield $F/\lambda V$. In general however we do also accept the hypothesis that diffusion limitation will be more pronounced at higher flow rates if all other factors

are kept constant. This very important question will be discussed later, when the double circulation hypothesis is considered.

Besides the first order kinetics models, not many predictions as to the shape of h(t) have been made. Strangely enough, even when a first order process seems unlikely on theoretical grounds, a small series of exponentials have been found to fit h(t) very well. In this way, by injecting and sampling at different sites of the central circulation Pearce (1953) showed that the density functions of transit times for the lungs is nearly exponential. But this is contradicted by Parrish (1959) who found by analogue simulation fitting, this function to follow a laminar flow model, not dissimilar to Bassinghwaight's prediction (1966).

Of all the shapes predicted for the density function of transit times, the lagged (with a normal distributed time delay convoluted on a single exponential) normal distribution as defined by Bassinghwaight (1966a-b), is the one that influenced methods and thinking most after the exponential model. The rationale for Bassinghwaight's approach is that one expects a "normal" dispersion in tubular vessels, due to turbulence and pulsative flow, but in cardiac chambers, or in any intermediate mixing volume, a first order process is assumed. Hence if the normal is given by

$$Ke^{-\frac{1}{2}\left(\frac{t-te}{\sigma}\right)^2} \qquad (1.29)$$

the output function is defined by the following differential

equation:

$$\dot{h}(t) = Ke^{-\frac{1}{2}\frac{(t-te)^2}{\sigma}} - \frac{1}{\tau} h(t) \qquad (1.30)$$

There is no analytical closed expression for the solution of Eq.(1.30), but it can be shown that

$$\bar{t} = t_e + \tau \qquad (1.31)$$

and that the variance is

$$\sigma^2 + \tau^2$$

Section 3. Recirculation

At this point it is important to discuss recirculation. Indeed, why would one when using the integral method find any advantage in defining the shape of h(t) a priori? The reason is obvious: h(t) cannot be measured directly. Before h(t) reaches its endpoint, recirculation appears. The derivation of h(t) can theoretically be done using the convolution theorem for linear transformations. One can use the upstream-downstream sampling method, and a single isotope injection, or a dual isotope injection with single sampling site (see Fig. 1). This last one is the method used by Maseri (1970). Isotope 1 is injected upstream of the studied organ, Isotope 2 downstream. The blood samples yield values respectively $c_1(t)$ and $c_2(t)$, both at the exit of the organ.

Let:

i(t) be the injection function

v(t) the density function of transit times in the general circulation

Fig. 1 Schematic representation of the dual isotope-single sampling site recirculation correction method

The first tracer is injected upstream of the studied system whose density distribution of transit times is h(t). The second tracer is injected downstream, and behaves in the general system (in which the system under study is included) in such a manner that at the sampling site one detects r(t). If r(t) is continuous and has a finite integral in the space t = 0 to t = ∞, h(t) can be isolated from h(t)*r(t) with a linear operation.

Alternatively it can be said that h(t) is found as the input function one needs to obtain the observed function h(t)*r(t) at the output of a system which has an output function r(t) when the input function is a delta function.

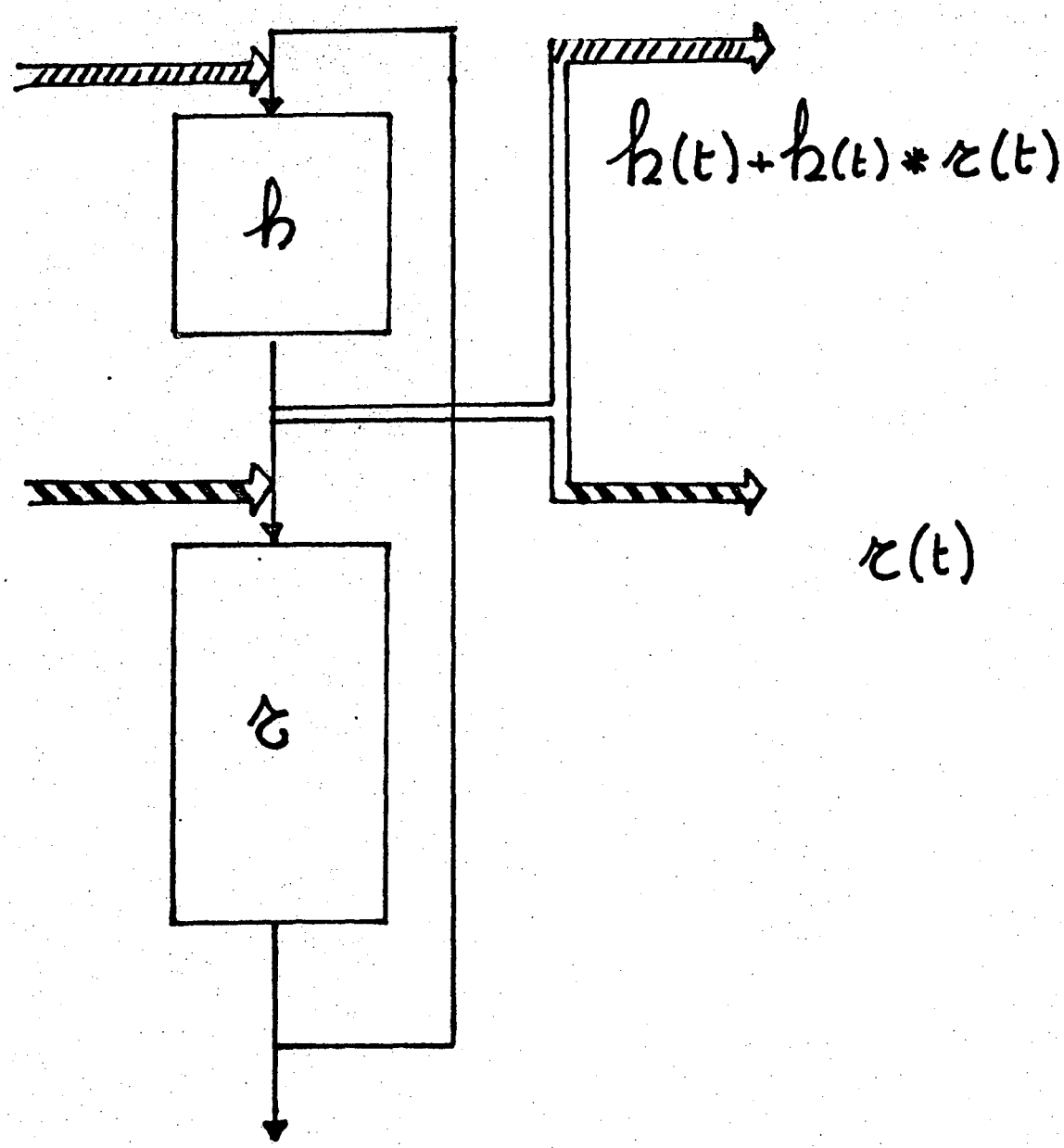

Figure 1

$h(t)$ the density function of transit times through the system

$*$ represents the convolution operation

$c_1(t)$ the concentration of tracer 1 in the output vein

$c_2(t)$ the concentration of tracer 2 in the output vein

F the stationary flow

Then

$$F\,c_1(t) = i(t)*h(t) + i(t)*h(t)*v(t)*h(t) + i(t)*h(t)*v(t)*h(t)*v(t)*h(t) + \ldots\ldots\ldots$$

$$F\,c_2(t) = i(t) + i(t)*v(t)*h(t) + i(t)*v(t)*h(t)*v(t)*h(t)$$

We now define the Laplace transform, symbolically represented by the capital letter representing the original function. In this way we find

$$F\,C_1(S) = I(s)\cdot H(s)\cdot \sum_{i=0}^{i=\infty} (V(s)H(s))^i$$

$$F\,C_2(S) = I(s)\cdot \sum_{i=0}^{i=\infty} (V(s)H(s))^i$$

hence

$$C_1(s)/C_2(S) = H(s)$$

It is interesting to note that both $C_1(s)$ and $C_2(s)$ have the term

$$\sum_{i=1}^{i=\infty} (V(s).H(s))^i$$

which in fact is the recirculation term.

Rewriting the equations as

$$FC_1(s) = I(s).H(s) + I(s).H(s) \sum_{1}^{\infty} (V(s).H(s))^i$$

$$FC_2(s) = I(s) + I(s) \sum_{1}^{\infty} (V(s).H(s))^i$$

shows how after the first passage the system (with transit function h(t)) becomes part of the general system, which is globally described by a transit function r(t), representing an infinity of recirculation cycles, and whose Laplace transform is

$$R(s) = \sum_{1}^{\infty} (V(s).H(s))$$

Therefore, if i(t) is a delta function injection we now have

$$Fc_1(t) = h(t) + h(t)*r(t)$$

$$Fc_2(t) = r(t)$$

This model is shown in Fig. 1. The main features, which we introduced in the preceding derivation are:

1. After the first pass, the system under study becomes part of the general circulation.

2. A delta function injection of a quantity Q, upstream from the sampling site at the output vein of the system,

yields a sampled function r(t).Q representative for the general system.

3. A delta function injection downstream of the same quantity Q yields at the same sampling site a sampled function in two terms. The first term h(t).Q is the first pass function, the second term Q.(h(t)*r(t)) is the recirculation function.

4. If one predetermines r(t), one can derive h(t) from [h(t) + h(t)*r(t)] by deconvolution.

Maseri (1970) did it numerically, that is, without assuming any specific analytical expression for h(t) or r(t). The solution proves not to be entirely satisfactory, since at the end of h(s) oscillations appear, which are due to the errors inherent in this type of analysis or noisy data. The authors also discuss what happens if not all of the tracer recirculates, and to what extent both tracers have to behave linearily in the same manner.

Indeed, for practical reasons one wants r(t) to have a finite integral between t = 0 and t = ∞. This is achieved if the tracer is lost to the system at a constant fractional rate α. The expression for $Fc_2(t)$ becomes a series as follows:

$$i(t) + i(t)*v(t)*h(t)\cdot\alpha + i(t)*v(t)*h(t)*v(t)*h(t)\cdot\alpha^2$$

and so on.

If α is a function of the concentration, or if the re-

moval of tracer is a zero order process, the removal is not necessarily the same for both injections. This discussion is important, but does not change the general outlook of the theory. Coulam (1966) uses the upstream-downstream type of analysis, still using a numerical method in finding the Fourrier transforms of the observed function in a method analogous to that described above.

In both cases the range of time over which sampling is performed, and the fact that one has to assume v(t) and h(t) to have a finite integral in the time interval in which it is completely described are critical aspects of the method. This explains why most authors assume something about the shape of the tail of the curve, by normalizing a lagged normal to the last observed points as does Bassinghwaight who also uses numerical deconvolution, or to assume the function to be periodic, as does Coulam.

Section 4. The diffusable tracer

In the next chapter we will present a circulation-perfusion model where the parallel circulation hypothesis and the difference in dilution volumes for different tracers are integrated. We are not the first to do so: Dobson et al (1955) already compared plasma turnover (Albumin as tracer) with sodium turnover, to determine the ratio of the different pools (8/1). The information one would get from using two isotopes with different distribution volumes will of course depend on the model one can safely use. Zierler (1963) used the most general model with a diffusable and

non-diffusable tracer to define both the bypass fraction of flow and the extravascular turnover (see Chapter II).

Perl (1968) considers three cases in a tubular model. If convection >> diffusion, he finds, as we do in the next chapter, that the wave of a diffusable tracer is simply delayed relative to that of a non-diffusable tracer. If convection << diffusion the extravascular space acts as a first order compartment. Unlike we, he does not consider the fact that the reference tracer may have a different intravascular volume (plasma) than the diffusable tracer (plasma + erythrocytes), but in those two limiting cases the conclusion is the same. Goresky (1970) finds the same results for one of the limiting cases, which he calls flow limited (convection >> diffusion)*. However, if the permeability is not very large, the output function has a spike at the same time as the reference tracer, but is followed by a first order process. This case is very interesting. As we shall see this is not different from a functional shunt situation. In any vessel i the output function is given as

*At this point however it may be necessary to reconsider some of the definitions. Goresky's definition of a system where convection >> diffusion as flow limited raises an interesting conceptual problem. Indeed, what is meant here is that the motion of the tracer is mostly due to convection, but that, over the small distances where it occurs, diffusion is essentially instantaneous.

$$Q_i \left[(1-\alpha)\delta(t-to) + \alpha e^{-k(t-to)} \right] \qquad (1.32)$$

If Q_i is the fraction of the total entering vessel i

δ is the delta function spike, appearing at the exit at the same time as the reference tracer

k is the fractional turnover rate of the first order compartment.

If one then combines this local result, assuming that k is the same in all tubular elements, as is α

$$h(t) = [(1-\alpha)\, n(t) + \alpha\, n(t)^* e^{-kt}] \qquad (1.33)$$

One will note however that Perl finds in his limiting case that $\alpha = 1$ in any vessel, because there is immediate lateral and longitudinal diffusion. We will incorporate immediate longitudinal diffusion (see farther) as did Zierler (1963), but we do consider the possibility that what is actually detected as "bypass flow" may be functional as in Eq. (1.32), leading to Eq. (1.33) for the whole system.

Section 5. Bypass and Diffusion Limitation

There have been many arguments about the existence of bypass flow. The first evidence is somewhat anatomical or structural.

Boestroem (1953) and Piiper (1959) showed how the fraction of microspheres of different diameters reappearing in the venous outflow after intraarterial injection is a function of their diameter, and may be influenced by denervation, or in the case of the dog, by tying off the paws,

where most of the bypass vessels seem to be located. We are not entirely confident that the case is this simple. Although for 50 μ diameter spheres, a morphological wider vessel has to be assumed, it is not clear that nutrient vessels need to have small diameters. Quantitation of the bypass with microspheres is even more complicated, since the microspheres may selectively go through wider channels, and not be distributed between small and wide vessels according to the flow distribution. However, the concept of bypass is an important one.

The issue has been somewhat clouded by the approach to the problem. Sapirstein (1956) defined the fraction of the cardiac output going to different organs by looking at the fraction of ^{42}K tracer found in that organ within a minute after intravenous injection. The author did assume initially first pass uptake. The theoretical derivation, assuming complete first pass uptake, and no back-flow, is straightforward

$$\dot{Q}_i = F_i C_a \tag{1.34}$$

where Q_i is the amount of potassium 42 in organ i

F_i is the flow to organ i

C_a is the overall arterial concentration.

Hence

$$Q_i(t) = F_i \int_o^t C_a(t)dt \tag{1.35}$$

Since C_a is the same for all organs

$$\frac{Q_i}{\Sigma Q_i} = \frac{F_i}{\Sigma F_i} \tag{1.36}$$

One sees undoubtedly that F_i is really only the nutrient flow to the organ, and, still assuming the validity of the model, $Q_i/\Sigma Q_i$ would then represent the fraction of the total nutrient flow, to organ i. Bypass flow is not detected.

The similarity, to some extent, of the physiological behavior of Rb and K led to the indiscriminate use of one isotope for the other, although some striking differences were noted early (Love 1954). That there is no backflow cannot safely be assumed. Indeed, it seems that up to 85% of intraarterially injected potassium-42 reappears at the venous output, and behaves in a manner similar to injected radioactive sodium. (Dobson, Hippensteele, Parker: Personal communication).

If backflow is indeed taken into account, and assuming that there is a single extravascular compartment (which in itself is a very important simplification) the basic differential equation now becomes

$$\dot{Q}_i = F_i C_a - kQ_i \tag{1.37}$$

whose solution is

$$Q_i(t) = F_i \left[\int_o^t C_a(t)\, e^{kt}\, dt \right] e^{-kt} \tag{1.38}$$

where k is defined by the steady state equation for stable potassium.

The total extraction concept is however popular, against all reasons. Tillich (1971) still uses it for effective coronary flow.

Friedman (1968) using Rubidium advanced the hypothesis

that if $(C_A-C_v)/C_A \neq 1$ during a constant infusion experiment there is bypass. However, since he cannot deny the existence of backflow, in 1969 he looked at the ratio of Rb/siderophylline ^{59}Fe. He observes 3 phases in this ratio, the early one expressing bypass, the next one backflow, the last one cell membrane permeability.

But it is really Martin and Yudelevich (1964) who first described the equations needed to understand the behavior of the tracer, and the extraction ratio method.

They first point out that only for an infinite pool the venous concentration of the diffusing tracer c(t) is related to the venous concentration of the reference tracer C(t) as

$$c(t) = (1-E)C(t) \qquad (1.40)$$

when one assumes that in all capillaries the same fraction E is extracted.

However, if there is backflow, the tracer may spend some time in the extravascular system, described by the probability function $\phi(t)$. In that case

$$Fc(t) = (1-E)FC(t) + EF\int_o^t C(\theta)\,\phi(t-\theta)d\theta \qquad (1.41)$$

and since

$$\lim_{t\to 0} \frac{\int_o^{\alpha} C(\theta)\,\phi(t-\theta)d\theta}{c(t)} = 0$$

Eq. (1.41) can be transformed to

$$E = 1 - \lim_{t\to 0} \frac{c(t)}{C(t)} \qquad (1.42)$$

We doubt very much that c(t)/C(t) close to t = 0 can be

measured with any confidence. Still, assuming that it can, and considering as we did up to now a unique $\phi(t)$, Eq. (1.41) can be transformed by a Laplace operator to

$$L(c(s)) = (1-E)L(C(s)) + EL(C(s)).L(\phi(s))$$

so that

$$L(\phi(s)) = \frac{1}{E}\left[\frac{L(c(s))}{L(C(s))} - (1-E)\right] \qquad (1.43)$$

In point of fact this model is not without problems, but Yudelevich (1968) used it to define capillary permeability as

$$PS = -F \ln(1-E) \qquad (1.44)$$

There are multiple problems: neither $\phi(t)$ or E are necessarily unique. In fact E could have any number of values between 1 and 0, the latter value indicating bypass flow. It is Renkin who proposed (1971,1955) that the shunt flow represents flow through a vascular bed with diffusion limitation ($E \neq 1$) where E decreases as the flow rate increases.

Conclusion

The multiplicity of models, and the somewhat confusing terminology makes it difficult to realize what the different models have in common, and how they differ. On the microscopic level one can distinguish several cases.

(1) In the first case, there is no diffusion possible across the vascular membrane. This is the case in the "bypass" vessels. In those vessels all tracers behave in the same way, if one disregards the difference in linear velocity of plasma and erythrocytes. Hence, if simultaneously

introduced, the reference (non-diffusable) tracer, and the diffusable tracer, will appear at the same time at the exit. In the absence of turbulence, and disregarding laminar flow, a delta function injection at the input, yields a delta function at the output.

(2) In the second case (Perl 1968), lateral equilibration is immediate, but there is no longitudinal diffusion. Although this model seems to lack in realism it has some valuable aspects, since the difference in time of appearance for both tracers is defined by their equilibrium distribution volume (see Chapter II).

(3) More realistically, there is some longitudinal distribution; the diffusable tracer has an output function whose mode is retarded relative to the appearance of the reference tracer, but whose shape is very complicated (Perl 1968).

(4) In the fourth case equilibration is instantaneous, and the extravascular distribution volume is combined in a single compartment with the intravascular compartment (Perl 1968, Goresky 1970). This is strictly speaking the flow limited case.

(5) The fifth case is the most general diffusion limited case, as described by Yudelevich (1968) and Martin (1964). Only a fraction of the tracer crosses the vascular membrane. This fraction is lower when flow is higher (Renkin 1955, 1971). The rest of the tracer appears as the reference tracer, but in the extravascular compartment back

diffusion begins. To simplify analysis, no diffusion restriction is assumed within the compartment.

(6) Finally, Dobson's (1957) model combines many elements as in case 4, all equilibrating in a large single pool. Within each system there may be many of those pools, but the attempt at globalization is worth noting.

Attempts at globalization, starting from the microscopic levels have failed, as is to be expected, unless drastic assumptions are made.

It is too early to reject any of the possibilities, even if case 2 seems unlikely. Obviously case 3 would be more realistic. Exclusive lateral equilibration, however, can be imagined if the tubular unit is very long, surrounded by a very narrow extravascular space. If the whole vascular system can be described by this, then an obvious relation exists between the density function of transit times of both tracers (Chapter II). This is also true for a combination of 1 and 2.

The disadvantage of Dobson's model lies in the fact that no transportation time to and from the compartments is assumed. Furthermore, the model makes no allowance for bypass flow.

As for the fourth case, it can be made close to Dobson's model, if one can group the elements in a restricted number of sets having the same first order coefficient while assuming that those "larger compartments" are partially in series with the intravascular pathways (Chapter II).

The final model will therefore be a combination of 1, 2 and 4.

However, one has to keep in mind that if at the microscopic level the empirical distinction between a combination of case 1 and case 2, 3 or 4 in parallel and case 5 is obvious, at the macroscopic level the observed function is in both cases of the general form of Eq. (1.33). This explains, we think, why the parallel network hypothesis coexists side by side with the Renkin model.

In any case, both phenomena are bypass phenomena in the sense we defined. Hence case 5 is implicit in the analysis when the model contains cases 1 in parallel with 2, 3 or 4. It differs only in the very important aspect that it allows the kinetics of a fraction of the tracer to be diffusion limited (Chapter II, Section 2).

CHAPTER II. THE MODEL

In this chapter the integrated model we will use is presented. This model of tissue perfusion is by no means ideal. It represents a compromise between exact representation of the physical reality, and the ability to collect the data necessary to its resolution.

Indeed, the paucity of applications of very complex tracer kinetics models, is indicative of the restriction of the method in general. On the other hand, it can be claimed that some models in general use may be too simplistic to yield real information. Since one of the main points of our method is an improvement of data collection (overcoming geometry factors and recirculation), it follows that we should be able to apply the improved observational method to a model slightly more complex (and closer to reality), but not necessarily to the "ideal" model, if there is such a thing.

At the end of the preceding chapter five distinct microscopic models were presented. We already pointed out how the macroscopic data do not allow one to distinguish between two alternatives. In that case (bypass flow as parallel circuit or as diffusion limitation) the formal analysis of the global data remained the same, in the two modalities.

We will show in this chapter how the same is true to some extent whether one considers tubular flow or a compartmental model, how, under certain specific conditions extravascular circuits in series with the intravascular ones cannot be distinguished from cases where the extravascular dis-

tribution volume includes the intravascular one.

Finally then we will hope to have shown that the analysis of the data, with the ambiguities about the model, allows one nevertheless to determine physiological parameters of importance.

Section 1. Transit Times - Flow and Volumes

The relation between the output function of a tracer injected - in a delta function injection - into an arterio-capillary-venous system, and the flow and distribution volume of the tracer can be defined in different ways. The most common model is the simple compartmental system. For one compartment, the output function is defined as

$$Q\ k\ \exp(-kt)$$

where k is defined as F/V.

Another approach is the transit time analysis. This section analyzes the relation between transit times and flow and volumes, (1) for diffusable tracers, without diffusion limitation in a direction normal to the flow, but no longitudinal diffusion extravascularly, and (2) for a non-diffusable tracer.

Obviously those are stringent conditions and the model can hardly be considered as general. However, the model allows us to analyze closely two important relations: The first one is the relation between $\bar{t}$ and V/F; the second one is the degree to which the output functions for two different (diffusable and non-diffusable) tracers are related. At the end of this section a parallel will be drawn with a com-

partmental model.

A. The Tubular Flow Model

It is easy to see how, for a pure plasma tracer, the transit times of the tracer elements are related to the transit times of the plasma elements, and how the transit time of plasma is related to the plasma's linear velocity, and the path length. Indeed, since flow is equal to dV/dt, and volume V is $\int_o^L A(x)dx$, where A(x) is a cross section area of the plasma volume, one can even intuitively perceive that there must be a relation between linear velocity and flow, as there is one between path length and volume.

Formally one has the following relations and definition: A(x) is the cross section area of the plasma volume, perpendicular to the flow. It is easy to imagine A(x) in a single tubular vessel (Fig. 2).

L is the length of the vessel.

The volume V of the vessel is defined by

$$V = \int_o^L A(x)dx \qquad (2.1)$$

On the other hand, since through the vessel the flow is conserved, and since flow is given by the defining equation

$$F = A(x)dx/dt \qquad (2.2)$$

while the time t spent in the vessel by a tracer element is given by the equation

$$L = \int_o^t v(\tau)d\tau \qquad (2.3)$$

where v(t) is the linear velocity, one sees that the intro-

Fig. 2 Schematic Representation of a Tubular Unit

On top, the figure shows the tubular unit of length L, with 3 cross sectional areas drawn in.

At the bottom, A(x) is plotted as a function of x (full line), while $\overline{A}$, the average cross sectional area is indicated in a dashed line.

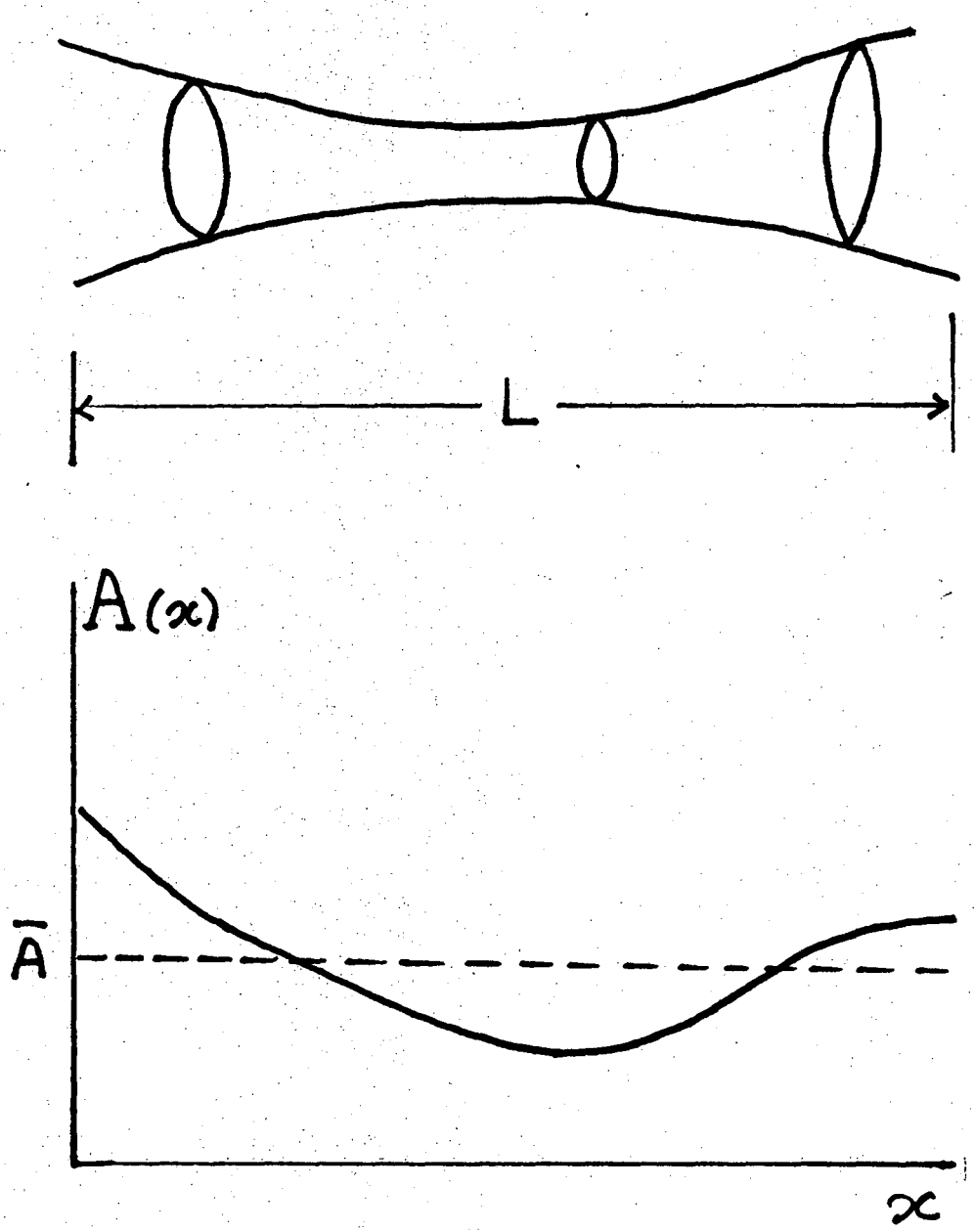

Figure 2

duction of average values for A and v immediately yields t as a function of V and F. Indeed, consider

$$\bar{A} = \int_o^L A(x)\, dx \Big/ \int_o^L dx \qquad (2.4)$$

then

$$V = \bar{A}L$$

$$F = \bar{A}\bar{v}$$

$$L = \bar{v}t$$

and finally

$$V = Ft \qquad (2.5)$$

This simple relation of Eq. (2.5) is less obvious if a tracer diffuses from the tubular vessel into the interstitial tissues. However, if one restricts the volume of extravascular space to which the tracer can diffuse, the situation changes.

As in the definitions of the capillaron we define a vascular unit as a single tubular vessel surrounded by its own extravascular region (Fig. 3).

In the very restricted model that we are discussing now, there is instantaneous lateral equilibration, but no longitudinal diffusion. The assumption has some validity in cases where the tubular vessel is very long and the surrounding extravascular space has a small depth.

At any rate, for this diffusable tracer, neither the flow, nor the length of the vessel have changed. What changes is the volume in its cross section area A'(x), with its average value.

For the plasma, the cross section area A(x), was the

Fig. 3 Schematic representation of the vascular unit

On top the tubular vessel (full line) is shown. Over part of its length, its wall is permeable, and the tracer equilibrates over the volume shown with the dashed line.

The dashed line represents either a capsular separation, or the distance beyond which, in an alternative model, diffusion limitation occurs.

On the bottom we have as a function of x:

$A(x)$, the lower full line representing the physical cross sectional area of the tubular element.

$Ap(x)$, the dashed line, representing the physical cross sectional area of the extravascular space.

$Ap(x).\lambda$, the dotted line, representing the virtual extravascular volume cross sectional area.

$A'(x)$, represented by the upper full line, and being the cross sectional area of the total virtual distribution volume:

$$A'(x) = A(x) + Ap(x).\lambda$$

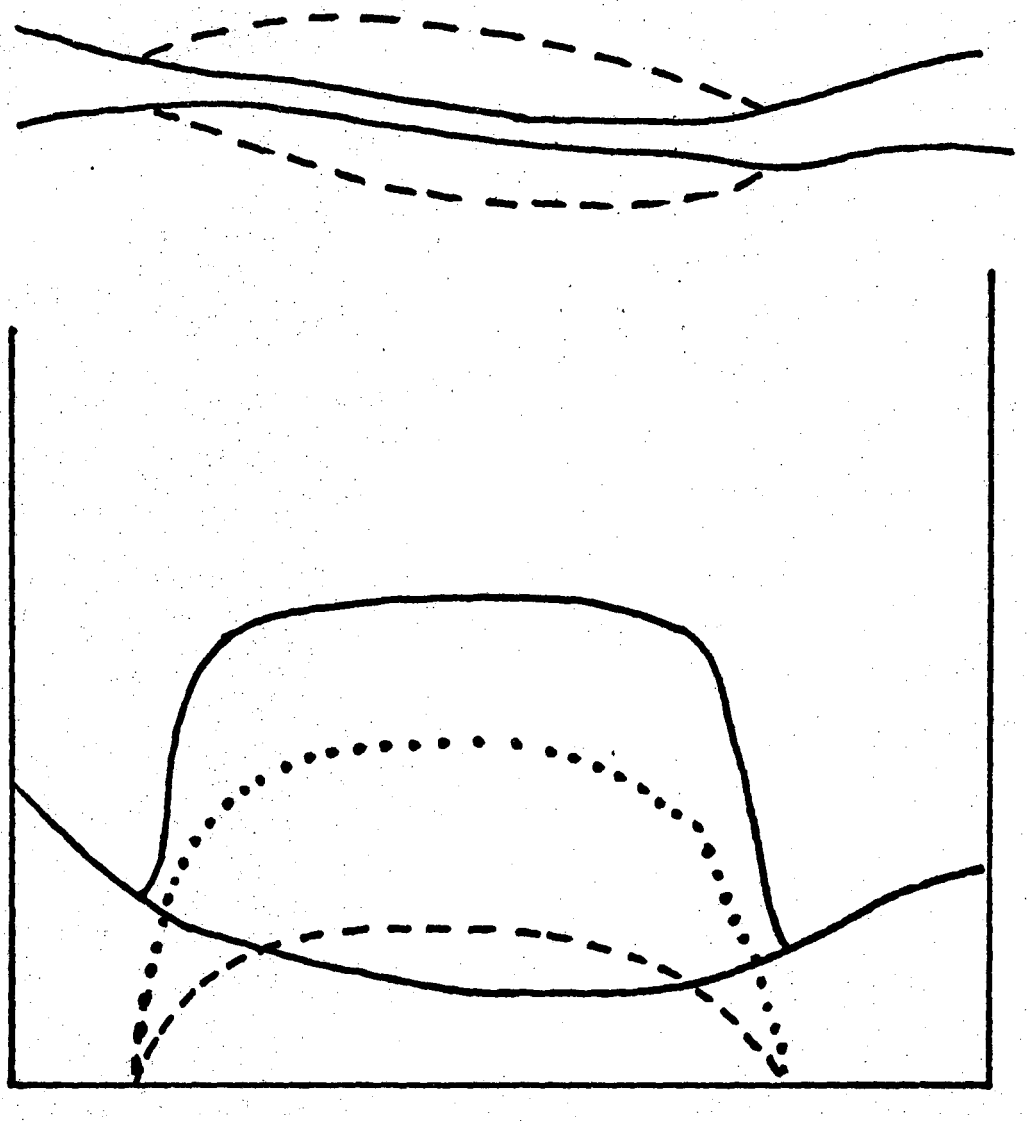

Figure 3

physical cross section area of the vessel (minus the part of it occupied by erythrocytes). Let the physical cross section area of the extravascular region be Ap(x).

At equilibration the concentration of the tracer in the plasma is Cp, the concentration in the extravascular space is Ce.*

We define

$$\lambda = Ce/Cp \tag{2.6}$$

and therefore

$$A'(x) = A(x) + Ap(x)\lambda \tag{2.7}$$

We then have, as for the plasma tracer from Eq. (2.1)

$$V' = \int_0^L A'(x)dx$$

from Eq. (2.4)

$$\bar{A}' = \int_0^L A'(x)dx/L$$

and from this we can define

$$V' = \bar{A}L + \bar{A}p\lambda L \tag{2.8}$$

There are two important points. The flow has not changed. Furthermore, $\bar{A}p\lambda L$ is a virtual volume for the tracer in the extravascular space, which we will call V'e. The transit time t' for this diffusable tracer is given by

$$V' = Ft' \tag{2.9}$$

and from (2.9) and (2.5) we have

*If the extravascular space is not homogeneous there is more than one equilibration concentration, and Ce is an average. This does not influence our derivation.

$$t' - t = V'e/F \qquad (2.9)'$$

If the tubular wall is not permeable for the tracer, both diffusable and non-diffusable tracers have the same transit times since λ obviously will be zero and

$$\bar{A}p\lambda = 0$$

$$Ve = 0$$

The problem is that if the tracer is diffusable, it may also diffuse into the erythrocytes. In that case the flow, which is flow of carrier in the first place, changes from plasma flow to blood flow. In this case there is a special problem when the erythrocytes have a different linear velocity than the plasma elements. We will not discuss this problem yet, but will only say that both velocities are close, if not equal.

Going back to Eq. (2.2), the relation between flow and cross section area remains the same but the cross sectional area one uses is the sum of plasma cross sectional area $A(x)$, + the tracers virtual cross sectional area in the erythrocytes $A''(x)$.

Hence

$$F' = (A(x) + A''(x))\, dx/dt$$

However there is also a change in volume, given by an equation similar to (2.8)

$$V' = \bar{A}L + \bar{A}''L + \bar{A}'L \qquad (2.10)$$

and Eq. (2.5) still holds

$$V' = F't \qquad (2.11)$$

Two cases have to be considered. In the non-permeable vessels, $\lambda = 0$, and $\bar{A}'L = 0$, therefore

$$V' = \bar{A}L + \bar{A}''L$$

and

$$t'' = \frac{L(\bar{A} + \bar{A}'')}{v(\bar{A} + \bar{A}'')} = \frac{L}{v} = t \qquad (2.12)$$

exactly as for the pure plasma tracer.

Otherwise, when $\lambda \neq 0$

$$t'' = \frac{L(A + A'' + A')}{v(A + A'')} = t + \frac{V'e}{F'} \qquad (2.13)$$

We see that in the non-permeable or bypass vessels the transit time for the diffusable tracer is the same as for the non-diffusable one, regardless of the fact that the diffusable tracer does or does not equilibrate in the erythrocytes. But we assumed both erythrocytes and plasma to have the same velocity, and a correction factor may have to be introduced.

More important, in the exchange vessels, depending on whether the tracer does or does not penetrate in the erythrocytes, the difference between the transit time of the diffusable and the non-diffusable tracer is either V'e/F', (Eq. 2.13) or V'e/F (Eq. 2.9)'. Note however that for different tracers V'e may be different, since it represents a virtual volume.

In general, if h(t) is a density function of transit times, the mean transit time is defined as

$$\bar{t} = \int_0^\infty th(t)dt \qquad (2.14)$$

and since in general in any tubular vessel i, the transit time ti is

$$ti = V_i/F_i \qquad (2.15)$$

where V_i and F_i may vary depending on the tracer and the vessel type, the mean transit time is

$$\bar{t} = \sum_{i=1}^{N} t_i/N \qquad (2.16)$$

where N is the number of vascular elements in parallel. Substitution of Eq. (2.15) in Eq. (2.16) yields

$$\bar{t} = \sum \frac{V_i}{F_i N} \qquad (2.17)$$

At this point, to reach the final solution proposed by Zierler, one has to introduce a new concept of volume. Consider

$$\frac{V_i}{F_i} = \frac{V_i/M_i}{F_i/M_i} = \frac{V_i/M_i}{f}$$

so that $Nf = F$, or the total flow,

then

$$\bar{t} = \sum_{i=1}^{N} \frac{V_i/M_i}{fN}$$

$$\bar{t} = \frac{1}{F} \sum_{i=1}^{N} \frac{V_i}{M_i}$$

and hence V in the equation $\bar{t} = V/F$ is not ΣV_i, but a weighted sum $\Sigma V_i/M_i$. (2.18)

One can now define the density functions of transit times (n(t) and d(t)) for both tracers. However, since two

types of vessels are assumed to be present (permeable and non-permeable) the functions are respectively:

$$n(t) = (1-\alpha)n_1(t) + \alpha n_2(t) \qquad (2.19)$$

$$d(t) = (1-\alpha)d_1(t) + \alpha d_2(t) \qquad (2.19)$$

where α is the fraction of F or F' going to the permeable vessel circuit (or exchange vessels), while $(1-\alpha)F$ or $(1-\alpha)F'$ goes to the non-permeable (or bypass) vessel circuit. Both circuits are assumed to be in parallel. Since in the bypass vessels the transit times are the same, regardless of the tracer, we have

$$d_1(t) = n_1(t) \qquad (2.20)$$

The mean transit times are found in the usual way

$$\bar{t}n = \int_o^\infty tn(t)dt = \int_o^\infty (1-\alpha)tn_1(t)dt + \int_o^\infty \alpha tn_2(t)dt$$

$$\bar{t}d = \int_o^\infty td(t)dt = \int_o^\infty (1-\alpha)tn_1(t)dt + \int_o^\infty \alpha td_2(t)dt$$

One can now define the following mean transit times

$$\bar{t}_1n = \int_o^\infty tn_1(t)dt = V_1/(1-\alpha)F \qquad (2.21)$$

$$\bar{t}_2n = \int_o^\infty tn_2(t)dt = V_2/\alpha F \qquad (2.22)$$

$$\bar{t}_2d = \int_o^\infty td_2(t)dt = (V_2 + Ve')/\alpha F \qquad (2.23)$$

or in cases where the diffusable tracer penetrates the erythrocytes

$$\bar{t}_2d = \int_o^\infty td_2(t)dt = (V_2' + V_e')/\alpha F' \qquad (2.23)'$$

where

V_1 is the plasma volume in the bypass circuit

V_2 is the plasma volume in the exchange circuit

V_2' is the blood volume in the exchange circuit

F is plasma flow

F' is blood flow (virtual)

Ve' is the virtual extravascular space of the exchange circuit.

In this way two global mean transit times were defined, $\bar{t}d$ and $\bar{t}n$, respectively for the diffusable and the non-diffusable tracer. However, the presence of bypass made it necessary to define three more.

$\bar{t}_1n$ is the mean transit time of both tracers in the bypass circuit.

$\bar{t}_2n$ is the mean transit time of the non-diffusable tracer in the exchange circuit

$\bar{t}_2d$ is the mean transit time of the diffusable tracer in the exchange circuit

Of course, unless $n_1(t)$, $n_2(t)$ and $d_2(t)$ are defined independently, the values one can derive from direct observation are $\bar{t}n$ and $\bar{t}d$.

However, from the preceding, it follows that

$$\bar{t}n = (1-\alpha)\bar{t}_1n + \alpha\,\bar{t}_2n$$

$$\bar{t}d = (1-\alpha)\bar{t}_1n + \alpha\,\bar{t}_2d$$

and hence

$$\bar{t}d - \bar{t}n = \alpha(t_2d - t_2n)$$

Two things, although obvious, are worth noting. First,

the extravascular volume in the bypass circuit is not detected. Secondly, by subtracting $\bar{t}n$ from $\bar{t}d$ one obtains Ve'/F, and not $Ve'/\alpha F$, the value of interest. Therefore, α has to be estimated independently.

It is worth noting that if there is a constant ratio between Ve' and the blood or plasma volume V, so that

$$S = \frac{Ve' + V}{V} \tag{2.24}$$

it follows that

$$t_i' = St_i \tag{2.25}$$

and also

$$\bar{t}_2 d = S\, \bar{t}_2 n \tag{2.26}$$

Eq.(2.25) and (2.26) will be used later.

B. The compartmental analogue

In what preceded the basic assumption is that lateral equilibration is immediate, while extravascular longitudinal diffusion does not happen.

Parker and Hippensteel (1972), among others, pointed out that for all practical purposes, if the output function for a tracer (in this case intravascular) can be fitted by a sum of exponentials, one can to a point consider the system as made up of compartments, but that a first order process does not have to be assumed. Indeed, so they argue, the exponential distribution of transit times may be due to an exponential distribution of tubular lengths, for equal linear velocities, or of tubular volumes, for equal flows.

Hence, if $n_2(t) = Ae^{-at}$, then if in general the proportion of intra and extravascular volume is constant, then $d_2(t) = A/S\ e^{-at/S}$ where S is defined as in Eq. (2.24) for the permeable units.

The output functions for the two tracers (barring by-pass flow) are then as one would expect them also in cases where the distribution volume for the diffusable tracer simply includes the intravascular volume, in such a way that in each parallel circuit the proportion of intra and extravascular volumes (virtual) is the same. Indeed, in each of the circuits, we have, for the non-diffusable tracer

$$\dot{q}_i(t) = \frac{F_i}{V_i}\, q_i(o) e^{-F_i/V_i\, t}$$

and for the diffusable tracer

$$\dot{q}_i(t) = \frac{F_i}{SV_i}\, q_i(o) e^{-F_i/SV_i\, t}$$

The model is represented in Fig. 4.

Obviously as far as diffusion goes between the two models (tubular flow and compartmental) the correspondence lies in the fact that flow is the limiting factor. But the diffusion factor is not the same in both cases. Contrary to the tubular model, the compartmental model has no diffusion limitation in any specific direction (relative to the flow), but an instantaneous mixing is assumed.

In this section we considered two cases of strict flow limitation. It is important to consider all assumptions explicitly.

Figure 4. Schematic Representation of a Single Compartment System.

The non-diffusable tracer, whose flow is indicated by the white part of the arrow "sees" only the small intravascular compartment V_1 (dashed square). The diffusable tracer, transported by the same flow, indicated here by the shaded arrow, "sees" the larger compartment as a single one, and is not influenced by the separation between extra and intravascular volumes (dashed line). In steady state, the rate of disappearance (after equilibration) is for the non-diffusable tracer F/V_1, for the diffusable tracer $F/(V_1+V_2)$. The mean transit times are respectively:

$$\bar{t}n = V_1/F$$

$$\bar{t}d = (V_1+V_2)/F. = S\bar{t}n$$

In this simple case no bypass circuit is assumed (or - $1-\alpha) = 0$).

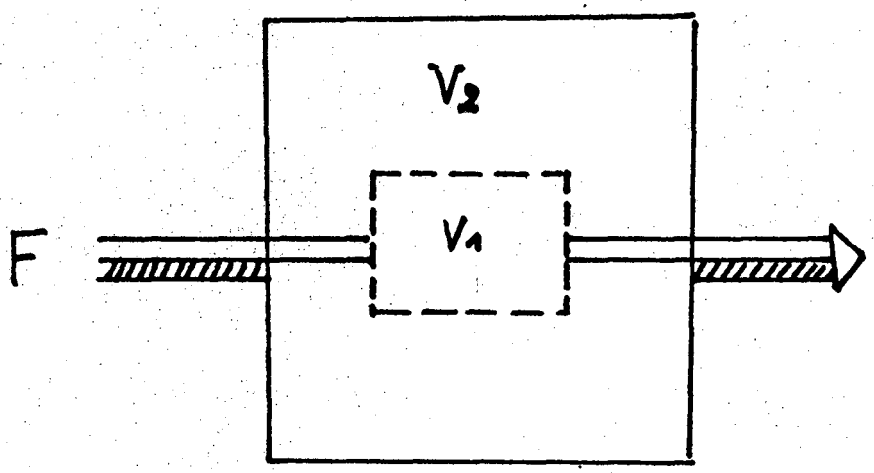

Figure 4

1. The tubular model assumes:

   unlimited lateral diffusion within the vascular unit, but no longitudinal diffusion.

2. The compartmental model assumes:

   uniform mixing;

   no diffusion limitation within compartments.

3. Coincidence between the two is found for permeable vessels if:

   the vascular transit times have exponential distribution;

   the intra and extravascular volumes are in constant proportion in all capillary units.

Obviously, in this case the emphasis lies in free diffusion. If the diffusable tracer is an inert gas like Xe or Kr, or an ion like sodium, the model may apply, but in poorly vascularized regions the assumption may be strained. Therefore, without prejudice as to the importance of the phenomenon, the model should take this factor into account. This will be presented in the next section.

Section 2. The extravascular compartment or volume in series.

It is difficult to assess what exactly will happen if the immediate equilibration (lateral in the tubular model, or throughout the compartment in the compartmental model) condition is not met.

Zierler (1963) presented a model in which one simply considers the time spent by tracer elements in the extra-

vascular space. The rationale is not immediately clear. Partly it is based on the conception that the motion of the tracer particle is possible only by some flow of carrier (fluid). On the average the tracer particles leave the vascular compartment and re-enter it at the same point (in Zierler's model). For each particle to the intravascular transit time an extravascular transit time is added. For this fraction of the tracer amount injected a distribution function of transit time is convoluted on the intravascular transit time.

There is more to this than meets the eye. Two elements of Zierler's model have to be explained.

If as he concludes, the distribution function of transit times is given by convoluting the distribution function of extravascular transit times on the intravascular one, then one assumes that both systems are completely in series, and not, as Zierler suggests, that to each intravascular tubular pathway an extravascular pathway is added, unless to each tubular element pathway the distribution of extratubular pathways added is the same, which amounts to the same thing.

Secondly, if a relation between transit time and volume and flow exists, it can only be so if the motion of the tracer is due to flow of carrier. Therefore, diffusion is not considered.

To introduce the solution one has to reconsider the basic formalism. Two functions have been defined, respec-

tively, for the non-diffusable and the diffusable tracer, as follows:

$$n(t) = (1-\alpha)n_1(t) + \alpha n_2(t)$$
$$d(t) = (1-\alpha)n_1(t) + \alpha d_2(t)$$

In the preceding section it appeared that under certain assumptions $d_2(t) = n_2(tS)$, which means that all transit times are multiplied by S. Up to now the relation $t = V/F$ is obvious. If a third process is introduced d(t) becomes

$$d(t) = (1-\alpha)n_1(t) + \alpha\beta\, d_2(t) + \alpha(1-\beta)\, d_2(t)*e(t).$$

The term $(1-\beta)\, d_2(t)*e(t)$ indicates that for a fraction $\alpha(1-\beta)$ of the injected amount, the model needs a distribution volume in series with the vascular units allowing diffusion. If the motion in this volume is flow limited there is no problem. Diffusion limitation would mean that the transit time is defined as V/F only for a fraction of the tracer. In that case

(1) $(1-\alpha)\, n_1(t)$ is indicative of the bypass flow

(2) $\alpha\beta\, n_2(t/W)$ is indicative of tissue perfusion

(3) $\alpha(1-\beta)\, n_2(t/W)*e(t)$ is indicative of diffusion exchange.

And while only (2) is tissue perfusion in the strict sense, (3) is indicative of exchange, although very much tracer specific. In the case of flow limitation in the volume in series (Zierler's hypothesis) both (2) and (3) are indicators of tissue perfusion.

But how can a volume in series be imagined with flow

limitation? We will consider the anatomical equivalents in Chapter IV (Results and Discussion). At this point however the following can be said:

For an intravascular (non-diffusable) tracer, the fraction of the total transit time spent in the large vessels is relatively large, while for a diffusable tracer most of the time is spent in the tissue compartments.

Hence, allowing for some error, for each tracer element of the diffusable tracer one can simply add to the intravascular transit time an extravascular transit time, which leads to the concepts of compartments or systems in series.

In Fig. 5 the model is schematically shown. Each circle corresponds to a subdivision of the systems where some time is spent. The time spent is proportional to the diameter of the circle.*

Up to now we did not use analytical expressions for $d(t)$ or $n(t)$, or any of their components. The tubular model as such gives no clues to the analytical form of these functions, but we considered briefly one case in which $d_2(t)$ is analytically defined by the analytical form of $n_2(t)$.

In the next section we will derive all expressions as they follow from a compartmental model, which will allow us to make the different possibilities clearer.

*Note that in this figure, as in all others of the same kind, the arrows indicate direction of flow, and no time is spent along the arrow.

Fig. 5 Schematic representation of the extravascular compartment in series, with flow limitation.

The intravascular tracer (white arrow) spends most of its transit time in the subsystems A and V, representing respectively the arterial and venous side of the vascular bed. Only a small fraction of its transit time is spent in C, at the capillary exchange level. This tracer does not see the tissue subsystem T.

The diffusable tracer spends the same time in A and V as does the non-diffusable, but spends a much larger time in the systems T and C. Hence

$$tn = tn(A) + tn(C) + tn(V)$$

$$td = tn(A) + td(C+T) + tn(V)$$

since $tn(C)/tn \ll 1$

and $td(C+T)/td \sim 1$

we have

$$td(C+T) \approx td - tn$$

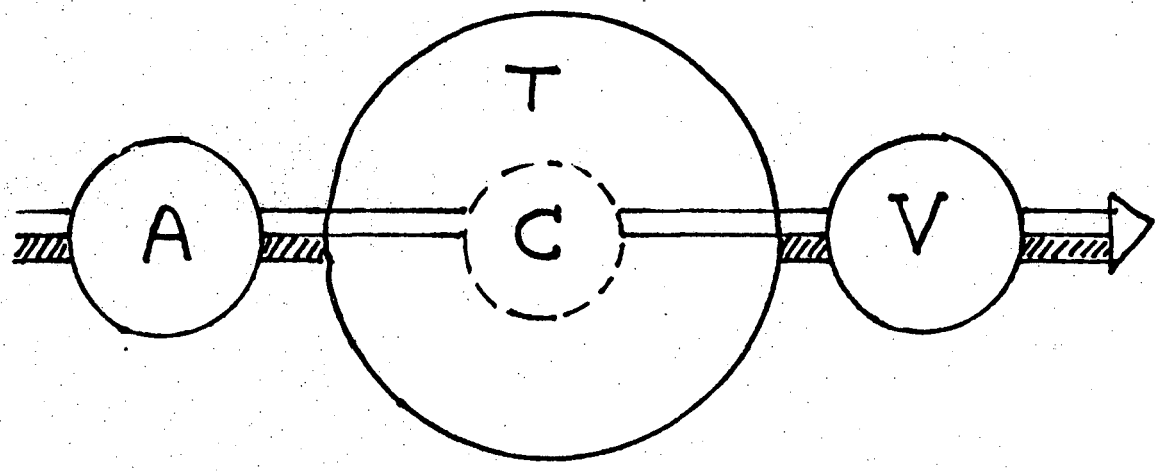

Figure 5

Section 3. Mathematical Formulation

In this section we will review the mathematical formulation. Because empirically the output function n(t) is well fitted by a restricted number of exponential terms, $n(t) = \Sigma A_i e^{-a_i t}$ will be the basis for all subsequent derivations. It so happens that the mathematical formulation is not different from that of pure compartmental analysis. Why then the non-compartmental derivation in the preceding section? This is a fine point. No realistic set of physical assumptions can make all capillaries into a small number of compartments. The good fit to exponentials is accidental. Zierler has made strong objections to the automatic compartmental approach. He points out the following objections:

(1) For a non-diffusable tracer the capillaries are too individual to be pooled in any sum of sets with instant equilibration.

(2) The general assumption that the compartments are parallel does not stand close inspection. Indeed, the output function h(t) does not jump abruptly from zero to maximum value at t = 0.

(3) Finally, there is a lag time between injection and the first appearance of the tracer in the output vein. In a strict compartmental situation this would not appear.

In what follows we have taken the pure time lag into account by translation of the time scale to the extent that it was necessary. The fact that we present the exponential

fitting as accidental will allow us to fit in such a way that after translation of the time scale, at $t = 0$, $h(t) = 0$, and remains continuous. In compartmental terms this means at least two compartments in series, but although this is hard to map from model to reality, it does not bother us since for the intravascular flow the fitting does not assume compartments.

1. Convolution of exponential functions

$Ae^{-at} * Be^{-bt}$ is analytically defined as

$$\frac{AB}{a - b}\left(e^{-bt} - e^{-at}\right) \tag{2.27}$$

unless $a = b$, in which case it is equal to

$$AB\, e^{-at}.t \tag{2.28}$$

2. In the simplest case, which will be finally used, one can fit the output function of the intravascular tracer as

$$n(t) = \sum_{1}^{N} A_i e^{-a_i t}$$

where $n(t)$ is normalized by the restriction that

$$\Sigma A_i / a_i = 1$$

This means of course that $n(t)$ is defined as the true output function, the observed one being $Q.n(t)$ where Q is the normalization factor. Furthermore, to keep the function continuous, even at $t = 0$, $\Sigma A_i = 0$. (a) If one then fits the data for the diffusable tracer regardless of the preceding, it appears that a fair fit is found by

$$d(t) = \sum_{1}^{M} B_i e^{-b_i t}$$

where once again $\Sigma B_i/b_i = 1$, and $\Sigma B_i = 0$.

(b) However, simply assuming independence of d(t) from n(t) is not realistic. The diffusable tracer has at least to travel the path of the non-diffusable (in part or totally). In one case (see Section 1), the assumption may be that the path is the same, as is the flow, but that the distribution volume is larger by a constant factor S all over the system. Then d(t) is in fact best fitted by

$$d(t) = \sum_{1}^{N} (A_i/S) e^{-a_i t/S} \qquad (2.29)$$

And from that it follows that $\Sigma A_i/S = 0$, but that the normalization is still $\Sigma A_i/a_i = 1$.

However, whether the fitting function for n(t) is a sum of exponentials because the system is truly compartmental, or whether it is so by a chance distribution of path lengths with equal linear velocities, it is not likely that S is constant for each compartment, or each tubular element.

In the compartmental hypothesis, still barring bypass, d(t) then becomes

$$d(t) = \sum_{1}^{N} (A_i/S_i) e^{-a_i t/S_i}$$

The concordance between n(t) and d(t) is not as loose as in the first case, since now

$$B_j = A_i/S_i \qquad \text{for } j = i$$

$$b_j = a_i/S_i \qquad \text{for } j = i$$

instead of being completely unrelated. However, if the number of compartments present, M, is larger than the number of terms, N, in the sum, then due to model bias the fitting may be purely accidental, and the relation between the B_j and A_i is lost. This is also what happens when the tubular model is assumed. Indeed, since in each individual tubular element the transit time for the diffusable tracer may be changed by any factor, S_i, if a fitting is found as

$$d(t) = \sum_{1}^{L} B_j \, e^{-b_j t}$$

there is no reason for L to be equal to N, nor is there any necessary relation between A_i and B_j for i = j.

(c) In a third approach it is assumed that the extra dilution volume of the diffusable tracer is in series with the intravascular one, and behaves as one single compartment (0.1) or one or more compartments in series (0.2) or parallel (0.3).

0.1) in this case

$$d(t) = (\Sigma A_i e^{-a_i t}) * e^{-kt} \qquad (2.30)$$

0.2) for two compartments in series

$$d(t) = (\Sigma A_i e^{-a_i t}) * (\sum_{1}^{2} K_j e^{-k_j t}) \qquad (2.31)$$

with the restrictions that

$$\sum_{1}^{2} K_j = 0 \quad \text{(0 and continuous at t = 0)}$$

$$\Sigma \, K_j/k_j = 1 \quad \text{(normalized)}$$

0.3) for two compartments in parallel

$$d(t) = (\Sigma A_i e^{-a_i t}) * (\sum_{1}^{2} K_j \, e^{-k_j t}) \qquad (2.32$$

with only the normalizing restriction $\Sigma K_j/k_j = 1$.

It is interesting to note the analytical expression of 2 or 3 which is as follows if $k_j \neq a_i \; V_{i,j}$

$$d(t) = \sum_i A_i \sum_j \frac{K_j}{(a_i - k_j)} \; (e^{-k_j t} - e^{-a_i t}) \qquad (2.33)$$

Indeed, assuming that the a_i have a tendency to be larger than the k_j, and to the extent that the difference is larger d(t) is soon reduced to

$$d(t) = \sum A_i \sum \frac{K_j}{(a_i - k_j)} \; e^{-k_j t}$$

or proceeding further

$$d(t) = \sum K_j \, e^{-k_j t} \qquad (2.34)$$

this explains the relative success of the independent solution of the type

$$d(t) = \Sigma \, B_j e^{-b_j t}$$

in this case again, since the simplification assumes for all practical purposes that $\Sigma A_i e^{-a_i t}$ is a delta function ($t \geq 0$).

(d) Under a different assumption the phenomenon described in b and c both occur, then the solution is of the form

$$d(t) = \sum A_i \sum \frac{K_j}{(a_i - k_j S)} \; (e^{-k_j t} - e^{-a_i t}/S) \qquad (2.35)$$

An unlikely case arises when $a_i = k_j S$ because then the expression is reduced for i and j to

$$A_i K_j \; t \; e^{-a_i t/S}$$

as was pointed out before.

(e) Finally one could have a combination of c and d, and therefore the output function would be described by

$$d(t) = \beta \sum \frac{A_i}{S} e^{-a_i t/S}$$

$$+ (1-\beta) \sum K_j \sum \frac{A_i}{a_i - S k_j} (e^{-k_j t} - e^{-a_i t/S}) \qquad (2.36)$$

When $a_i >> S \; k_j \; V_{i,j}$ this last expression reduces to

$$d(t) = \beta \sum \frac{A_i}{S} e^{-a_i t/S} + (1-\beta) \sum K_j \; e^{-k_j t} \qquad (2.37)$$

or if the factor S is not constant from element to element

$$d(t) = \beta \sum B_i \; e^{-b_i t} + (1-\beta) \sum K_j \; e^{-k_j t} \qquad (2.37)'$$

The noteworthy thing about this assumption is the compartmental model fitting it. (Fig. 6). The existence of one tissular compartment in series with, and one including the intravascular compartment, is not impossible to visualize, and will be discussed in Chapter IV.

However, in this case the implicit assumption is that all the intravascular compartments, or alternatively all the tubular elements, are in series with a few common tissular

Fig. 6. Compartmental model showing the intravascular compartment (I), and two tissue compartments, with one of them (III) in series with the intravascular compartment or the intravascular compartment and the tissue compartment II.

The non-diffusable tracer detects only compartment I and passes, without "seeing" them, through the others (shaded arrow). A fraction of the diffusable tracer bypasses in the same sense compartment III (white arrow). But for all of the diffusable tracer there is complete equilibration between I and II.

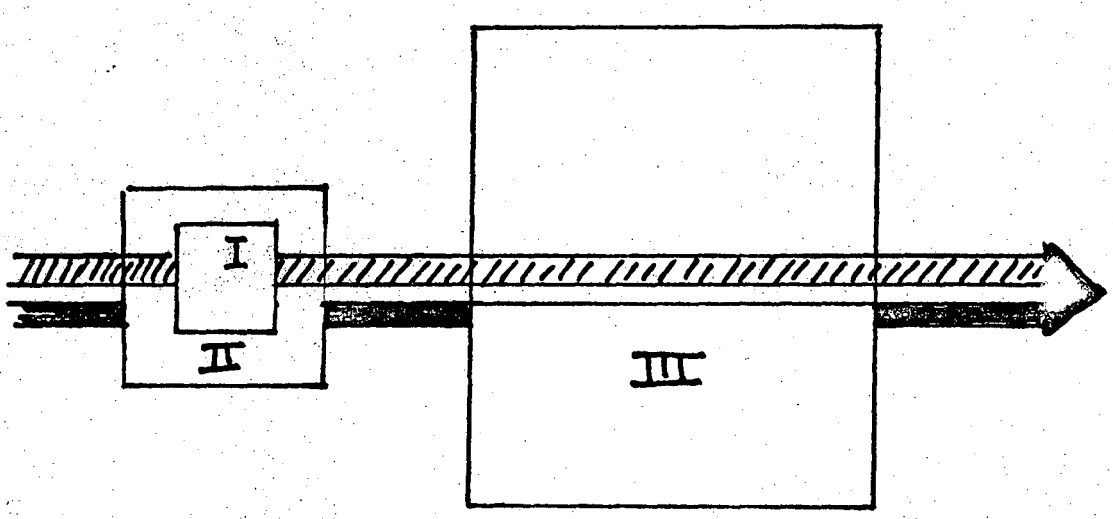

Figure 6

compartments. This is represented in Fig. 7. In this figure bypass is not considered, since it was not discussed at this stage. Formally then, the derivation was reduced to a comparison of $d_2(t)$ with $n_2(t)$.

We have then shown that $d_2(t)$ may have a functional form very different, and independent of, $n_2(t)$. The conditions needed are different in each modality.

In the tubular flow model the independence of $d_2(t)$ is guaranteed if S is not constant over all the elements.

In the compartmental model, with including compartments, the same condition is needed.

In the cases of compartments in series, the condition is for the intravascular transit time to be short relative to the residency time in the extravascular compartment.

3. In the derivation of the simplest case possible bypass was disregarded altogether. However, the bypass fraction is theoretically one of the most important parameters. One can assume that n(t) has two terms, one due to the tracer going through thoroughfare channels, the other due to the exchange vessels. n(t) therefore would be defined as

$$n(t) = \alpha \sum A_i e^{-a_i t} + (1-\alpha) \sum B_i e^{-b_i t}$$

$(1-\alpha)$ being the bypass fraction.

This however proves to be too much of a commitment to the parallel circuit theory. Empirically, we found (see Results) that n(t) can be fitted, with fair constancy from one exper-

Fig. 7 Schematic representation of a compartmental model with two parallel systems of two compartments in series, which for a fraction of their flow are in series with a single (larger) compartment.

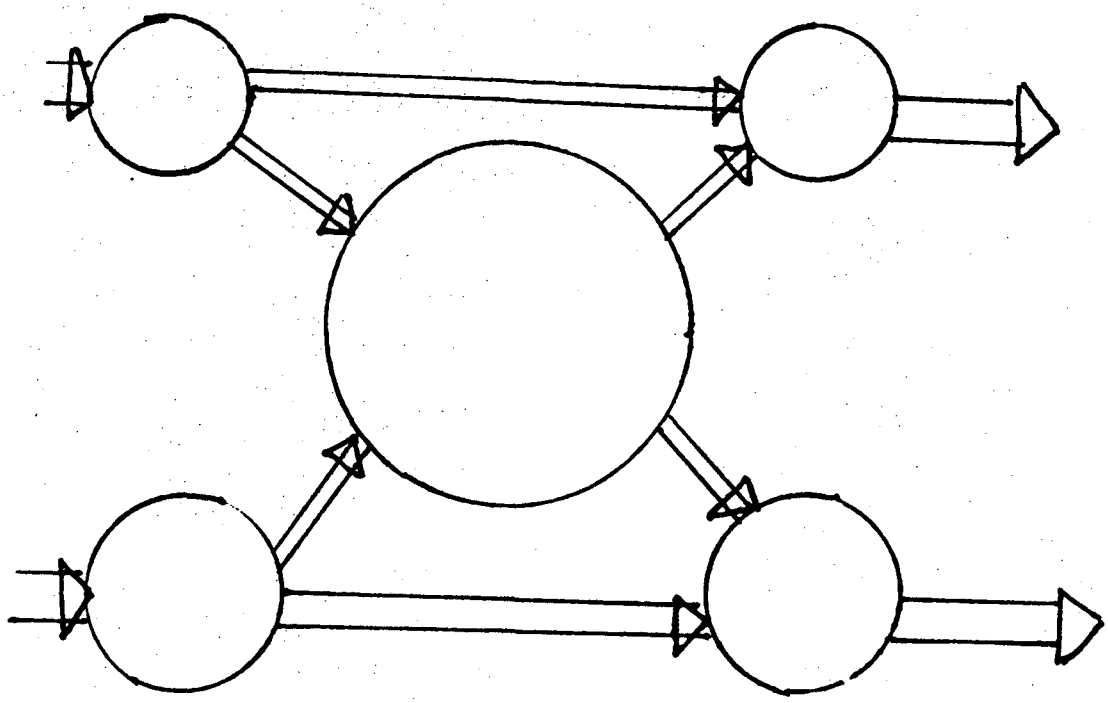

Figure 7

iment to another, by

$$\sum_{1}^{3} A_i(e^{-a_i t} - e^{-b_i t}) \tag{2.38}$$

and that maximizing the bypass element can be achieved by assuming

$$(1-\alpha)n_1(t) = \sum_{1}^{3} \gamma_i A_i(e^{-a_i t} - e^{-b_i t}) \tag{2.39}$$

In this fashion we found that d(t) is well fitted by

$$d(t) = (1-\alpha)n_1(t) + \sum_{4}^{6} A_i(e^{-a_i t} - e^{-b_i t})$$

where

$$\alpha d_2(t) = \sum_{4}^{6} A_i(e^{-a_i t} - e^{-b_i t}) \tag{2.40}$$

The compartmental model fitting those equations is shown in the most general way in Fig. 8. (See Appendix A).

4. In short, then, we will not assume any specific microscopic model, but we will use the characteristic they all have in common. We have already stated that the functional form

$$d(t) = (1-\alpha)n_1(t) + \alpha d_2(t)$$

can be expected whether at the microscopic level one has two parallel networks, or diffusion limitation in some or all of the vessels.

Furthermore, the independent functional form of $d_2(t)$ is consistent with the tubular flow model when S is not constant

Fig. 8 Generalized compartmental model

The flow is divided between 3 parallel circuits in fractions $f_i = A_i/\Sigma A_i$. In each parallel circuit there are again two paths, dividing the fraction of flow as $\gamma_i f_i$, so that $\Sigma\gamma_i f_i = \alpha F$.

It is important to note that if the tissue compartment is very large the equation is the same (in the limiting case) whether it is in series with the intravascular compartment, or, as shown here for aesthetic reasons, includes it.

Also, in cases where there is diffusion limitation the bypass circuits are not isolated from the exchange circuits, but the larger tissular compartment is still only seen by a fraction of the tracer going that way.

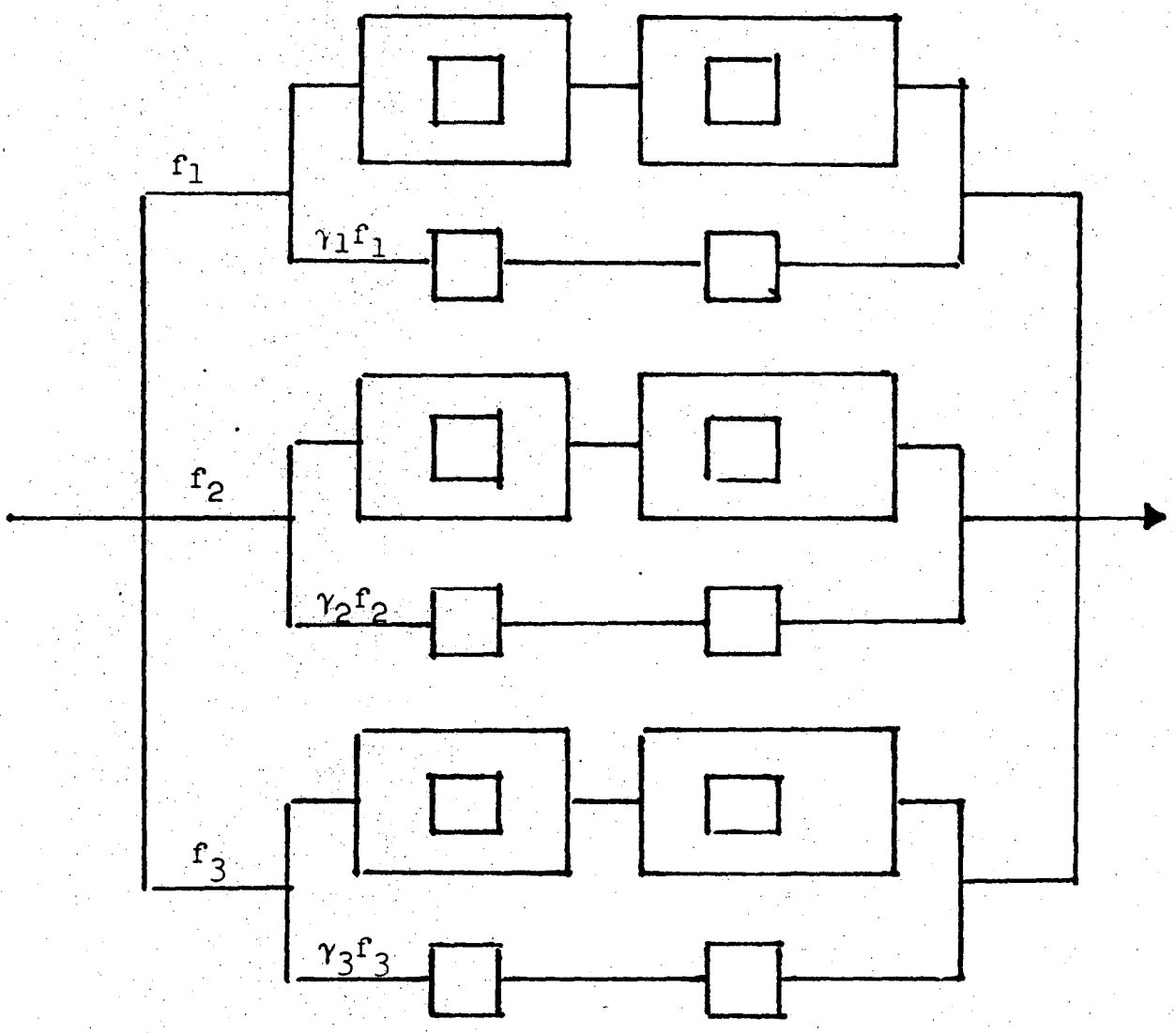

Figure 8

in all the capillary units, as it is, (in the limiting case) when the extravascular volumes are in series with the intravascular ones.

That this limiting case applies is supported by the fact that the transit times for Xenon are markedly longer than for colloid, so that the derivation leading to Eq. (2.34) is not far-fetched.

In the next chapter we will discuss how we determine n(t) and d(t) (by correcting for recirculation), and how the functional form we described here is applied after the recirculation correction.

CHAPTER III. MATERIALS AND METHODS

Section 1. Experimental design

In all experiments, beagle dogs, weighing approximately 10 kgr., were used. Anesthesia was induced by an intravenous injection of Suritol® (sodium thiamylal, Parke-Davis), and continued with Methophane® (Metoxyflurane:2,2-dichloro-1,1-difluroethyl-Methyl ether, Pittman-Moore).

The dogs were positioned in dorsal decubitus, with the hind limbs stretched. A PE50 catheter, measuring 50 cm., was introduced in the lateral or medial saphenic vein and pushed up six to nine inches, in such a manner that the end of the catheter would be localized in the iliacal vein, outside of the field of the vein detector over the inferior caval vein.

The tip of a 22 gauge needle was percutaneously introduced in the femoral artery, and threaded as far as possible upstream. The needle was fed by another PE50, 50 cm. long catheter (Fig. 9). If adrenalin was infused, this was done through the jugular vein.

In almost all experiments the arterial blood pressure was measured through a needle in the heterolateral femoral artery.

The pressure measurement was used to ascertain the effects of adrenalin, when infused, and to determine the period of relative steady state. Besides that, the pressure reading, the cornea reflex and the color of the tongue were used as indicators of the depth of the anesthesia.

Fig. 9 Experimental setup

This figure shows the location of the two heavily collimated scintillation detectors (3,4), the two venous catheters, one (6) used for the venous injections of both tracers, one (2) for the adrenalin infusion. The intraarterial needle (5) is threaded upstream in the femoral artery.

During the whole procedure the animal breathes through an endotracheal tube, but when Xenon is injected, the exhaled gases are pumped out of the room. Otherwise the dog breathes in a closed system with CO_2 absorption and O_2 supply from a gas cylinder (1).

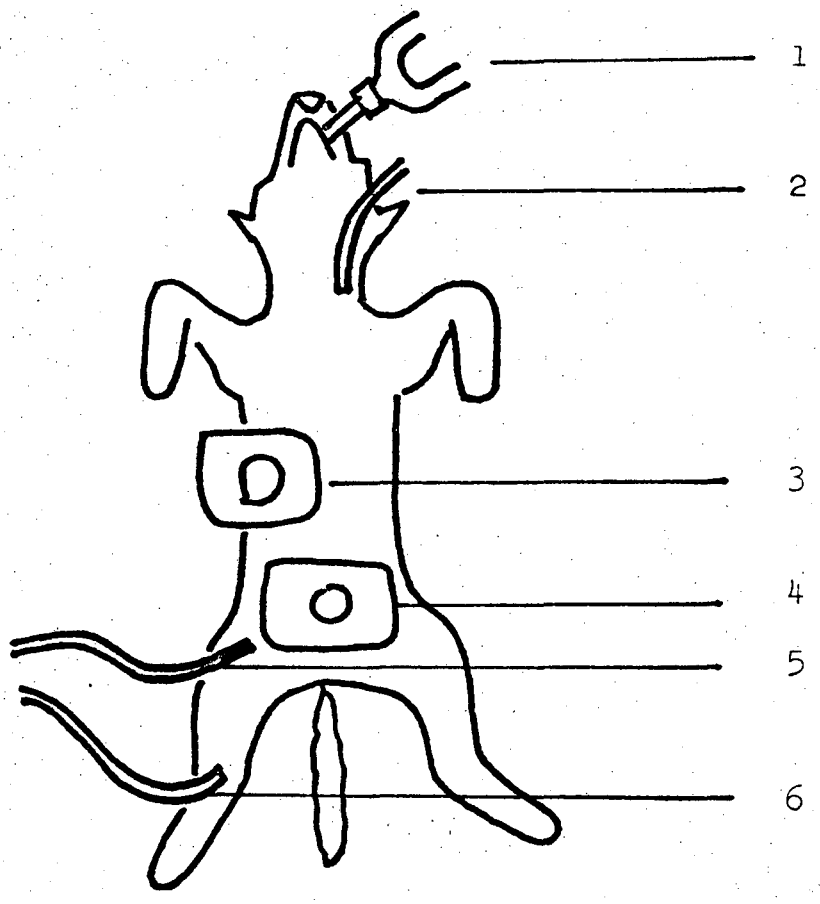

Figure 9

Two well-collimated sodium iodide crystals are positioned over the dog, the first one on the limit between the distal third and middle third on the line between the xyphoid processus and the symphysis pubica, the second one so that its field comprehends the basis of the right lung and the dome of the liver (Fig. 9).

Each detector is connected to two single channel analyzers, bringing the total of channels to four (Fig. 10). The pulses in each channel are subsequently collected and stored in a PDP-12 computer.

The timing of the injections, performed by an injection pump which injects and withdraws, was controlled by the same computer. We chose not to flush the catheter by injecting a supplementary volume, since the perturbation provoked by the fast infusion of large volumes would not be insignificant. However, if some activity remains in the catheter, diffusion or leaking may occur, which would render the shape of the injection function unpredictable, or at least invalidate the assumption that the injection of the tracer was a delta function injection. Flushing the catheter was therefore performed by withdrawing a volume of blood equal to the injected volume of tracer. The injection volume is between 0.25 and 0.35 cc in all experiments, but does not vary in any experiment. Injection time + withdrawal was less than 1 sec.

During the experiment the dog's temperature (esophagal) was maintained at 37°C with heating cushions.

For the non-diffusable tracer ^{99m}Tc-labelled sulfur colloid (Testuloid^{R}, Squibb) was used, and for the diffusable tracer ^{133}Xenon, in saline. The activity injected was respectively 200 μCi of ^{99m}Tc and 300 μCi of Xenon.

In a typical run there were 4 injections:

1. Xenon intravenous
2. Xenon intraarterial
3. Colloid intravenous
4. Colloid intraarterial

If the experiment was followed by a repeat during adrenalin infusion the sequence was:

1. Xenon intravenous
2. Colloid intravenous
3. Xenon + Colloid intraarterial

start adrenalin infusion

1. Xenon + Colloid intraarterial
2. Xenon + Colloid intravenous

Section 2. Data Collecting

The PDP-12 computer was programmed so that it could receive data from 1 to 8 channels, but in this set of experiments we consistently used four (Fig. 10).

Before the start of the experiment, the time length for each data point, the time of day, and the time of injection were fed into the computer. As the experiments proceeded, the time of integration could be changed, the range being from 0.20 sec to 1 minute.

Fig. 10 Schematic representation of the data collection system

The pulses coming from the sodium iodide scintillation detectors (D1, D2) are analyzed for pulse height and selected by two single channel analyzers (AN1, AN2, AN3, AN4) for each detector, and sent to a scaling unit (SC) in the PDP-12 computer, where they are collected in preset time in double precision mode.

When the integration time is over, depending on a programmed variable instruction, the recorded counts are scaled down by a factor 2^n, and sent to the central core memory. From there they are displayed in real time as count rates on the cathode ray tube (CRT) display.

At the end of the run, the data stored in core are written into a magnetic tape (MG TAPE), as are the times of integration of all data points.

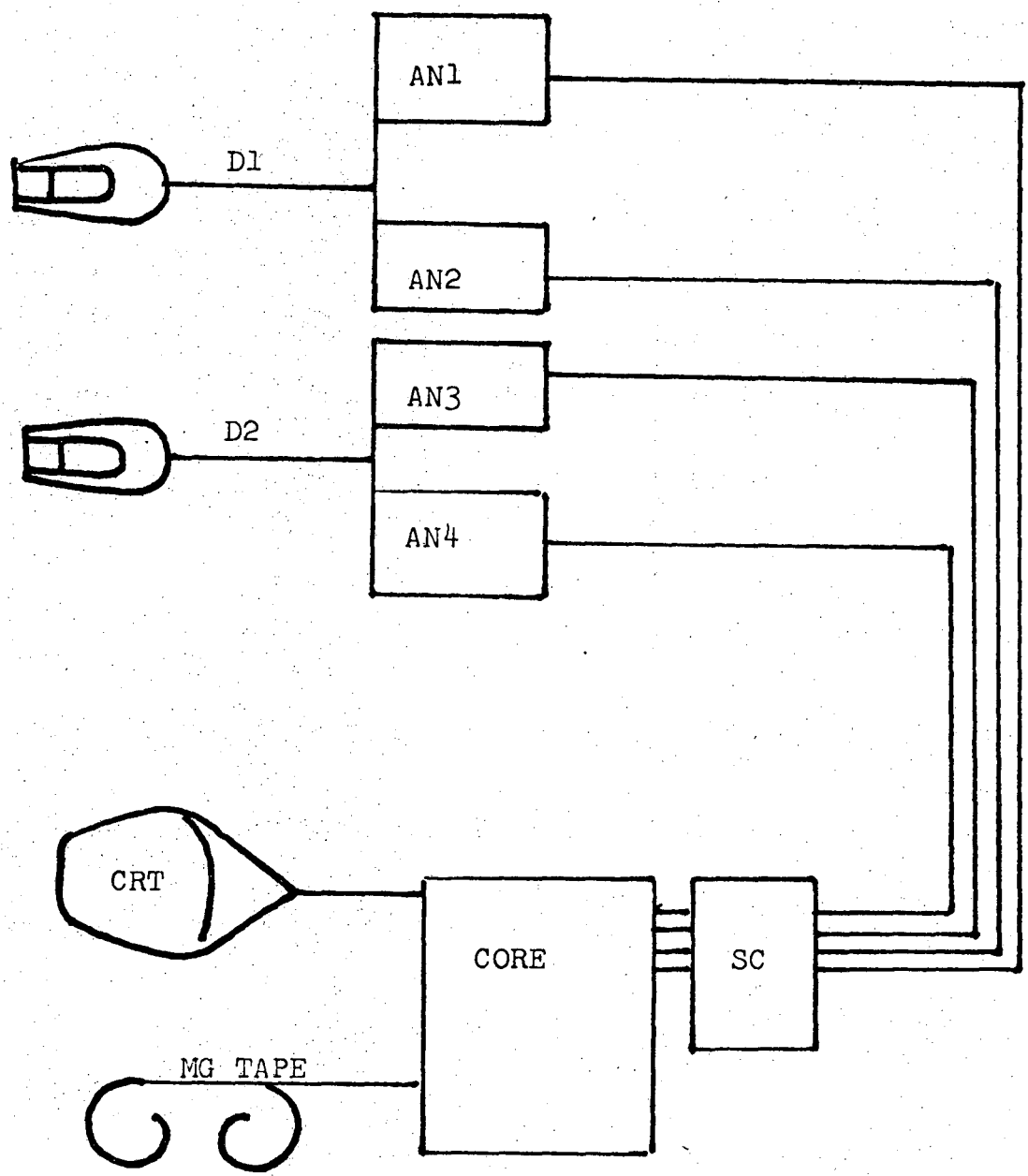

Figure 10

The count rate in each channel was followed on an oscilloscope screen, where the time function of the four channels could also be displayed.

When the experiment ended, the collected data were transferred to a magnetic tape, which was then used for all subsequent data handling.

At the start of each new experiment the memory was cleared automatically. Identification of the experiments was obtained by run number, a value which also defined the location of the data on the final tape.

Section 3. Data Handling

1. Smoothing and Cross-talk Correction

Smoothing, or regrouping of the data is made necessary because of the time factor in the final curve-fitting program. Least-square subsequent approximation programs tend to be long in themselves, and an unnecessarily large number of data points becomes very expensive. The smoothing program, devised by C. T. Schmidt (see appendix), is performed on the PDP computer itself, as is the cross-talk correction. The principle is simple. Data points are pooled until one of the following situations arises: (1) a preset time of integration limit is reached; (2) a preset integrated count limit is reached; (3) the next data point represents a count rate which differs by more than two standard deviations from the count rate of the integrated interval up to that point. At that moment, a new pool is started. When defining the

preset time and counts, care must be taken not to "smooth out" the functional form of the time function, especially if "peaks" are present.

In our method, cross-talk, which is the influence from one isotope on the count rate detected in the channel for the other isotope, or from one isotope in one location on the count rate detected in another location, has a unique feature.

Indeed, although the gamma rays from ^{133}Xenon have low energy, and do not interfere with the detection of the higher energy gamma photons from ^{99m}Tc, the redistribution of Tc-colloid, from the vein, at the start of the experiment, to the liver at the end, is bothersome.

Indeed, as shown in Fig. 11, the cross talk factor (channel cross talk) from ^{99m}Tc in the lower energy ^{133}Xenon channel is time dependent. The injection bolus, seen in the figure as the early sharp peak, is localized entirely in the vein, well in the field of the detector, so that the Compton scattered rays do not in general reach the detector. For this first peak, the channel cross talk is small. However, as more of the tracer is accumulated in the liver, outside of the detector's view, the direct interactions with the crystal are relatively rarer than the interactions after scattering. Hence, the channel cross talk factor seems to be higher, but is in fact a combination of channel and location cross talk.

Furthermore, although the collimation tends to minimize

Fig. 11 Effect of the redistribution of ^{99m}Tc colloid from vein to liver on the cross talk in the Xenon channel of the vein detector.

The full line is the count rate detected in the ^{99m}Tc channel of the vein detector. The first steep peak is due to the passage of the injection bolus. The second part of the curve is tissue clearance.

The dashed line is the count rate detected in the $^{133}Xenon$ channel of the same detector. While the injection bolus, well centered in the field of the detector, gives only minimal cross talk, as the time goes on the influence of liver accumulation is felt.

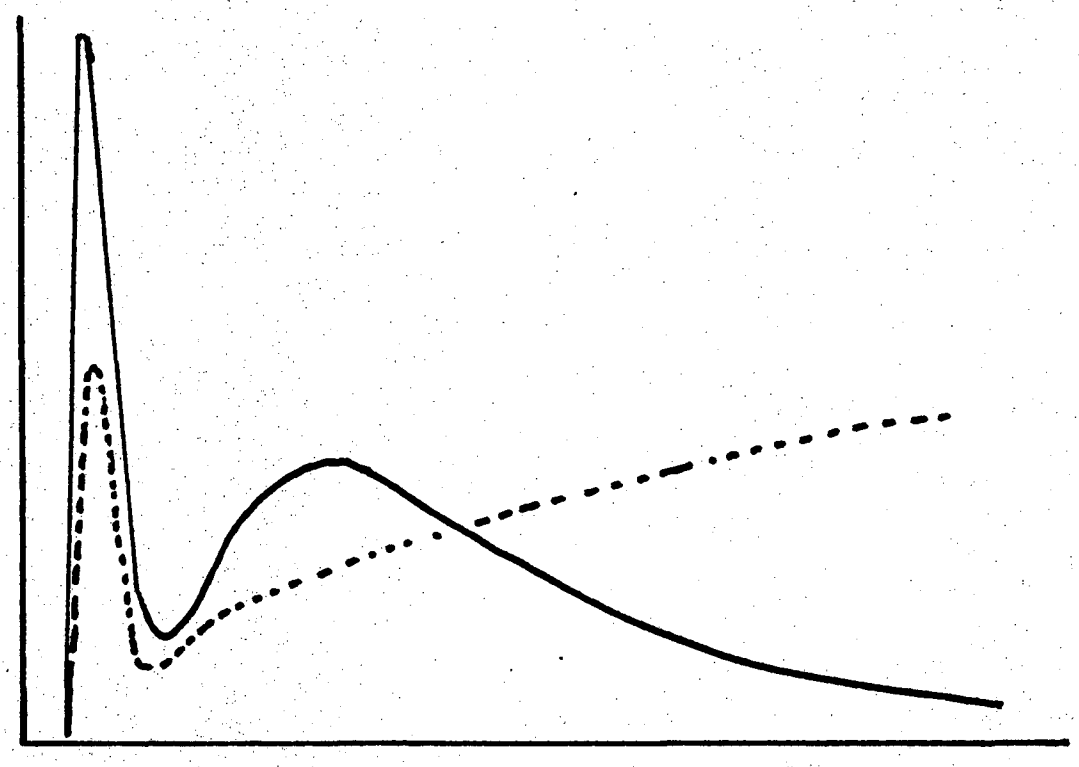

Figure 11

this effect, during recirculation the "vein detector" detects activity from within its direct field, which is not however localized in the vein, but in the surrounding tissues. This problem can be minimized, and when cross talk corrections were used, we did not take this into account.

Since, as we will see, there is no important recirculation factor for Xenon it would have been better had the Xenon had the higher energy. We have considered the problem, and in subsequent applications we will use $^{11}CH_4$ gas instead of Xenon. The counting efficiency for this positron-emitting isotope is expected to be better, and furthermore, since the Technetium colloid remains in the liver, as more injections are made, the higher ^{99m}Tc energy increases the background for Xenon to interfering levels.

Since our project was directed to solve a model and find appropriate data handling methods, in most cases when possible, we did subsequent injections of single isotopes, in such an order that the interference of Technetium was minimized.

When the two isotopes were injected simultaneously the following cross talk factors were used. Let Xij,kl be the cross talk from an isotope counted in channel j, situated in the field of detector i, affecting the count rate in channel l from detector k.

To situate the matter:

i or k are 1: detector over vein

2: detector over liver

j or l are 1: Xenon energy channel

2: Technetium energy channel

It is obvious that

$$X_{ij,ij} = 1$$

Furthermore, since ^{133}Xenon has the lower energy photons

$$X_{il,k2} = 0$$

A venous injection of Tc colloid at the first peak (Fig. 7) in channel 2 of detector 1 yields

$X_{12,11}$

$X_{12,21}$

$X_{12,22}$

While the value of channel 2 of detector 2 at the end of the experiment yields

$X_{22,11}$

$X_{22,12}$

$X_{22,21}$

The corresponding factors for Xenon are found with a single intravenous injection of Xenon. The final matrix is therefore

$$\begin{pmatrix} 1 & X_{12,11} & X_{21,11} & X_{22,11} \\ 0 & 1 & 0 & X_{22,12} \\ X_{11,21} & X_{12,21} & 1 & X_{22,21} \\ 0 & X_{12,22} & 0 & 1 \end{pmatrix}$$

so that, if (C) is the vector of the true counts in each channel and (O) the vector of the observed counts

$$(X)\ (C) = (O) \qquad (3.1)$$

A small program in the PDP library allows us to find the in-

verse of (X), or $(X)^{-1}$, after which this matrix is applied to the counts collected in each subsequent injection of mixed tracers (see appendix).

$$(X)^{-1}(O) = (C) \qquad (3.2)$$

2. Curve fitting

The curves were fitted to the functions described below by using Bremermann and Lam's (1970) optimization program. The only change made in their program was to make the steps proportional to the parameter value, and not absolute.

In what follows we will discuss the techniques used.

(a) Fitting of the venous curves: determination of the recirculation parameters.

We assume the injection to be a delta function injection. However, empirically we found that the time function, although nearly discontinuous at time zero, as expected, subsequently follows an exponential decrease. The vein, immediately distal of the detector, seems to act as a first order compartment. Furthermore, we assumed the central circulation time to provoke a simple time delay t_o between the injection and the appearance of recirculation. For both colloid and gas the recirculation compartment was assumed to be made up of two parallel first order compartments (Fig.12).

The functional form assumed for the observed data depends of course on where in the model the detector is placed.

For theoretical reasons it is easier to assume that the detected function represents the output function of the gen-

Fig. 12 Model of the venous injection curve

The tracer is injected in a small compartment V, with rapid turnover (fractional turnover rate k), from where it is distributed between two compartments in parallel, respectively f_1' to compartment 1, f_2' to compartment 2, but with a time delay t_o.

Those two compartments have a fractional turnover rate of respectively V_1 and V_2. The detector "sees" the output of V and of compartments 1 and 2 (shaded region), hence the detector "sees".

$$kV + v_1 q_1 + v_2 q_2$$

if the counting efficiency is the same for all the output functions.

In reality this is not so, while the detector really sees kV and a fraction of q_1, and a fraction of q_2. For those reasons the parameters f_1' and f_2' are replaced by f_1 and f_2 in the fitting function.

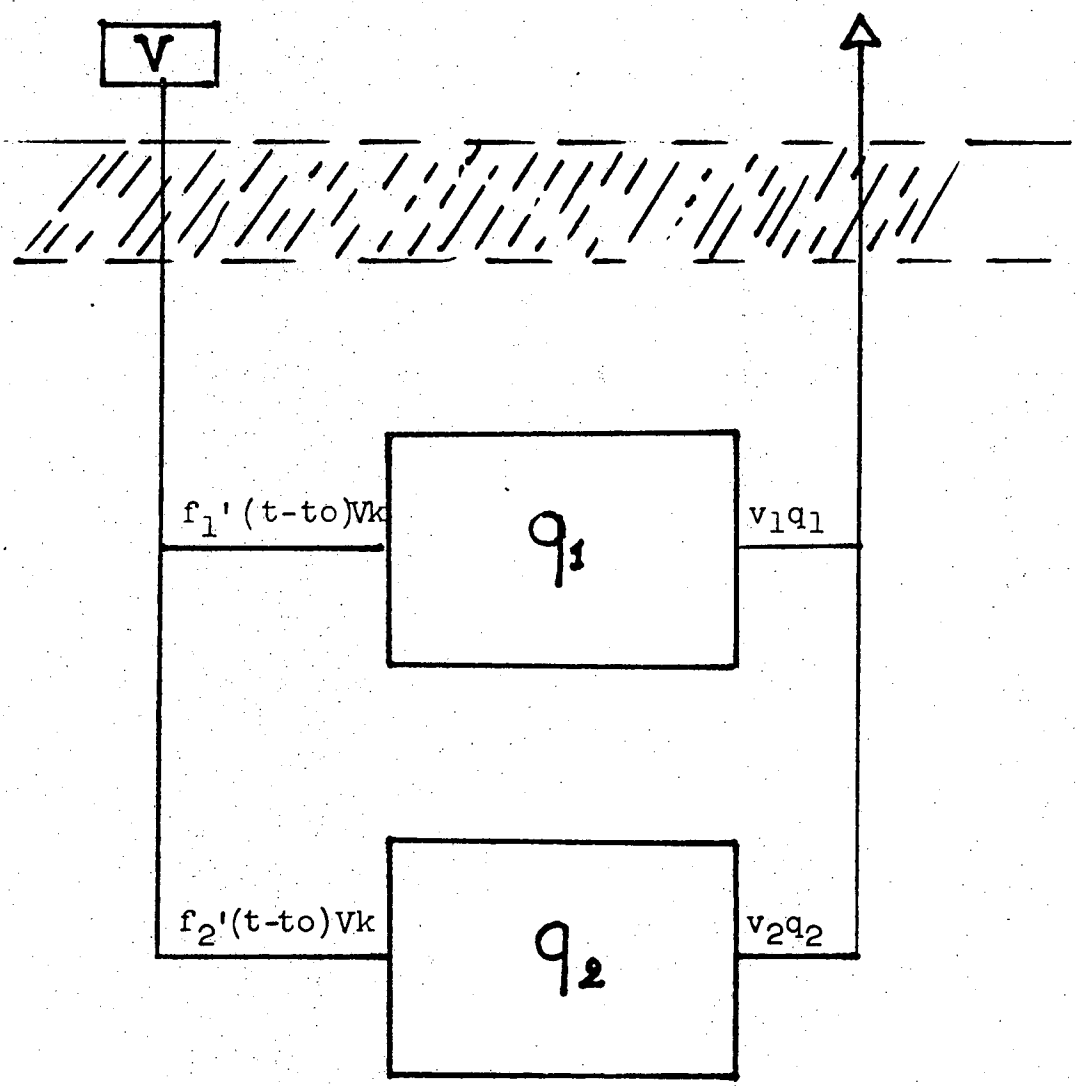

Figure 12

eral circulation compartments, added on the output function of the small, rapid-turnover, venous injection compartment. In reality, however, one detects a fraction of the two general circulation compartments, but since they do follow a first order process, if the activity present is

$$q_i(t) = e^{-v_i t}$$

the output function is

$$\dot{q}_i(t) = v_i e^{-v_i t}$$

Hence if the data follow a function

$$q_i(t) = ke^{-kt} * f_i' e^{-v_i t}$$

one can fit as

$$q_i'(t) = ke^{-kt} * f_i . v_i e^{-v_i t}$$

The model assumed for the data fitting is shown in Fig. 12. The observed function is therefore

$$A(ke^{-kt} + lag(t-t_o)ke^{-k(t-t_o)} * \Sigma f_i v_i e^{-v_i(t-t_o)} \qquad (3.3)$$

where

$$lag(t-t_o) = \frac{\exp[100(t-t_o)/t]}{1 - \exp[100(t-t_o)/t]} \qquad (3.4)$$

$t = t_o$, where t_o is the central circulation time

k is the turnover in the small venous compartment

v_1 and v_2 are the two central compartments

f_1 and f_2 are the scaling factors for each of them

It appears that since k is large relative to the integration intervals, and because there is some imprecision about the precise time $t = 0$, that f_1 and f_2 may be off by some factor.

Also, since f_2 is small, the definition of v_2 is very background-dependent. Those two factors will be taken into account later. The parameters to fit are A, k, v_1, v_2, f_1, f_2, and t_o (see appendix).

(b) The arterial data: recirculation correction

If the density function of transit times is n(t), the detected function is

$$B\left[n(t) + C\ \mathrm{lag}(t-t_o)\ n(t-t_o) * \Sigma v_i f_i e^{-v_i(t-t_o)}\right] \qquad (3.5)$$

where C is a correction factor introduced to account for the error in f_1 and f_2.

Note that the function ke^{-kt} does not appear in this expression, since it is supposed to be specific for a local process arising with a rapid intravenous injection. The underlying assumption is that in the artery there is no initial deformation of the injection function.

C is relatively easy to determine for the colloid, since after 6 minutes all activity detected is recirculation activity. Indeed, blood drop experiments indicate n(t) to be near zero after a very short time.

It would have been ideal to be able to fit the data immediately to the final analytical expression expected of n(t)

$$n(t) = \sum_{1}^{3} A_i(e^{-a_i t} - e^{-b_i t})$$

however, no good fit could be obtained that way. But at this point the only concern is to find n(t) without

$n(t)*\Sigma v_i f_i \exp(v_i t)$ interfering.

We found that it is easier to fit

$$Qn(t) = \sum_{1}^{9} B_i(t-L_i)e^{-b_i t} + \sum_{10}^{18} B_i te^{-b_i t} \qquad (3.6$$

Q is of course the normalization factor dependent on the injected amount and the counting efficiency, and is reflected in the B_i's.

L_i is defined as

$$L_i = (b_i\ t_M - 1)/b_i \qquad (3.7)$$

where t_M is the time at which the detected function reaches its maximum value. Introducing L_i allows the first nine terms to have their maximum value at t_M, independently of their slope.

This type of fitting function could of course correspond to a specific compartmental model. Indeed, the function

$$k^2te^{-kt}$$

is specific for two compartments in series with the same fractional turnover rate k, since

$$\int_o^t ke^{-k(t-\tau)}ke^{-k\tau}d\tau = k^2\ e^{-kt}.t$$

However, we used the expression for n(t) simply as a smoothing function for the exclusive purpose of finding an analytical expression for the recirculation term in Eq.(3.5).

$$C \text{ lag } (t-t_o)n(t-t_o)*\Sigma v_i f_i\ e^{-v_i(t-t_o)}$$

The main feature of the fitting function we use, besides its smoothness and continuity is the fact that for the

first nine terms the term $(t-L_i)$ will prevent oscillations,* while for the last nine terms oscillations are unlikely to appear if the b_i's are evenly distributed, with decreasing B_i values when b_i decreases.

This indeed appeared to give satisfactory results. The steep ascending part of the detected function is generally well fitted, as is the abrupt change in the first derivative at t_M.

There are more parameters than strictly needed, and the system appears to lack a unique solution: In general at the end of a satisfactory fitting some values of B_i are so small, that in fact some of the terms are not used to fit the function. However, since the fit seems to be satisfactory, and since further analysis is not based on those fitting parameters, we did not feel that this was an argument against the method. (see Appendix A)

Indeed, once n(t) has been determined as in Eq.(3.6) we determined from this function different data points at different times. On those data points the final analysis was performed.

*A sum of exponentials $\Sigma A_i e^{-a_i t}$ can oscillate if the A_i terms are allowed to be negative. The derivative of the sum of exponentials $\Sigma a_i A_i t\, e^{-a_i t}$, if $A_i \geq 0$ will oscillate if there is a term j reaching its maximum at time $t_j = 1/a_j$ when $a_j A_j t\, e^{-a_j t_j} \gg a_i A_i t\, e^{-a_i t_j}$ for all $i \neq j$.

For d(t) the same method is used, but for the fact that C is simply transposed from the preceding, since d(t) does not reach near zero values very soon.

Correction factors, held between 1.25 and 0.75 are allowed to operate as fitting parameters on v_1 and v_2 in the fit on the data from the colloid injection. During the fit on the Xenon data both are held at the value 1.0.

The main point of this section is that since the analytical expression used to "deconvolute" is in no way related to the model, the method amounts to a smoothing of the data, before the deconvolution. The difference with the numerical methods, which can also be carried out after smoothing, lies in the fact that in our case the functional form used does not yield oscillations in the tail of the deconvoluted function.

3. Analysis on h(t): Bypass and Tissue Perfusion Estimation

As mentioned before, we found the data points derived from n(t) to be well fitted by

$$\sum_{1}^{3} A_i(e^{-a_i t} - e^{-b_i t})$$

Using Bremermann and Lam's optimization program, adapted in F, we first fit the parameters to n(t). Subsequently, during the same run, after 100 to 150 iterations, d(t) is fitted using:

$$d(t) = \sum_{1}^{3} A_i\gamma_i(e^{-a_i t} - e^{-b_i t}) + \sum_{4}^{6} A_i(e^{-a_i t} - e^{-b_i t})$$

with the restriction that $0 \leq \gamma_i \leq 1$ for all i

and that

$$\int_0^\infty d(t)\, dt = 1$$

During the first subsequent 100 to 150 iterations A_i, a_i, b_i are kept constant for i = 1,3. Following this, all parameters are allowed to vary without restriction, but for the normalization conditions, and n(t) and d(t) are fitted simultaneously.

4. Analysis of the fitted functions

In this study the main objective was to determine the bypass fraction of flow (α) and the tissue perfusion, which has been defined as being characterized by the function $d_2(t)$ and the mean transit time $\bar{t}_2 d$.

If the data are indeed well fitted by the functional forms

$$n(t) = \sum_{i=1}^{3} \gamma_i A_i \left[e^{-a_i t} - e^{-b_i t}\right] + \sum_{i=1}^{3} (1-\gamma_i) A_i \left[e^{-a_i t} - e^{-b_i t}\right]$$

$$d(t) = \sum_{i=1}^{3} \gamma_i A_i \left[e^{-a_i t} - e^{-b_i t}\right] + \sum_{i=4}^{6} A_i \left[e^{-a_i t} - e^{-b_i t}\right]$$

in such a way that the first term in each equation has been maximized, one can consider this first term as the best estimate of the bypass with this method.

Since (see Eq. 2.39)

$$(1-\alpha) n_1(t) = \sum_{i=1}^{3} \gamma_i A_i \left[e^{-a_i t} - e^{-b_i t}\right]$$

and

$$\int_o^\infty n_1(t)dt = 1$$

we have

$$\int_o^\infty \sum_{i=1}^{3} \gamma_i A_i \left[e^{-a_i t} - e^{-b_i t}\right] dt = (1-\alpha) \qquad (3.8)$$

or the bypass fraction.

The whole system is further characterized by the different transit times (Eq. 2.21, 2.22, 2.23). (see Appendix A)

There is a global mean transit time for the non-diffusable tracer

$$\bar{t}n = \int_o^\infty t\, n(t)\, dt$$

and a global one for the diffusable tracer

$$\bar{t}d = \int_o^\infty t\, d(t)\, dt.$$

However, when bypass is considered, one needs the mean transit time in the bypass circuit (or alternatively for the fraction of the diffusable tracer which does not diffuse).

$$\bar{t}_1 n = \int_o^\infty t n_1(t)dt = \frac{\int_o^\infty t. \sum_{i=1}^{3} \gamma_i A_i \left[e^{-a_i t} - e^{-b_i t}\right]}{\int_o^\infty \sum_{i=1}^{3} \gamma_i A_i \left[e^{-a_i t} - e^{-b_i t}\right]} \qquad (3.9)$$

Finally the tissue perfusion parameter is

$$\bar{t}_2 d = \int_o^\infty t d_2(t) dt = \frac{\int_o^\infty \sum_{i=4}^{6} t A_i \left[e^{-a_i t} e^{-b_i t} \right] dt}{\int_o^\infty \sum_{1=4}^{6} A_i \left[e^{-a_i t} - e^{-b_i t} \right] dt} \qquad (3.10)$$

which is the mean transit time for the fraction of the diffusable tracer which did diffuse (out of the vascular bed).

Because of the popularity and wide understanding of the strict compartmental approach to this problem we did also compute the mean transit time of each of the parallel series of compartments as shown in Fig. 8. We have therefore

$$\bar{t}_i = \frac{\int_o^\infty t . A_i \left[e^{-a_i t} - e^{-b_i t} \right] dt}{\int_o^\infty A_i \left[e^{-a_i t} - e^{-b_i t} \right] dt} \qquad (3.11)$$

CHAPTER IV. RESULTS AND DISCUSSION

Section 1. Smoothing and the recirculation correction

In Figures 13 a,b,c,d,e we show some of the fittings on the venous data. The first steep part of the curve is the component due to the injection, or the output function of compartment V in Fig. 12. It is fitted by

$$Qke^{-kt} \tag{4.1}$$

where Q is the normalization factor and k the fractional turnover rate of the injection compartment V. Obviously, since the injection itself takes a finite time (< 1 sec), some of the time seemingly spent in V is really injection time. However, since in all experiments k was larger than 30 min^{-1}, which is very large compared to the components found in the circulation system, for all practical purposes the injection function can indeed be considered as a delta function injection. This is even more so since during intraarterial injection one does not expect to have a small intermediary compartment at the injection site.

The rest of the curve is due to recirculation. The model and equations used were discussed previously (Eq. 3.3 and Fig. 12). Since background subtraction is so critical in the slope determination, and corrections are applied in the subsequent arterial fitting, we did not feel that better fitting (at large expense) was necessary.

The fitting of the empirical smoothing function (Eq. 3.6) and the recirculation correction application for intraarterial injection data was less easy. For the colloid the

Fig. 13 This set of graphs shows the data collected after intravenous injection over the inferior caval vein as crosses, and the line representing the fitted function, for some of the experiments. All are plotted in semilogarithmic scale.

Figures 13a, 13b and 13d are from the ^{99m}Technetium-colloid intravenous injections. Figures 13c and 13e are from the venous injection of ^{133}Xenon.

In all the graphs the first, steep component represents the output function of the injection compartment (represented as V in Fig. 12).

The slower components are due to the recirculation. Obviously the recirculation fraction is smaller for Xenon.

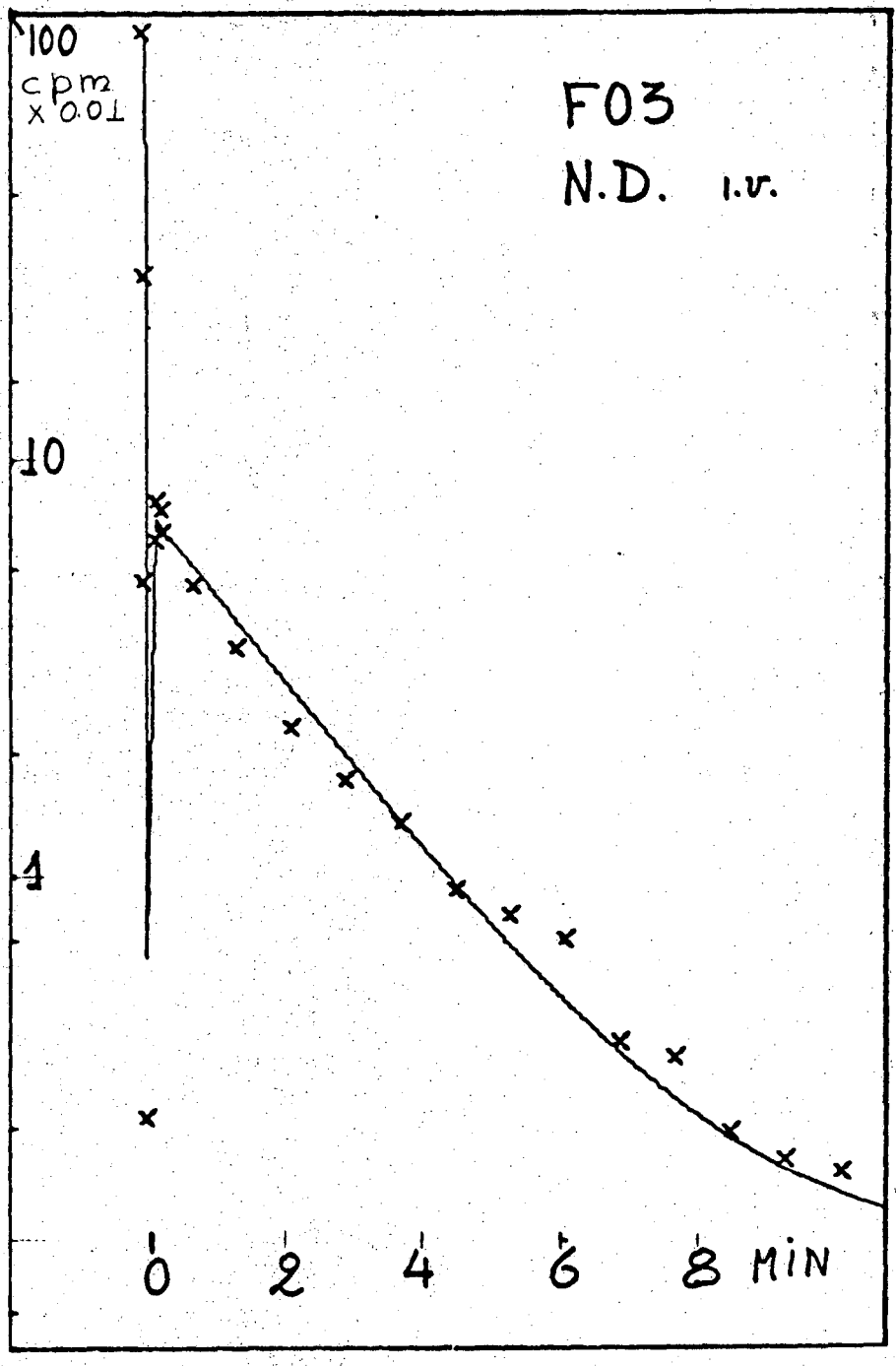

Figure 13a

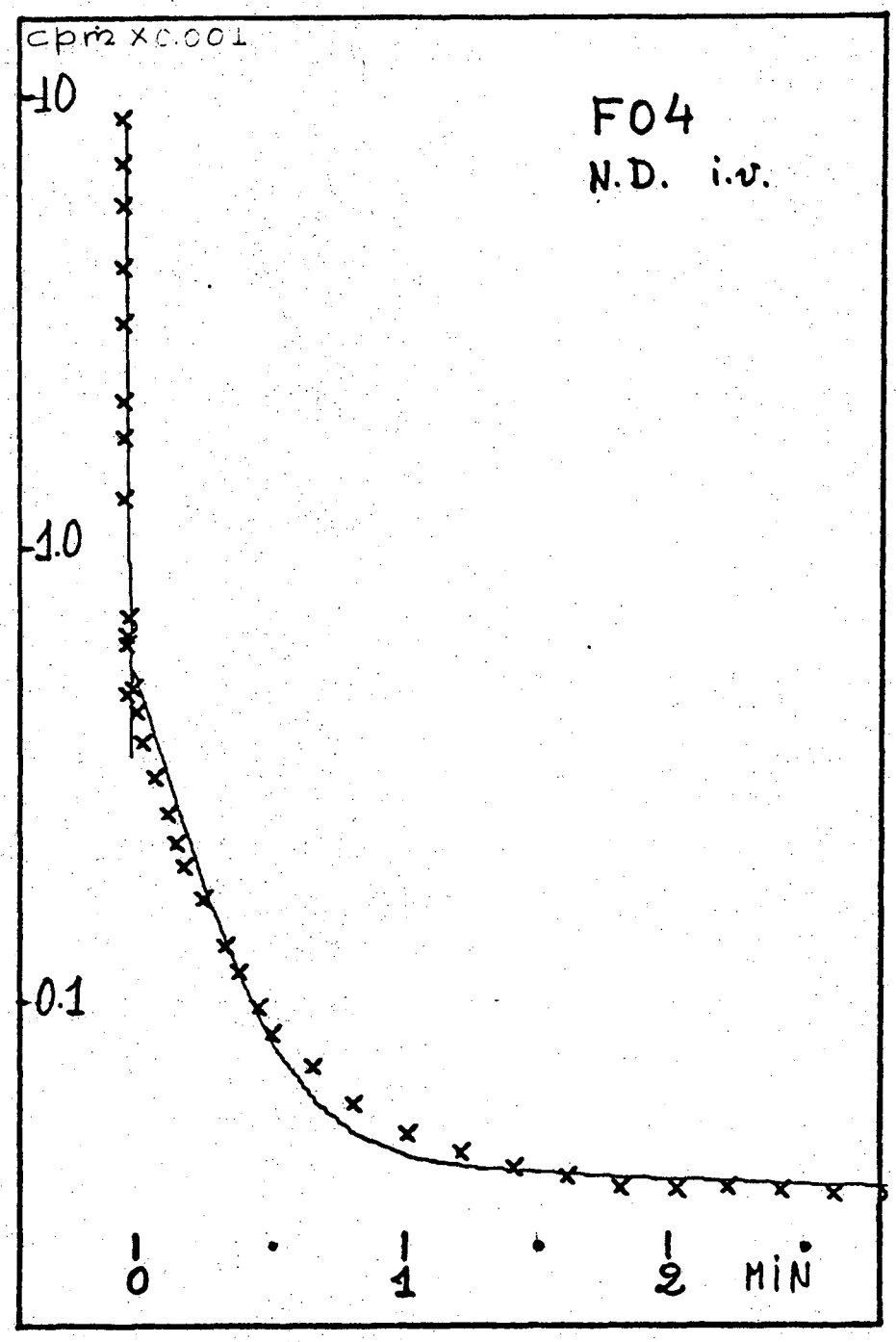

Figure 13b

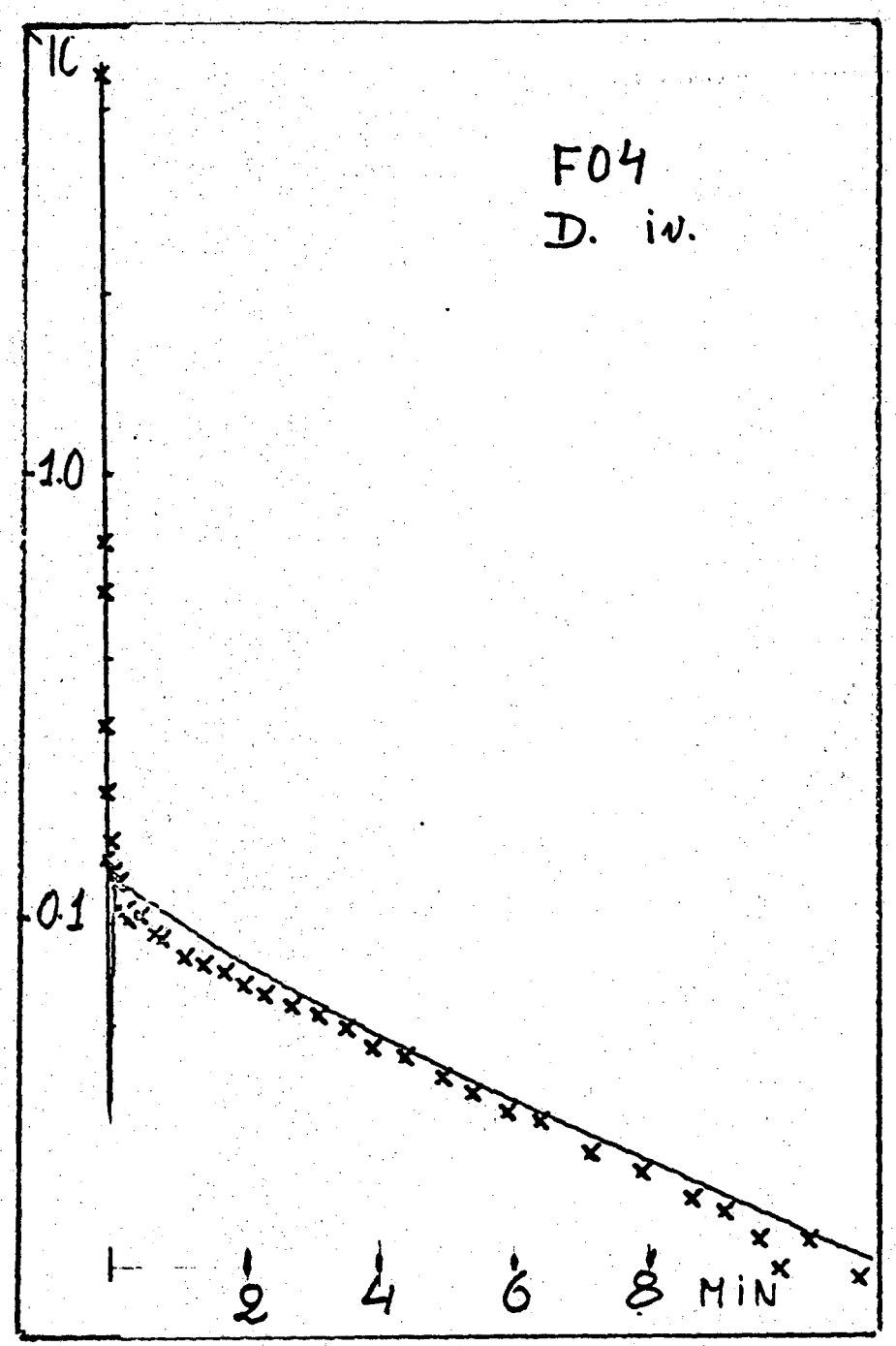

Figure 13c

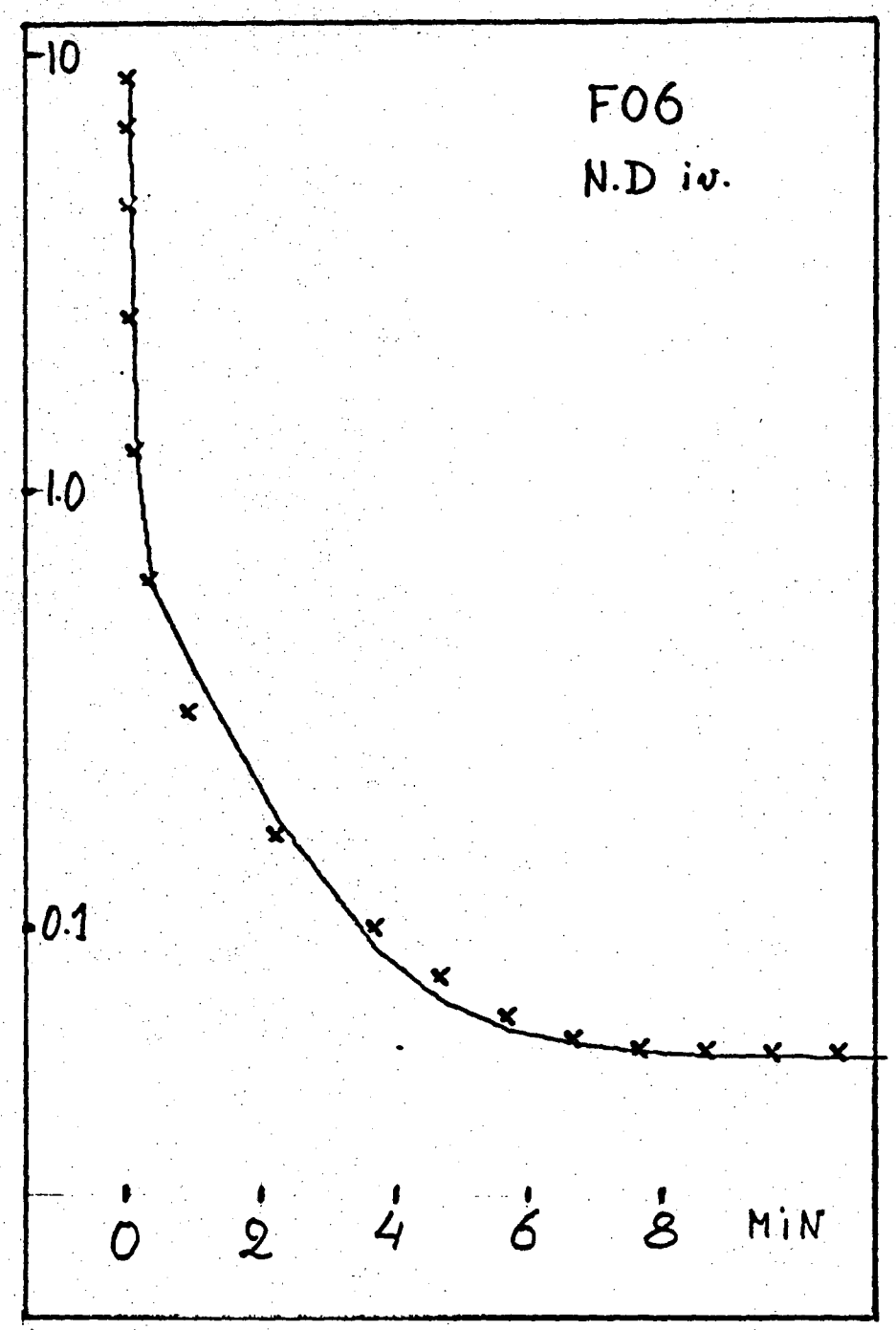

Figure 13d

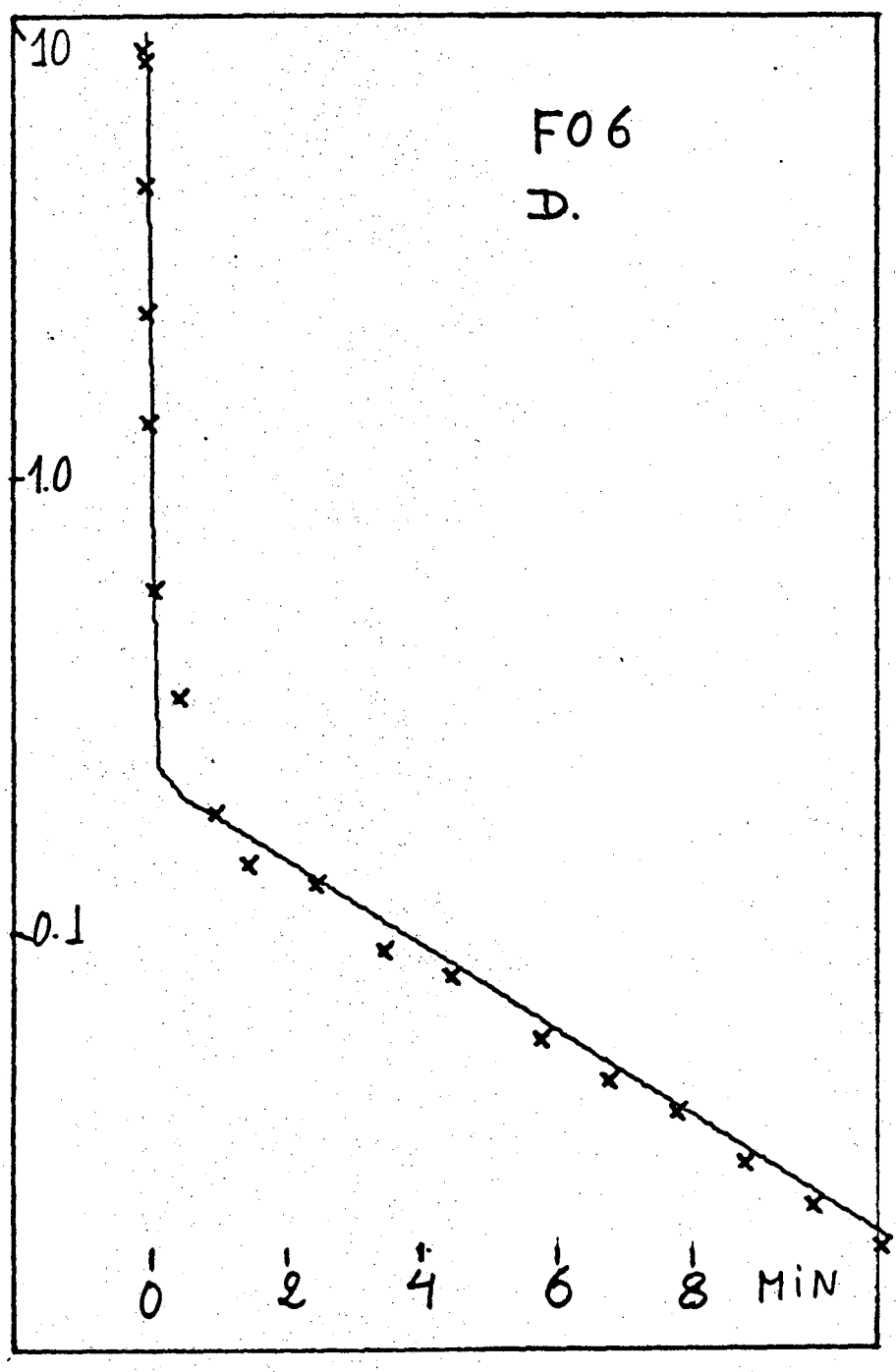

Figure 13e

recirculation becomes a major portion of the curve at a very early time (Figures 14a, 15a, 16a, 17a, 18a, 19a). The slope corrections, applied to the slopes determined during venous injections, combined with the scaling correction, are critical.

For Xenon the recirculation factor is smaller. The bulk of Xenon leaves the circulation after the first pass through the lungs (Figures 14b, 15b, 16b, 17b, 18b, 19b).

Since the smoothing function is related to the model only to the extent that it is a continuous positive function, it is not necessary to present the fitting parameters. However, it is interesting to note that the fitting function in this case had a relatively larger number of parameters, but that not all of them are always significantly used. Hence some of the

$$(A_i \; t \; a_i \; e^{-a_i t})$$

elements come out with such small A_i values that they were lost to the fitting.

The data points were fitted to

$$h(t) + h(t)*r(t) \qquad (4.1)$$

as explained in Chapter III. Once the best fit is found, using the smoothing function for h(t), expected count rates at different times are determined. Those expected count rates correspond to the count rate one would have detected in the absence of recirculation, and if the detection efficiency and the injected amount would have yielded

$$\int_0^\infty Fc(t)dt = 1$$

for all the experiments and both isotopes.

In other words, the data points so defined are corrected for recirculation, and normalized. We did already point out that the fitting function is empirical, and used exclusively for smoothing purposes, and to allow an analytical expression for the convolution of the recirculation function r(t) on the first pass function h(t). We also pointed out that the functional form used has a redundant number of parameters, and is not related to the model finally used. This very redundancy allows us, at the same time, to fit easily and to minimize the danger of model bias at this point.

The determination of data points from the smoothing function, after recirculation correction and normalization, corresponds in fact to what one would have done by smoothing first and then performing a numerical deconvolution. The analysis in terms of the model used can then be performed on those computed "corrected" data points.

Section 2. Analysis of the "corrected" data

We have at some length discussed in the previous chapters how different modalities could lead to the same functional form for n(t) and d(t).

The first point was that if n(t) can be fitted by a sum of exponentials, one need not necessarily feel committed to a compartmental model for the intravascular tracer. It is

Parker (Parker, Dobson, Hippensteele) who pointed out that a combination of different flows, tube diameters and tube lengths could lead to many forms for n(t), one of them possibly a sum of exponentials. The likelihood of this may seem remote. However, we did find consistently that the corrected data for n(t) could be fitted by

$$\sum_{i=1}^{3} A_i \left[e^{-a_i t} - e^{-b_i t} \right] \qquad (4.2)$$

In Figures 14c, 15c, 16c, 17c, 18c, 19c those data points are indicated as circles.

The strict compartmental model corresponding to this functional form has already been discussed. It is made of three sets in parallel of two compartments in series (Fig.8).

We have already pointed out what the main objection to a compartmental analysis for an intravascular tracer is: one cannot imagine good mixing - a compartmental assumption - in a restricted number of compartments, since the number of capillaries is extremely large, and have not many direct and "fast"* interconnections.

Besides the two modalities mentioned above we did consider a different interpretation. It relates to the concept of the extravascular compartments in series. If a large

*"fast" is used in the theoretical sense. To have good mixing one needs passage from one to another in a short time relative to the intracapillary turnover rate.

fraction of the time spent by the tracer in the system is actually spent in the large vessels (of which there are less) the compartmental concept may be less strained. The two compartments in series are easily imagined in this way.

We do not have of course direct evidence indicating which model does apply. But the good fitting to this restricted number of exponentials is consistent enough to be undeniable.

In Figures 14c, 15c, 16c, 17c, 18c, 19c, the corrected data for d(t) are represented as crosses. As explained before, the main point of the method is to fit as much as possible of d(t) by elements of n(t). We did this by maximizing the values of γ_i for which d(t) was well fitted by

$$d(t) = \sum_{i=1}^{3} \gamma_i A_i \left[e^{-a_i t} - e^{-b_i t} \right] + \sum_{i=4}^{6} A_i \left[e^{-a_i t} \; e^{-b_i t} \right] \qquad (4.3)$$

There is no conceptual difficulty in considering that the extravascular tracer is in fact distributed within a restricted number of compartments. In point of fact even this restricted number of terms for the "perfusion" term of d(t) which is:

$$d_2(t) = \sum_{i=4}^{6} A_i \left[e^{-a_i t} - e^{-b_i t} \right] \qquad (4.4)$$

are not all needed. (cf. Table II).

In the Figures 14c, 15c, 16c, 17c, 18c, 19c the line marked 1 represents the function n(t), which is the density function of transit times for the non-diffusable tracer.

The line marked 2 represents the global density function of transit times for the diffusable tracer (d(t)). Line 3 represents the density function of transit times which is common to both tracers ($n_1(t)$), or the density function of transit times in the bypass circuit. Finally, line 4 represents the density function of transit time which is exclusive for the diffusable tracer ($d_2(t)$), or the density function of transit times for the tissue perfusion proper.

The model implied here is of course that the three parallel networks of intravascular components are in connection with three common parallel sets of extravascular compartments.

Although one-to-one mapping from the model to anatomical concepts may be attractive, some caution should be used. What one detects as a fairly simple function may be a fortuitous combination of many undiscernable complicated functions. The test for the adequacy of the model should not be so much its anatomical correspondence, but its predictive value in functional determinations. However, the model should not be antithetic to every realistic anatomical consideration.

Thus, since the functional form used to analyze the "corrected" data introduces some implicit assumptions, in what follows we will try to show how they are not contradicted by generally accepted anatomical and physiological considerations.

The interpretation of the exponential fit for n(t) has

Legend to Figures 14, 15, 16, 17, 18, 19

The figures marked "numeral a" represent the data points (crosses) and fitting function (including the recirculation component) $Q(n(t) + n(t)*r(t))$ from the intraarterial ^{99m}Tc colloid injections. The lower line represents the recirculation component $Q(n(t)*r(t))$. The figures marked "numeral b" represent the same for the intraarterial ^{133}Xe-non injections. Note how the recirculation factor $Q(d(t)*r(t))$ is smaller, and sometimes not shown because it is off scale. The figures marked "numeral c" represent the "corrected" data points from n(t) as circles, and d(t) as crosses. Line 1 is the best fit for n(t) using the functional form corresponding to the model. Line 2 is d(t). Line 3 is the best fit for $(1-\alpha)n_1(t)$. Line 4 is the best fit for $\alpha d_2(t)$.

Figure 14a

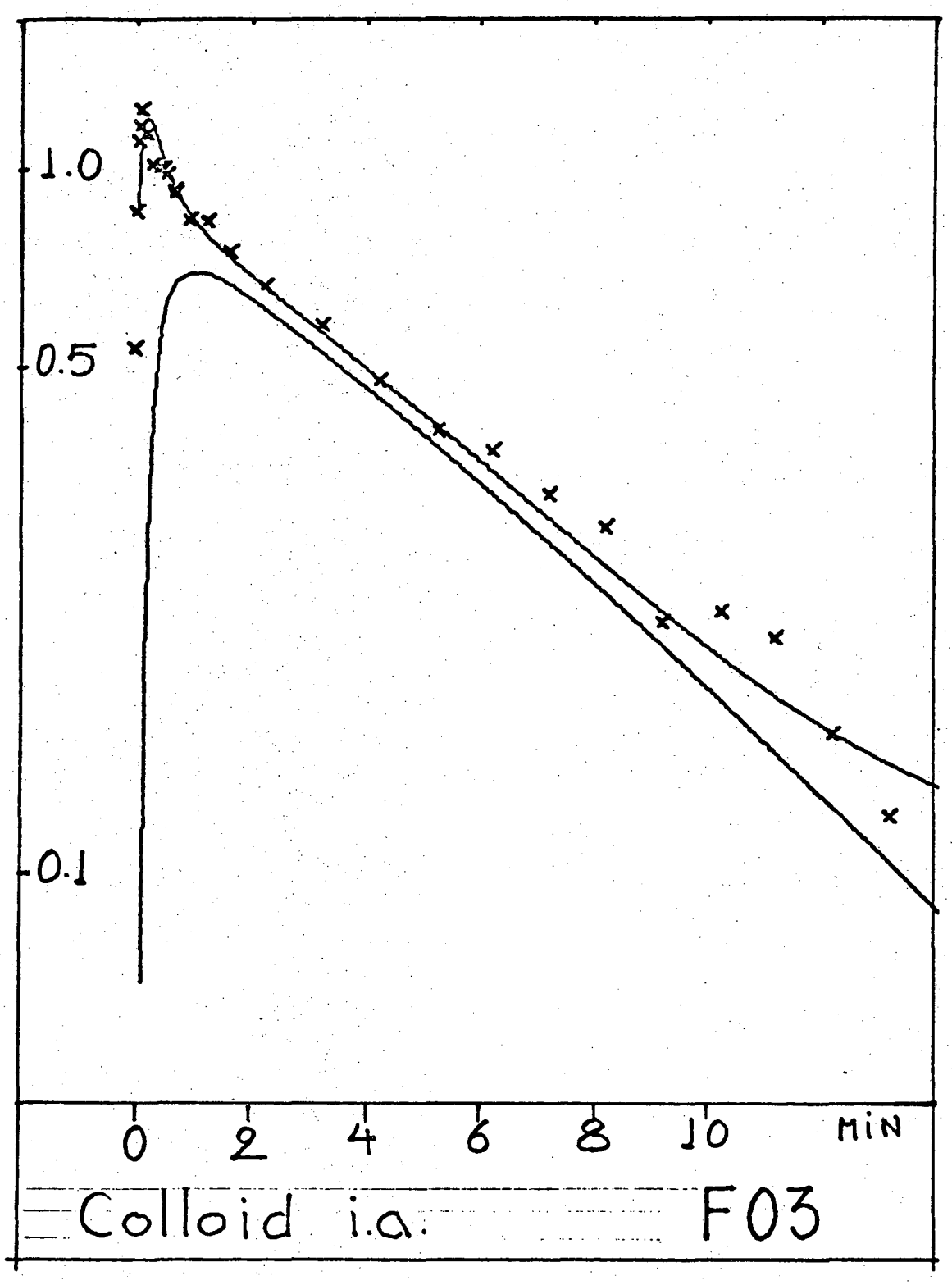

Figure 14b

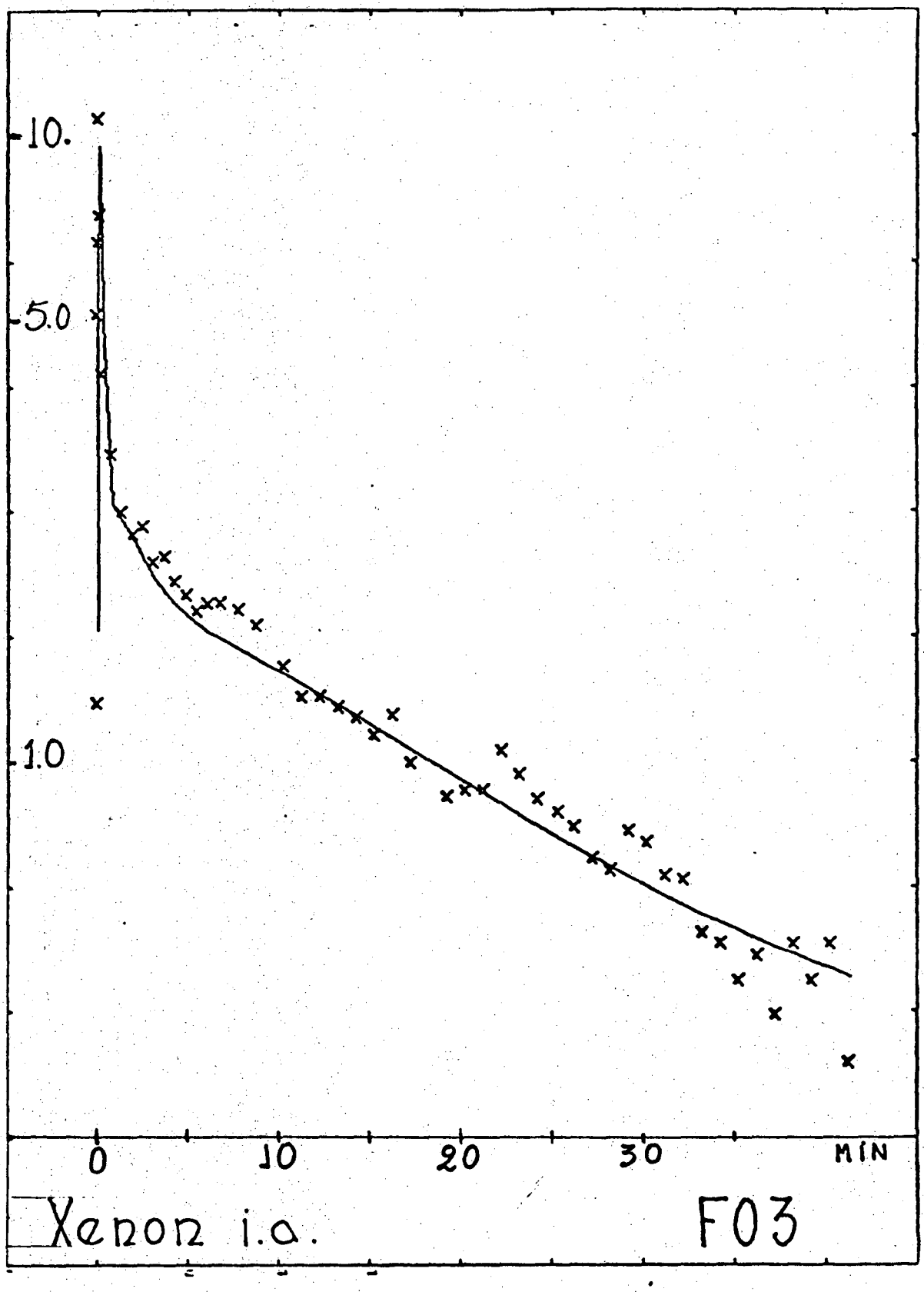

Figure 14c

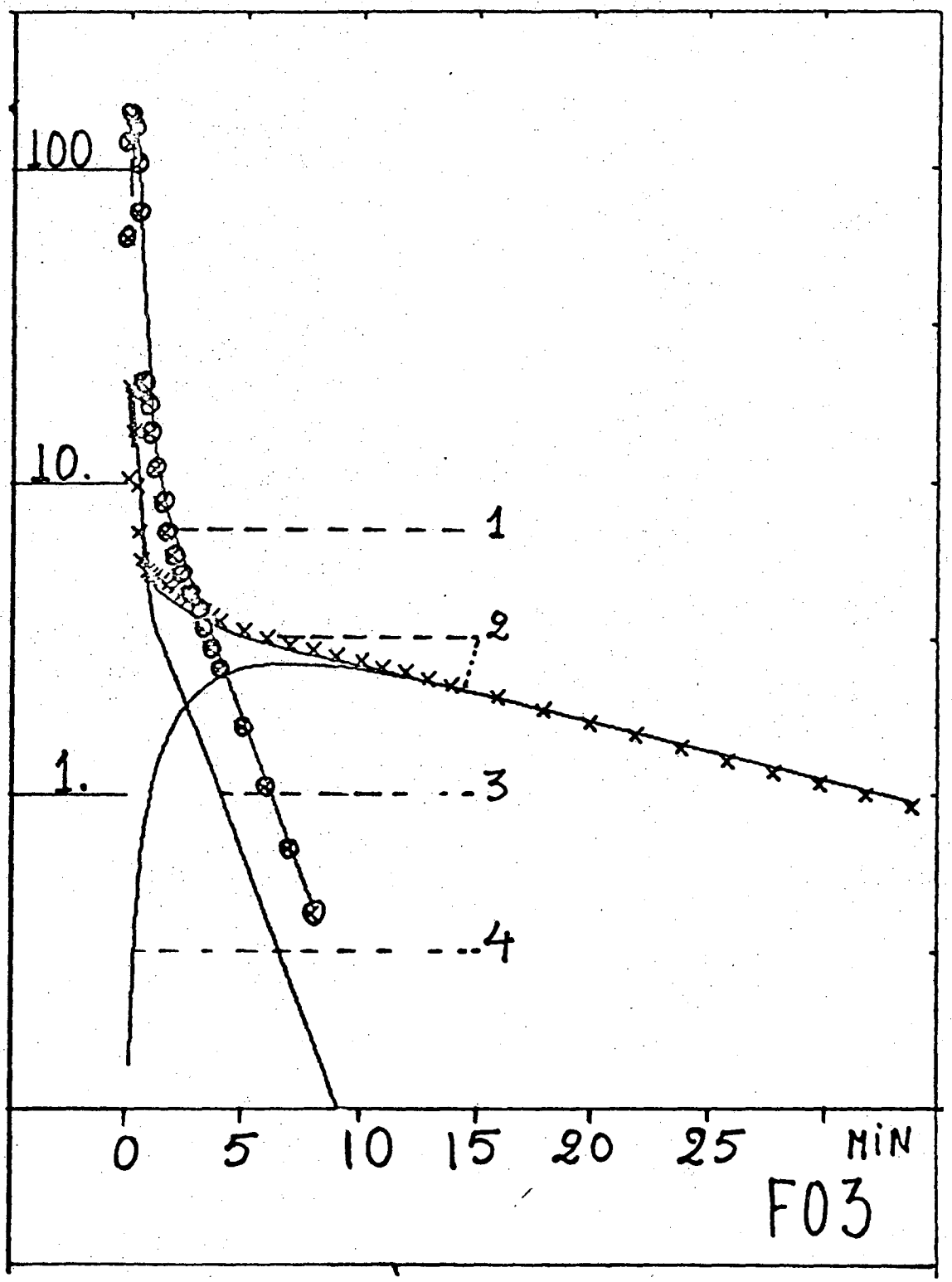

Figure 15a

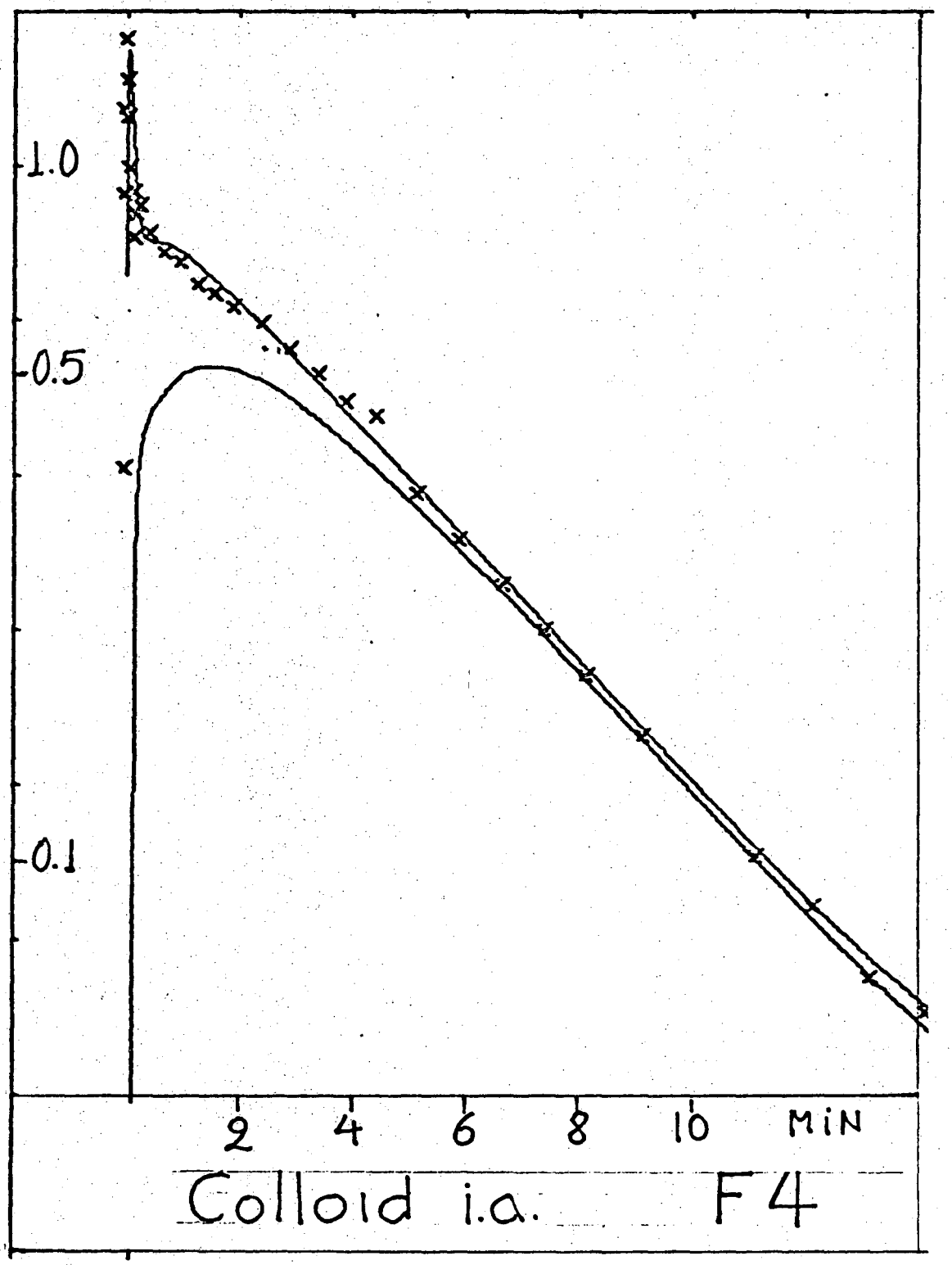

Figure 15b

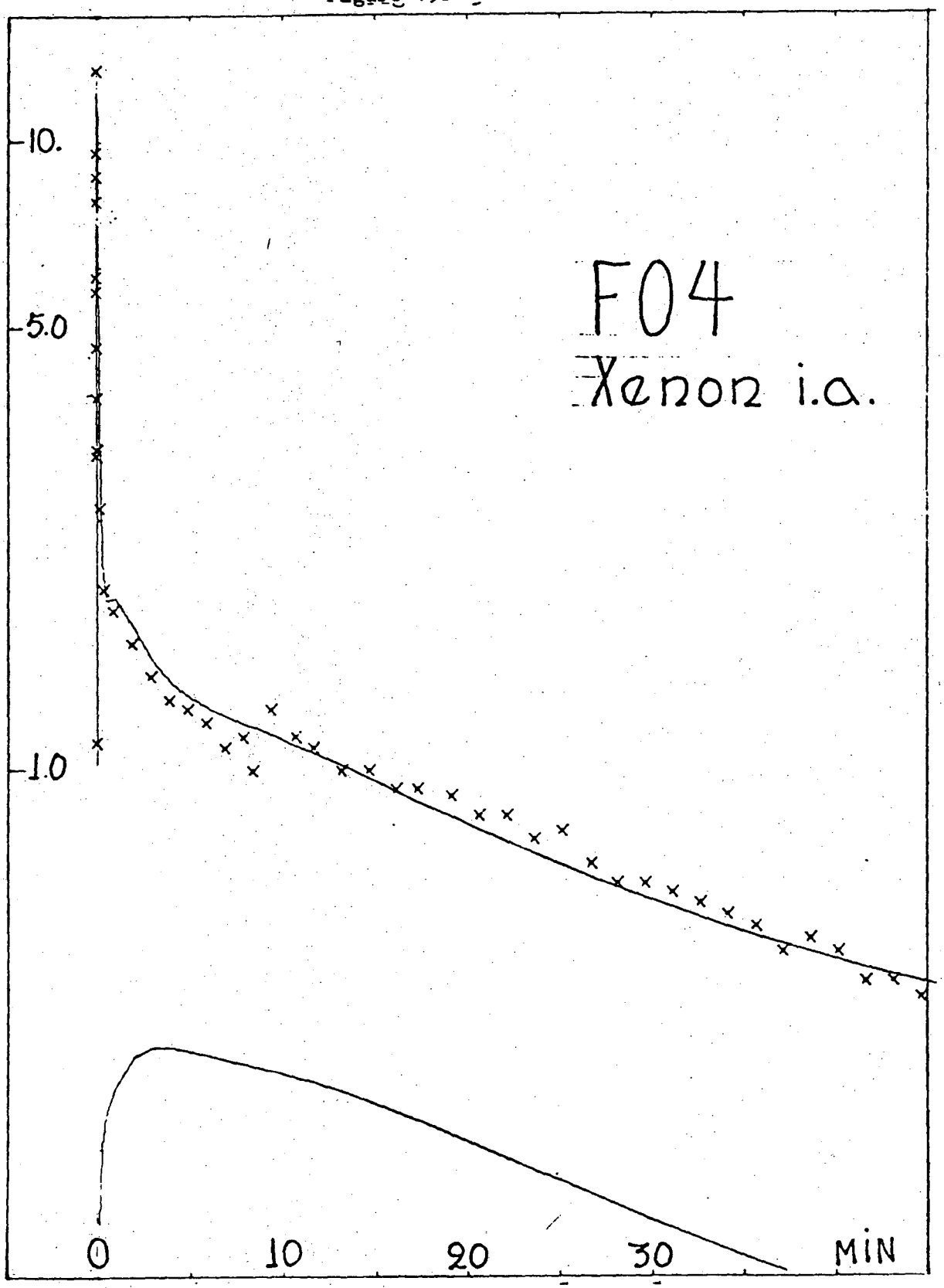

Figure 15c

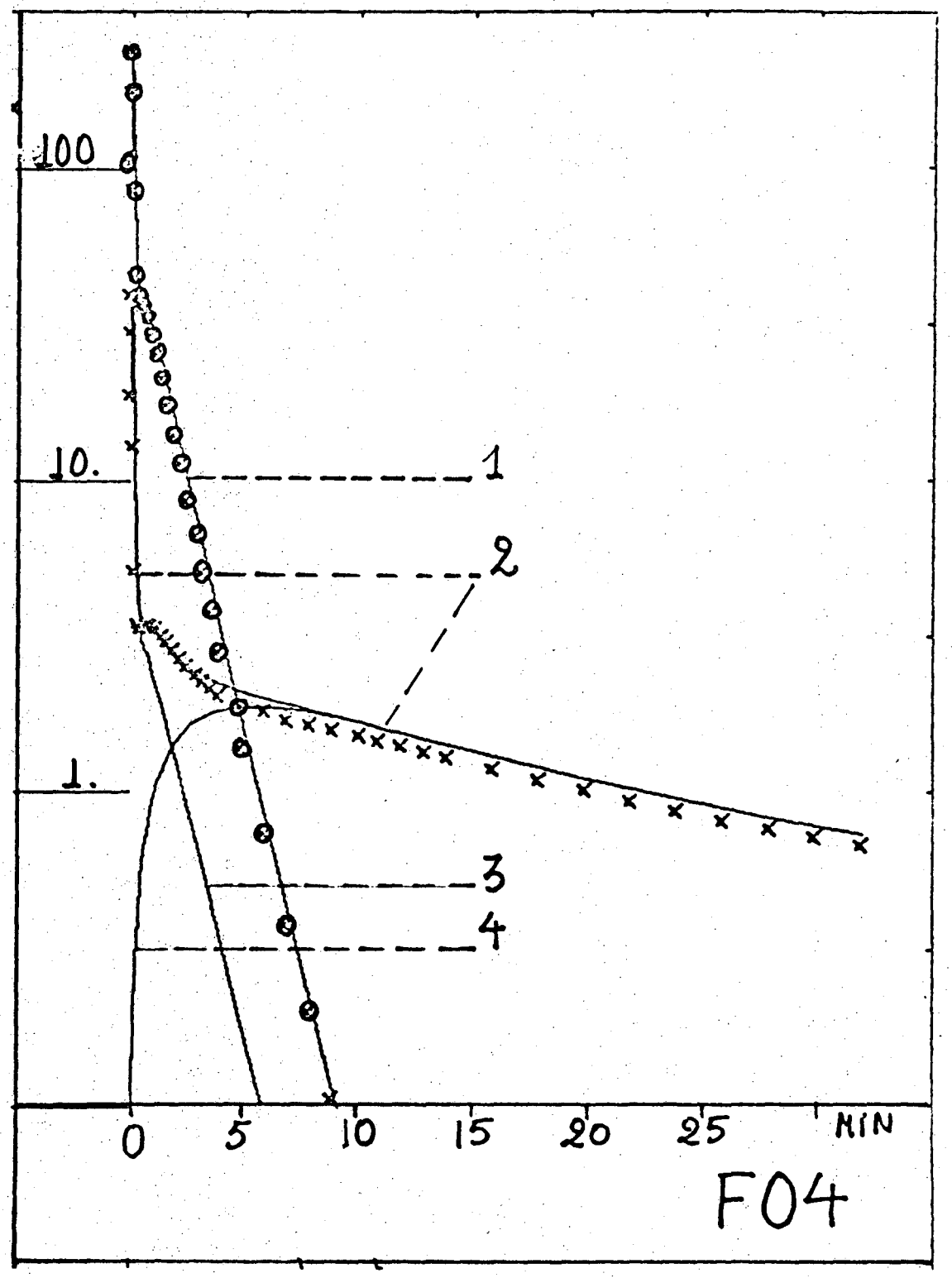

Figure 16a

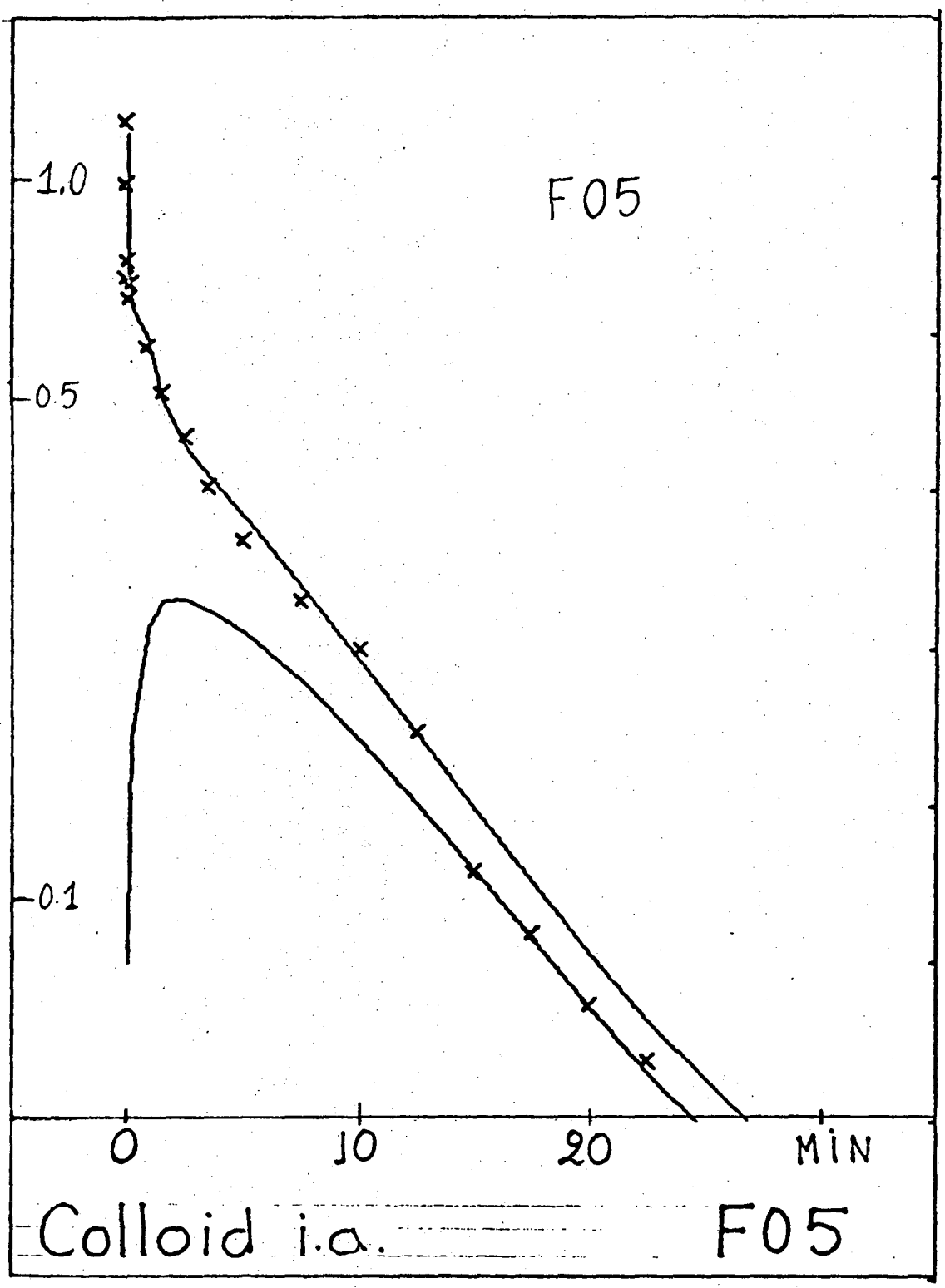

Figure 16b

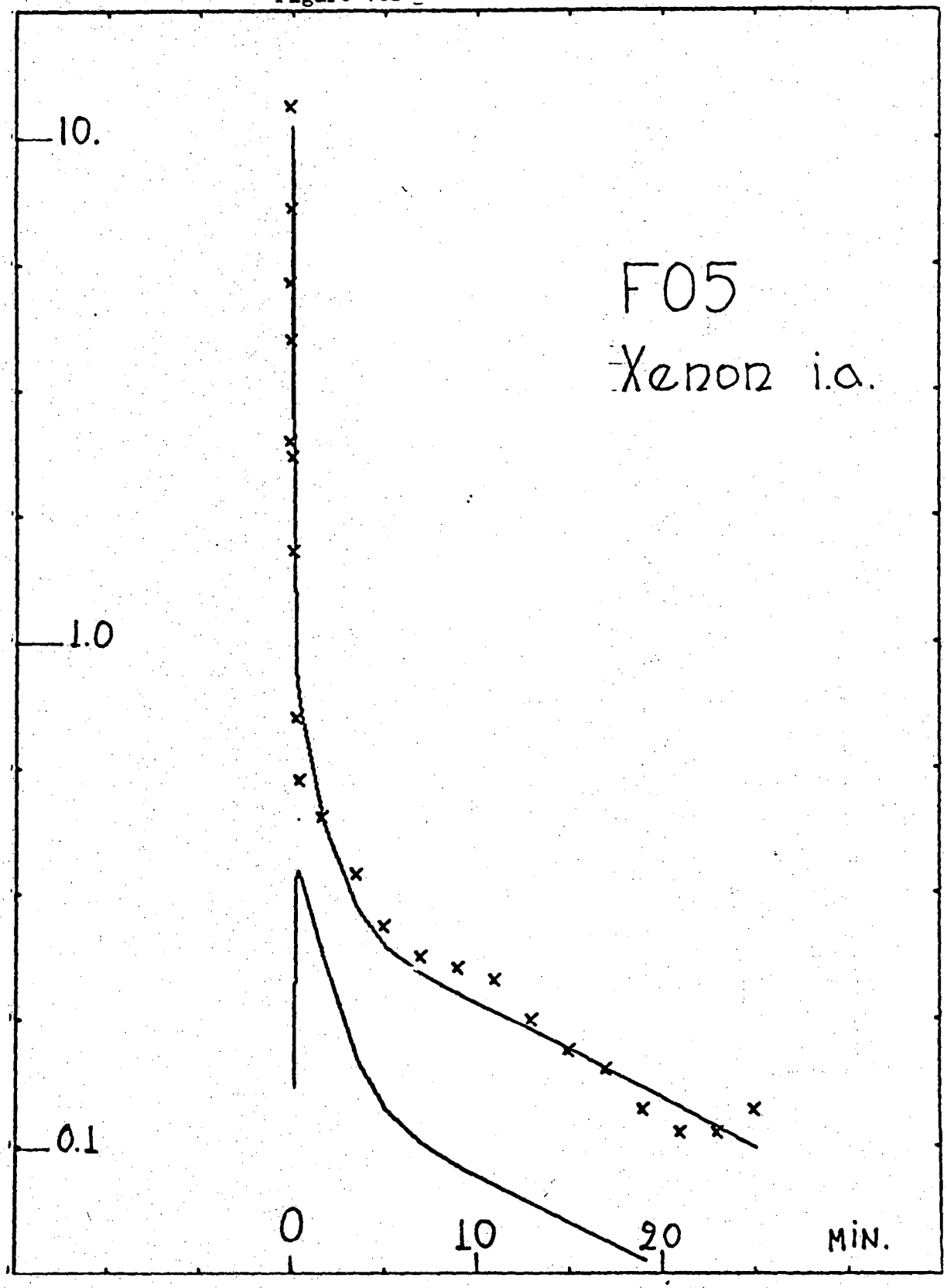

Figure 16c

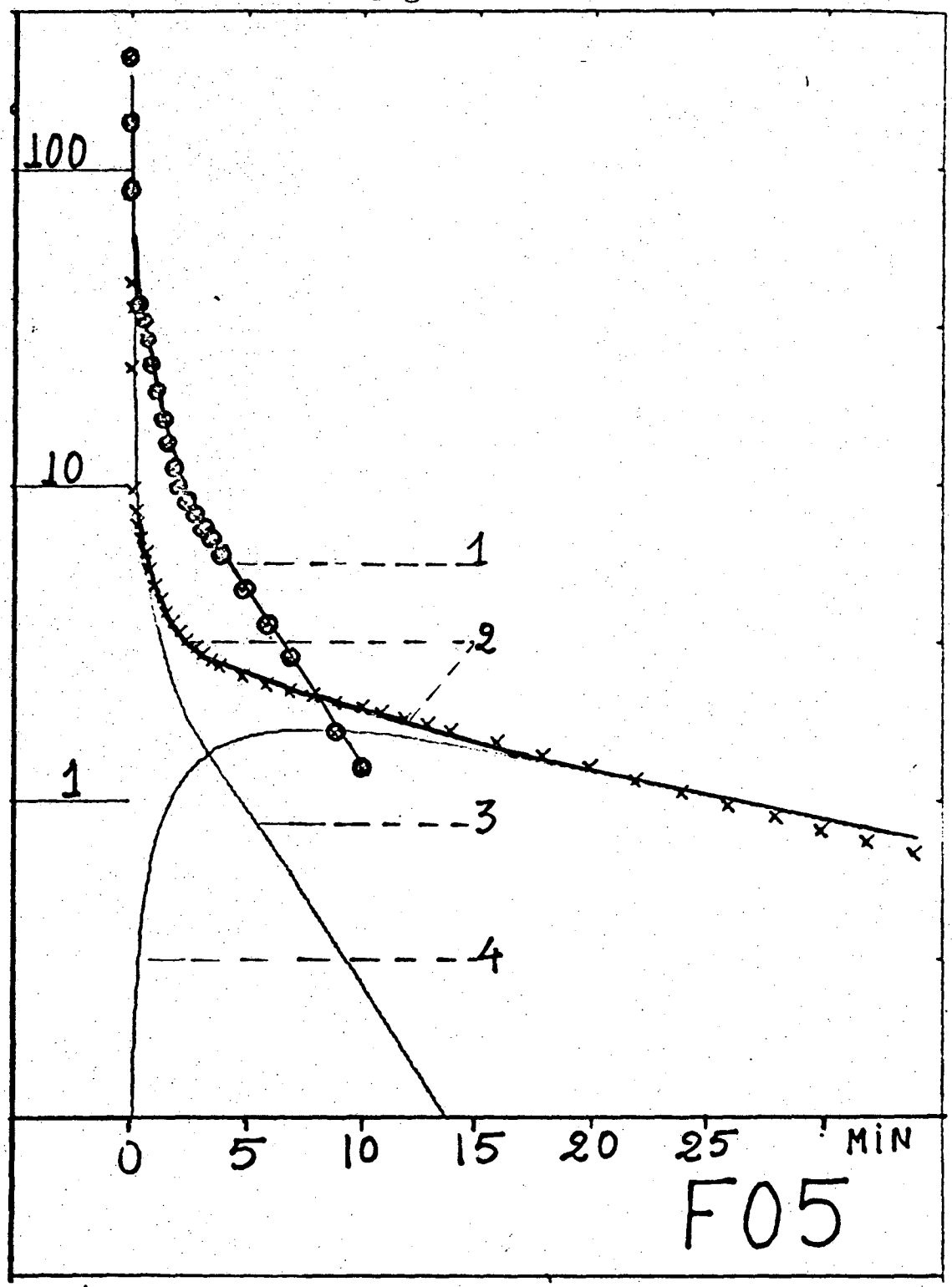

Figure 17a

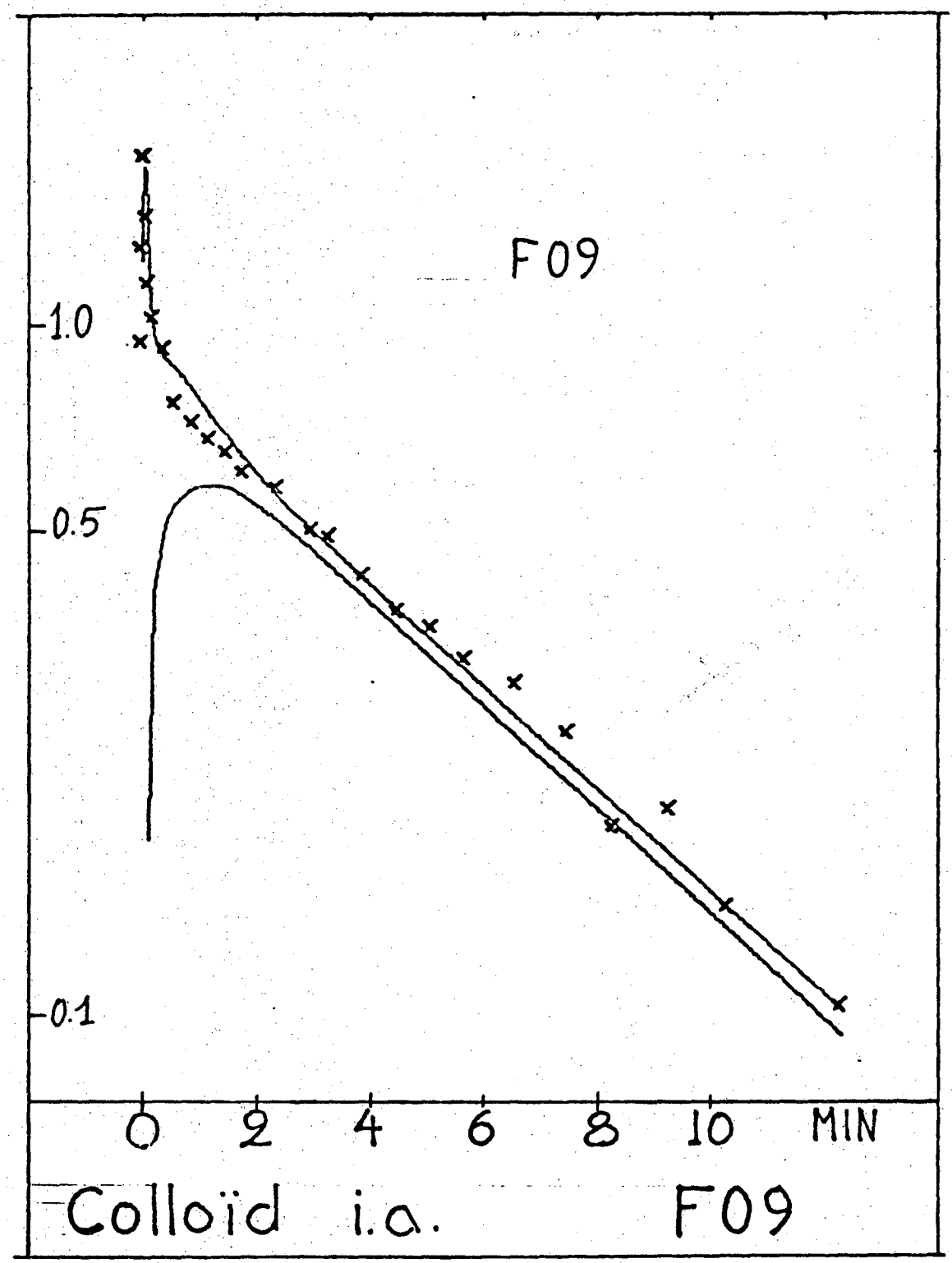

Figure 17b

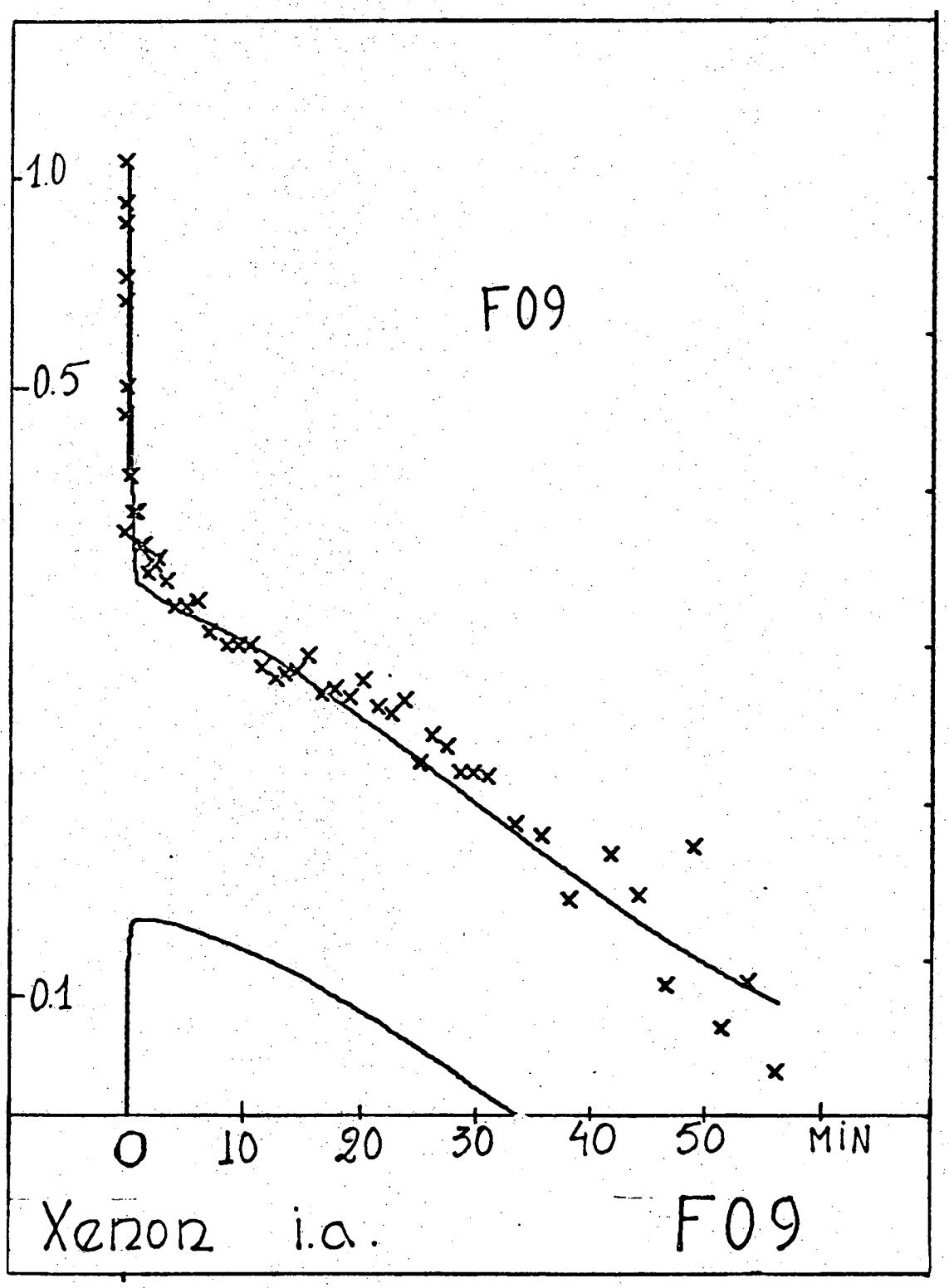

Figure 17c

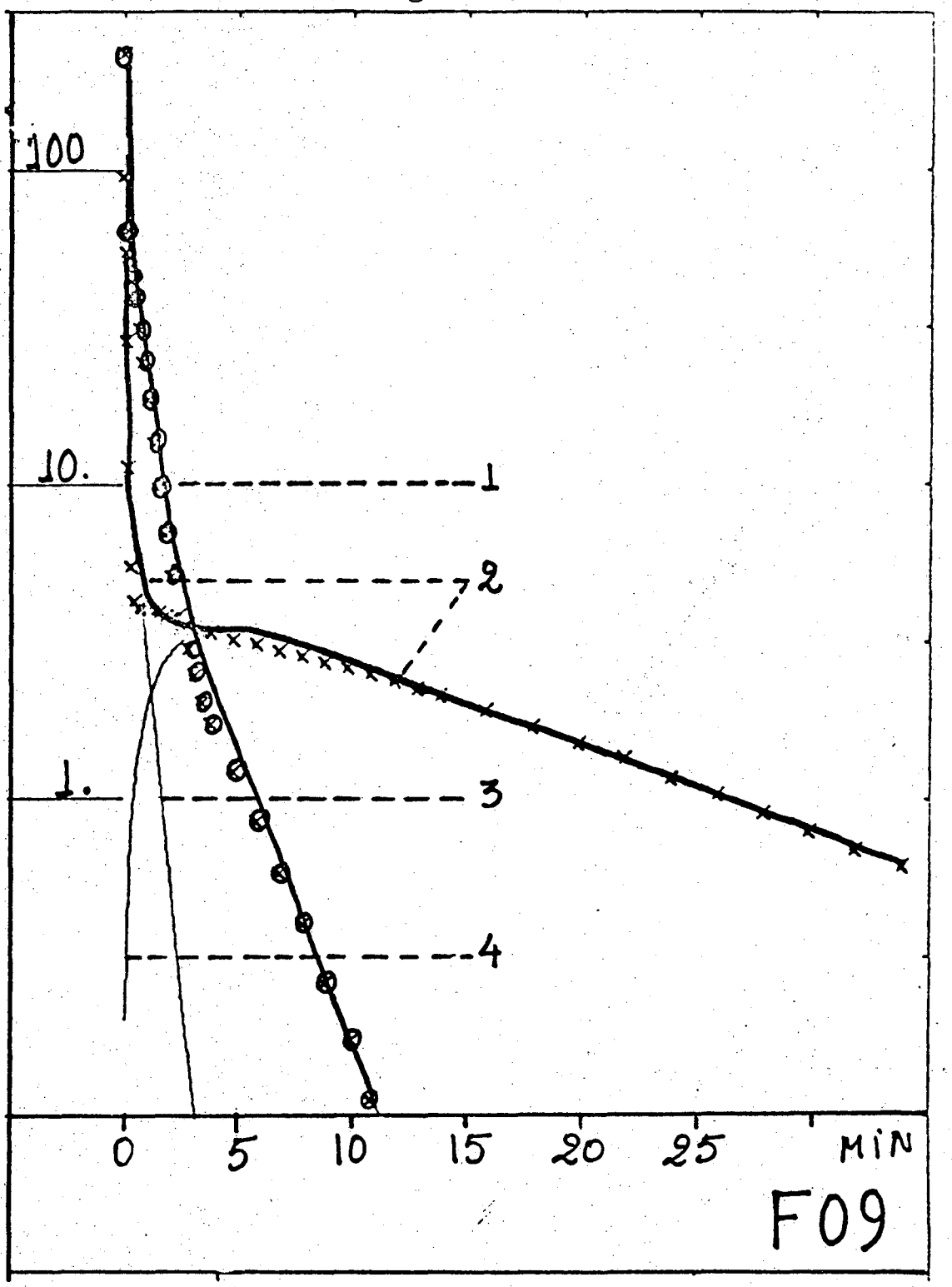

Figure 18a

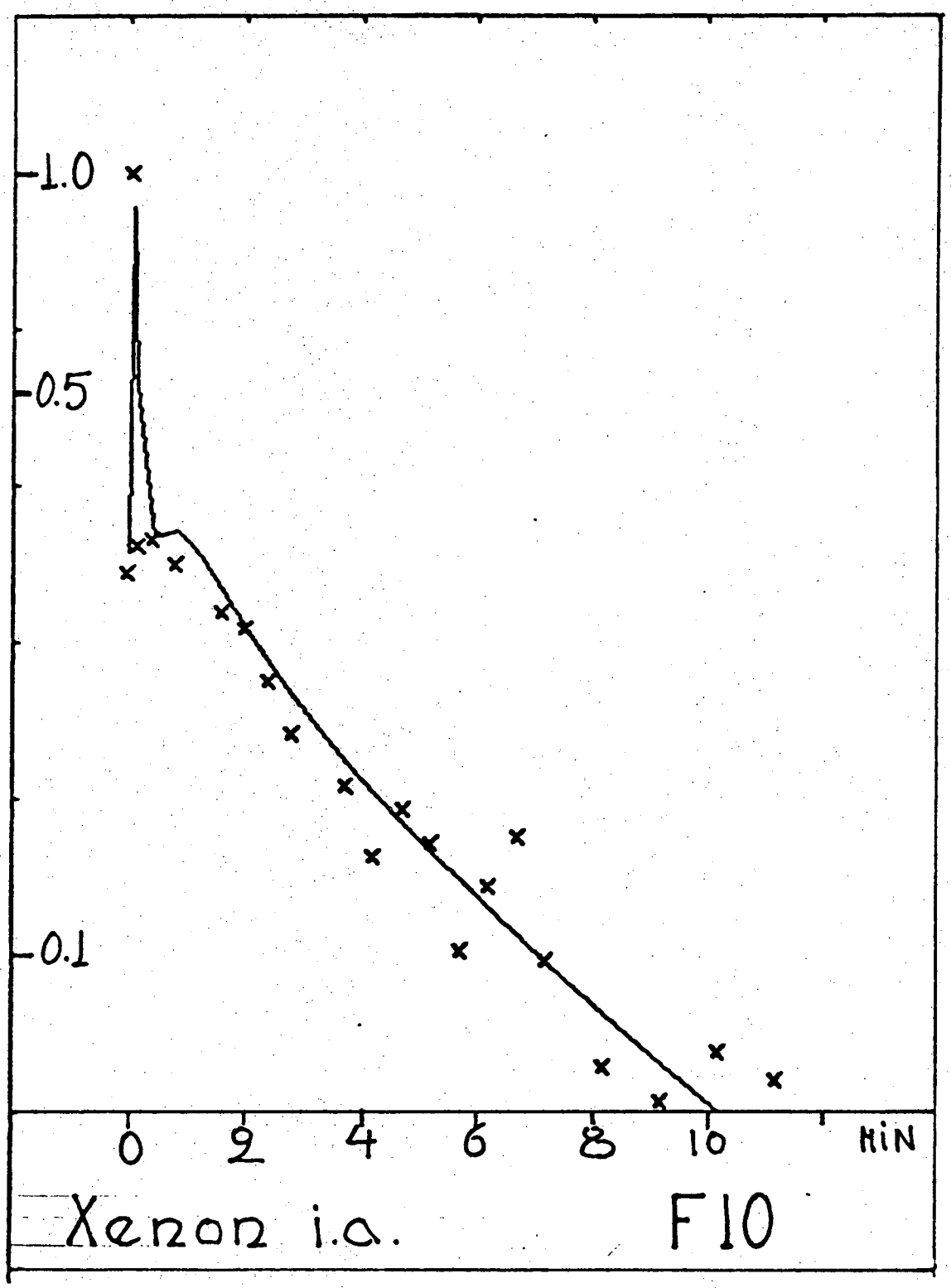

Figure 18b

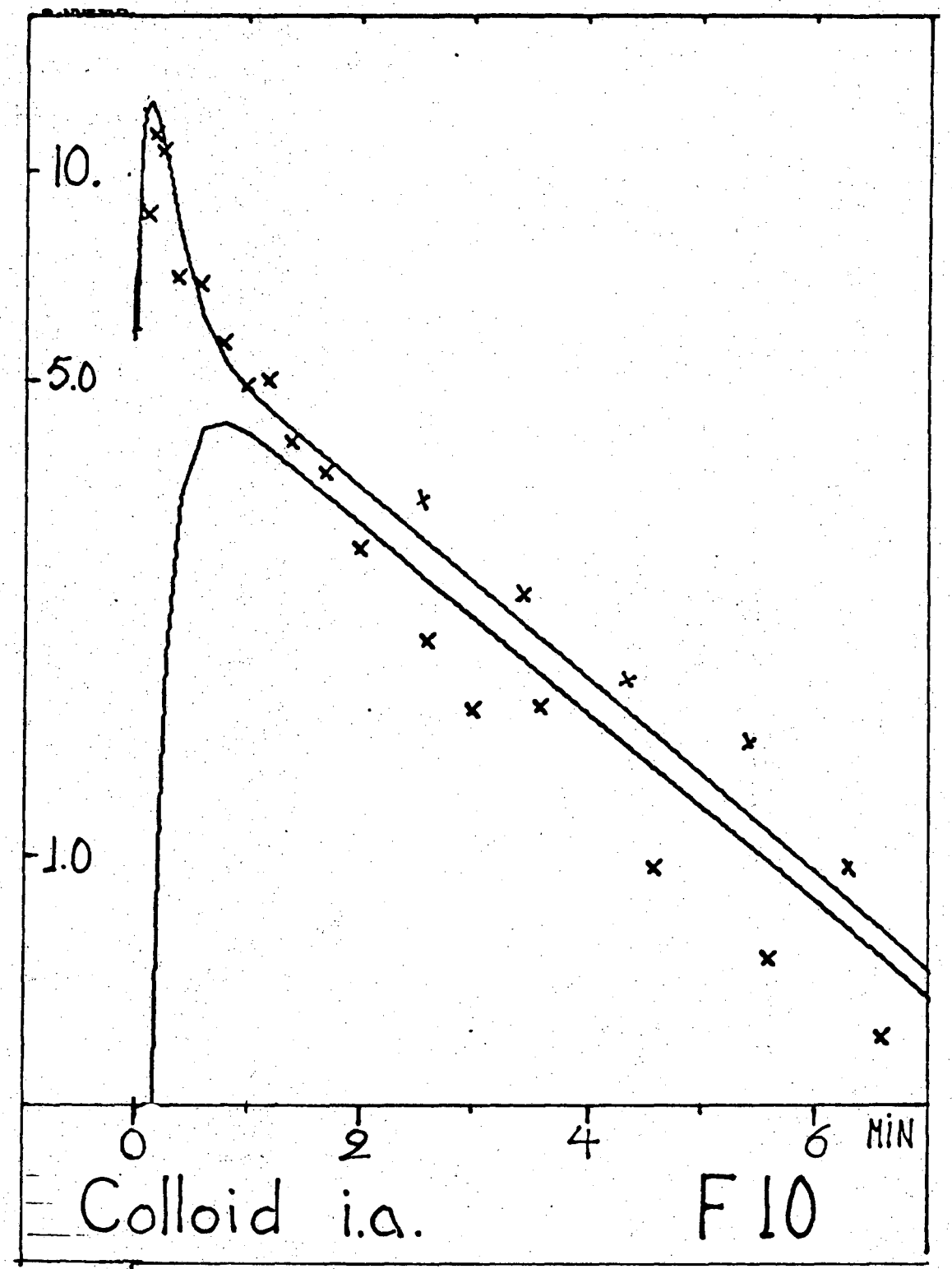

Figure 18c

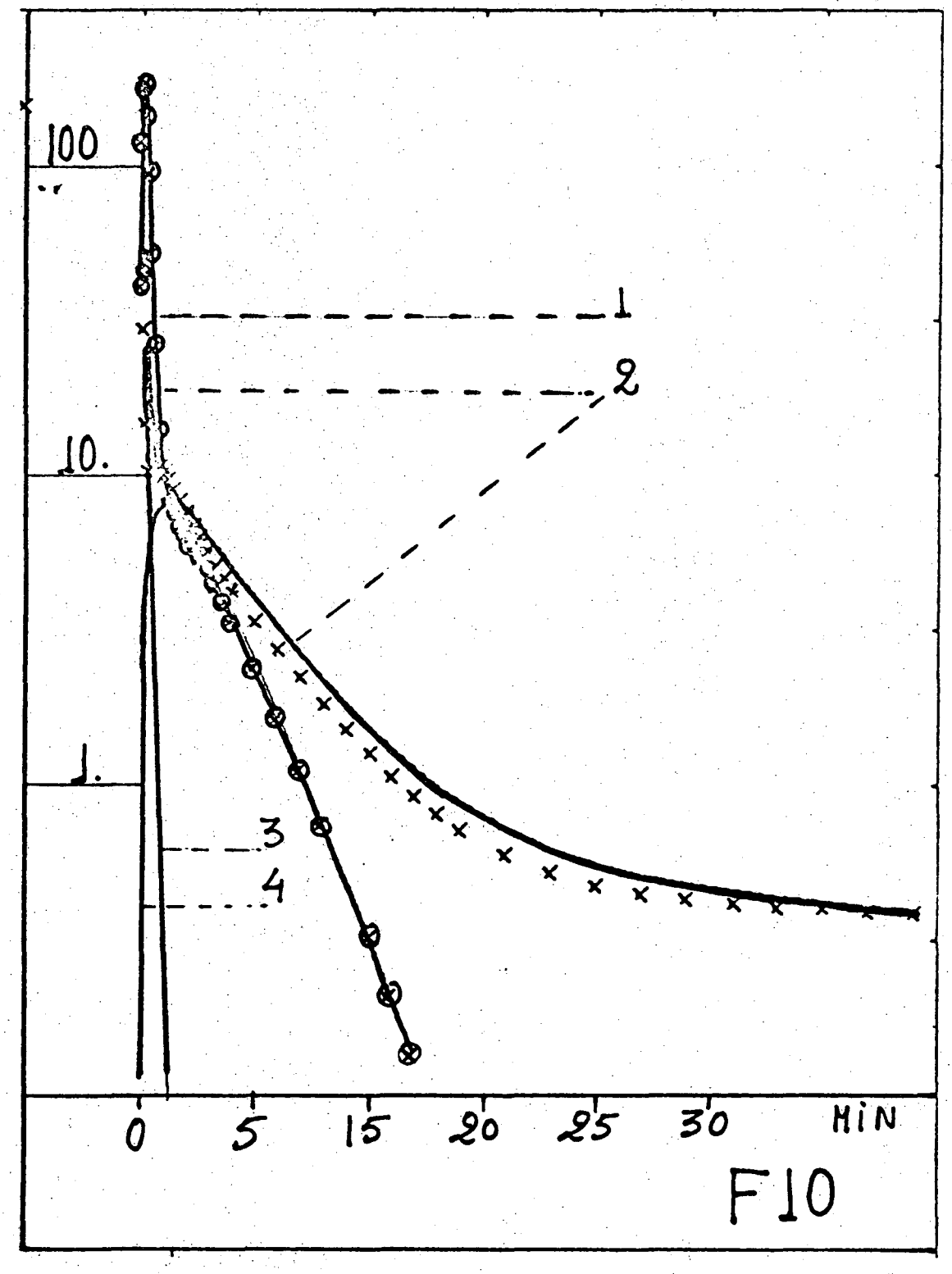

Figure 19a

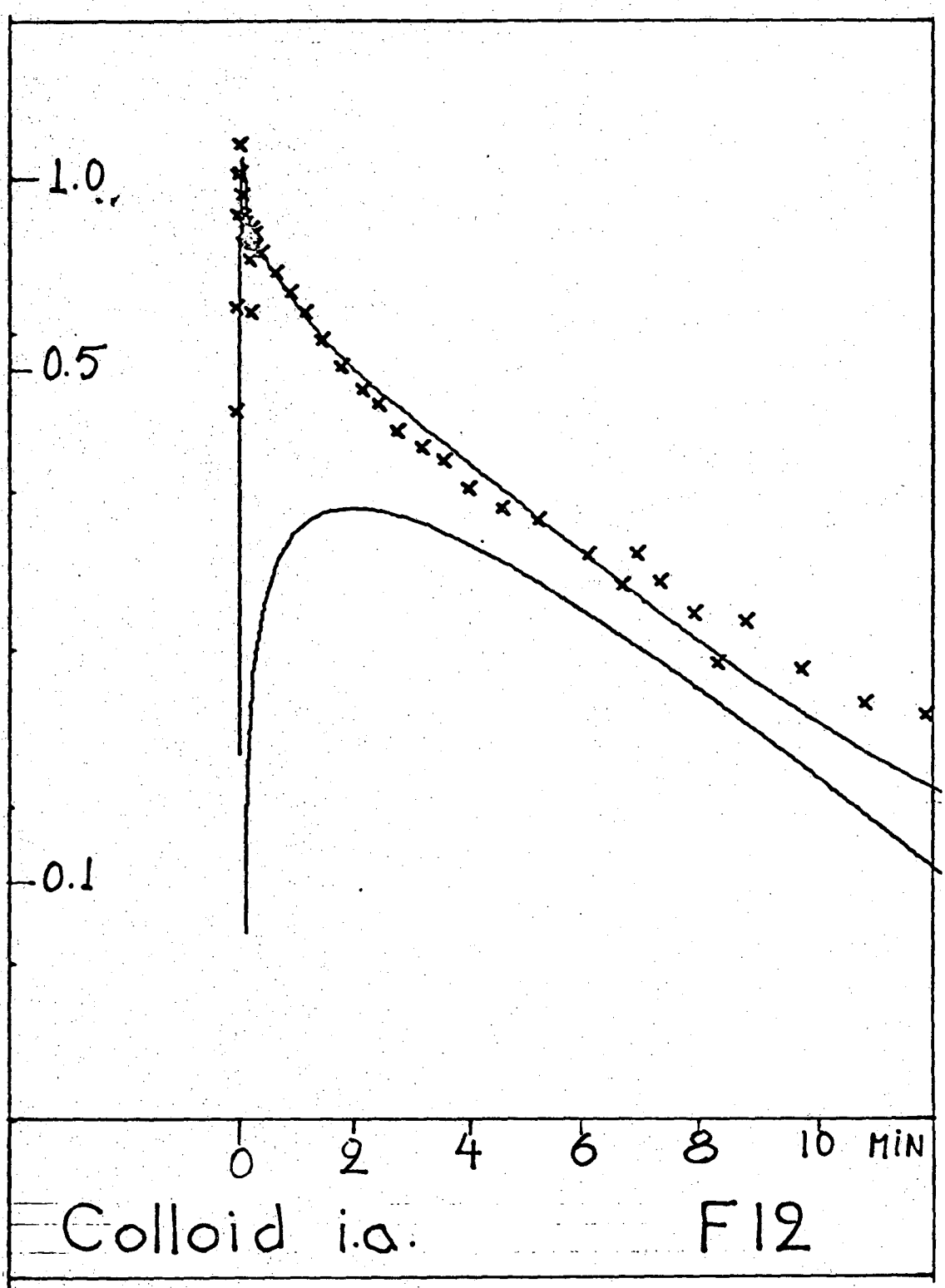

Figure 19b

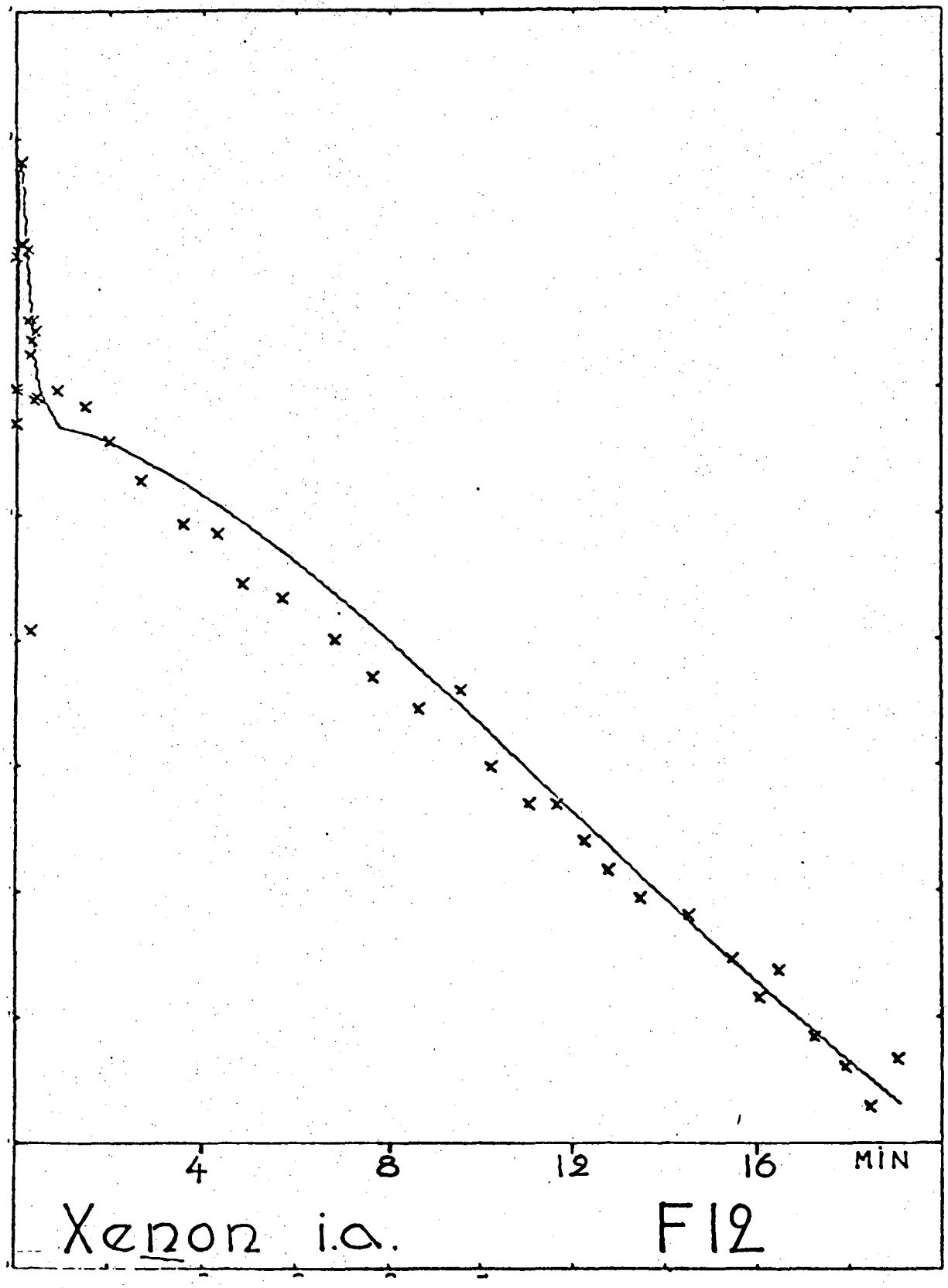

Figure 19c

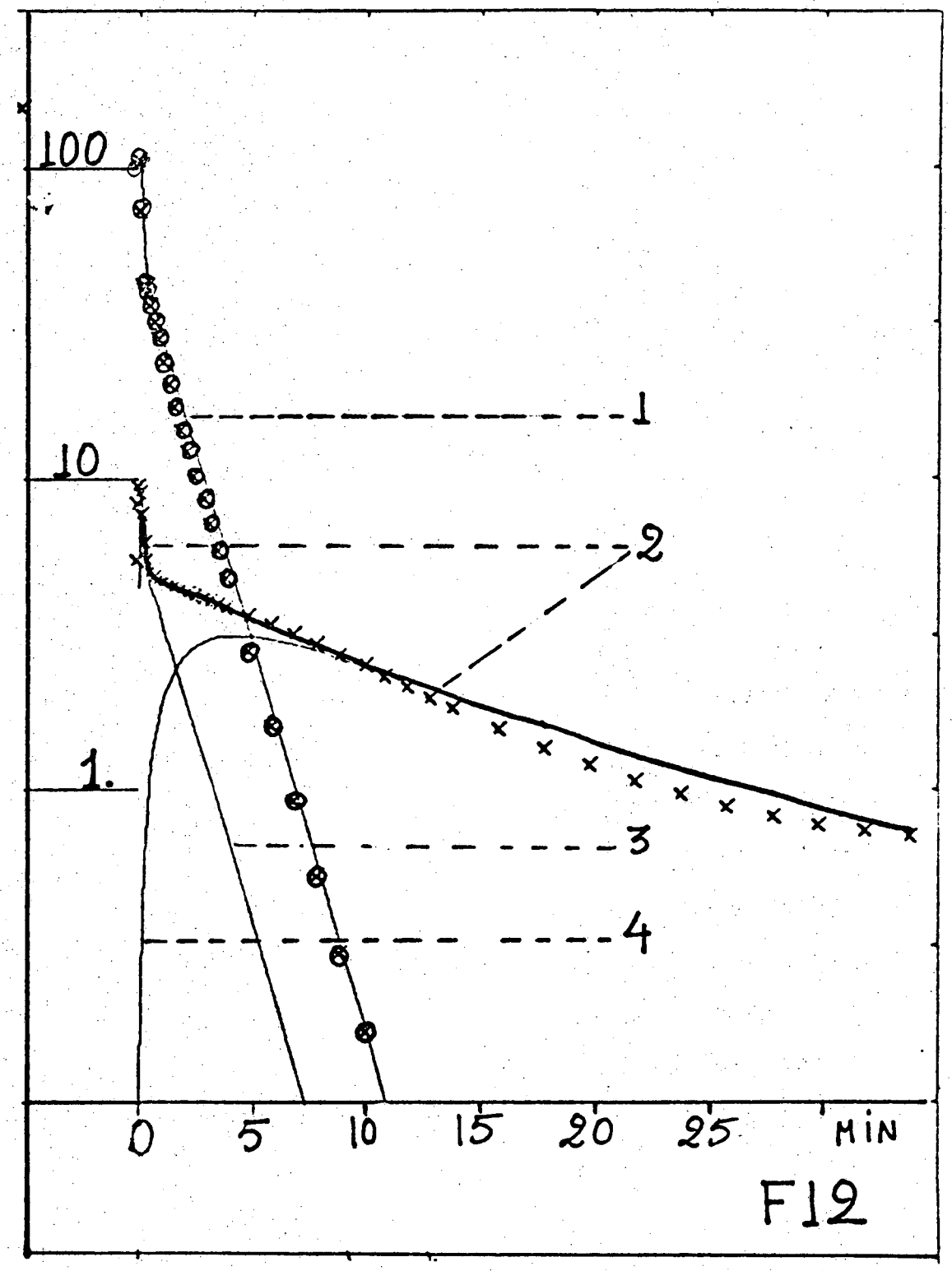

already been discussed.

The main point of our derivation lies in the concurrent fit of $n(t)$ and $d(t)$, so that

$$n(t) = (1-\alpha)n_1(t) + \alpha n_2(t)$$

$$d(t) = (1-\alpha)n_1(t) + \alpha d_2(t)$$

Assuming that $n(t)$ represents the density function of transit times through three parallel sets of two compartments in series, the splitting into $(1-\alpha)n_1(t)$ and $\alpha n_2(t)$ may be due to duplication of each of the sets, getting each respectively a fraction γ_i and $(1-\gamma_i)$ of the flow. This is the parallel bypass network hypothesis, and is the model represented in Fig. 8. In this model there is no permeability in the bypass network, and no diffusion limitation in the exchange networks.

But this exact reduplication of the fractional turnover rates in the bypass and exchange circuits is unlikely, unless one does indeed accept that the two compartments in series correspond to the large arteries and veins. The duplication would then be at the capillary level, where the residency time is too short to influence the global transit times (see legend of Fig. 5). In that case the independency of $d_2(t)$ from $n_2(t)$ follows, as demonstrated in Chapter II, Section 3, because for all practical purposes the extravascular compartments are in series with the intravascular ones, with transit times relatively large compared to the transit times within the vascular compartments.

One has then to explain why in the expression of $d_2(t)$

one uses terms such as

$$A_i(e^{-a_i t} - e^{-b_i t})$$

which implicitly assume two extravascular compartments in series. However, the term $e^{-b_i t}$, responsible for the ascending part of $d_2(t)$ may be not more than a carryover from the intravascular pools. The data resolution however does not allow us to ascertain that $d_2(t)$ could be better fitted by

$$\sum_{1}^{3} (1-\gamma_i)A_i(e^{-a_i t} - e^{-b_i t}) \; * e^{-k_j t}$$

Alternatively, one could assume diffusion limitation in the three parallel sets, so that only the fraction $(1-\gamma_i)$ in each of the sets diffuses into the extravascular compartment.

The analytical form of $d_2(t)$ could be the same as in the previous case. The physiological implications are very different. The choice of Xenon as the diffusable tracer decreases the likelihood of any important diffusion limitation factor. On the other hand, in this case the exact reduplication of the slopes in $n_1(t)$ and $n_2(t)$ is immediately explained, since physically the non-diffusable tracer is not divided between different paths.

A certain amount of diffusion limitation can be expected on theoretical grounds when the density of the exchange vessels is low, and thus, this modality of "functional bypass" should not be immediately rejected as possibly existing in muscles.

Section 3. The model parameters

Table I gives the values for $(1-\alpha)$, $\bar{t}_n$, $\bar{t}_{1n}$, $\bar{t}_{2d}$, and $\bar{t}_d$ in 10 different determinations.

Experiments 3 to 7 were performed on different dogs, without treatment. Experiments 9 and 10, 11 and 12 are on the same dogs, respectively before and during adrenalin infusion (1 µg/kg/min).

The parameters are

$(1-\alpha)$: the bypass fraction of flow

$\bar{t}_n$: the mean transit time for the non-diffusable tracer

$\bar{t}_d$: the mean transit time for the diffusable tracer

$\bar{t}_{1n}$: the mean transit time in the bypass circuit

$\bar{t}_{2d}$: the mean transit time for the tissue perfusion.

Interpretation of those values should be made in the light of the following:

In one ancillary experiment Krypton-^{81m} (Yano, 1970) was injected in the femoral artery of a dog placed under the gamma camera. The injection was repeated during an adrenalin infusion (1 µg/kg/min). The 80 lens camera pictures (taken at 0.2 min intervals) are shown in Fig. 20.

The striking fact is the redistribution of flow from the paw to the muscle. In his experiments C. T. Schmidt finds the same phenomenon, detected with microspheres.

However, there is some striking individual variation in dogs. Once in a while the flow, as detected by microspheres, to the paw is lower, even before adrenalin, while the bypass is lower.

Fig. 20. This figure shows the distribution of ^{81m}Kr in the leg of a dog, after a short intraarterial infusion, before (a) and during (b) adrenalin infusion. The pictures were taken with the gamma camera and an 80 lens photographic camera. Shown here from left to right, top to bottom, in Fig. 20a and b are the pictures taken at 10, 20, 30, 40, 110, 120, 130, 140, 210, 220, 230, and 240 seconds. The redistribution of flow is manifest.

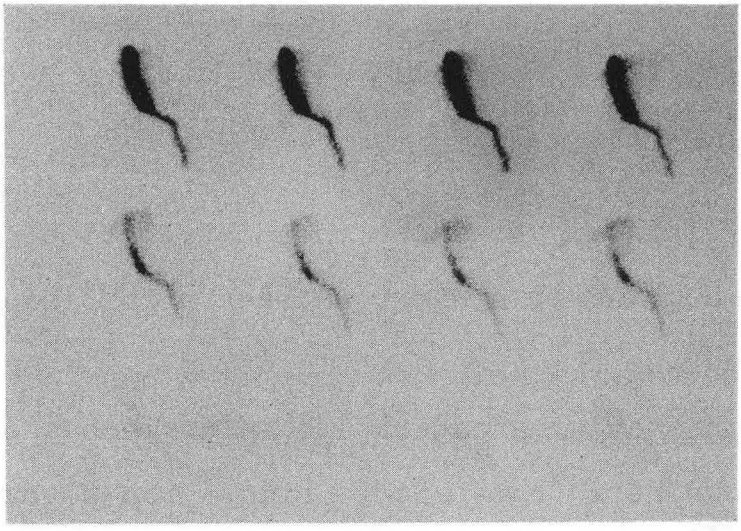

Figure 20a

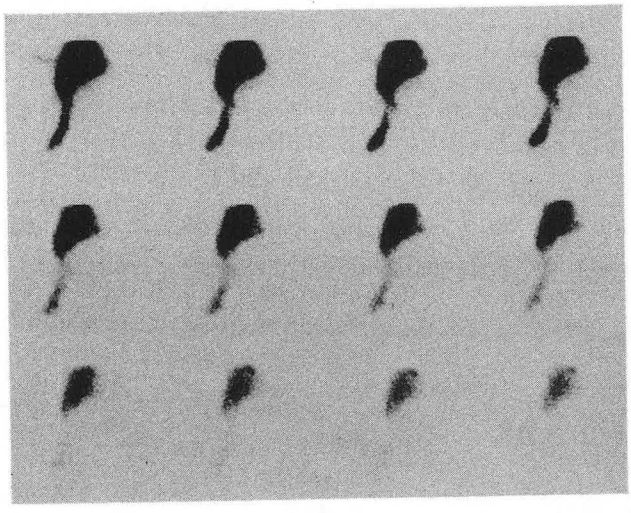

Figure 20b

XBB 728-4134

C. T. Schmidt finds, as Lopez-Magano (1969) does, a large individual variation in bypass fraction. In general, the bypass tends to be lower when the relative flow to the paw is lower.

In our experiments it appears also that in general when the bypass fraction is high, (and the flow to the paw supposedly high), $\bar{t}_{2d}$ is small. The inverse is also true. However, in the two cases where adrenalin is infused, the effect depends on the pretreatment condition.

In case 9, and 10, adrenalin decreases the bypass fraction (.24 to .07), but t_{2d} goes from 14 to 88 minutes.

In cases 11 and 12, the bypass fraction which was already low, remains essentially unchanged, while the originally long tissue perfusion transit time decreases.

Since the aim of this study was to demonstrate the feasibility of the method, rather than to apply it, the reason for the individual variations in pretreatment conditions was not investigated. However, the following can be derived:

(1) When bypass is evaluated by means of microspheres (C. T. Schmidt), this amount of adrenalin reduces the bypass, sometimes, to zero. But this is structural bypass, not functional, depending exclusively on the diameter of the vessels.

As we noted before, if diffusion limitation is to be expected, it will be in the muscle, with the low capillary density. Hence, the probability to detect functional bypass when flow is shifted to the muscles increases.

Table I

Experiment Number	Bypass Fraction (1-α)	$\bar{t}_n$ min	$\bar{t}_{1n}$ min	$\bar{t}_d$ min	$\bar{t}_{2d}$ min
3	.165	1.00	1.82	26.32	22.27
4	.107	1.18	1.08	74.26	66.41
5	.353	2.75	1.57	32.55	21.60
6	.092	1.68	0.71	76.73	69.72
9	.249	0.99	0.28	18.80	14.18
10	.070	1.20	0.33	95.36	88.61
11	.066	0.79	0.81	59.31	55.40
12	.116	1.62	1.73	38.99	34.63

Bypass fraction, and the mean transit times for the non-diffusable tracer ($\bar{t}_n$), the bypass circuit ($\bar{t}_{1n}$), the diffusable tracer ($\bar{t}_d$) and the tissue perfusion component ($\bar{t}_{2d}$) in minutes.

(2) Dobson found that for sodium the turnover rate increased when adrenalin was infused. But his detector was localized over the muscle. Since in our method the turnover in the whole limb is evaluated, a shift of flow from high turnover pools in the paw, to low turnover pools in the muscle, can result in a global decrease in the turnover rate even if the turnover in the slow pool does increase.

(3) When the fractional flow to the paw was originally low, adrenalin cannot shift much more of the total flow to the slow muscle pool, and hence, the increase in turnover becomes apparent.

(4) This is consistent with the observation that in low bypass situations the pretreatment state is characterized by larger values for $\bar{t}_{2d}$.

(5) Finally, it appears that the bypass fraction in general is small enough so that the difference between $\bar{t}_{2d}$ and $\bar{t}_{d}$ becomes negligible, in view of the biological variation.

No special relationship was found between $\bar{t}_{n}$ and $\bar{t}_{1n}$, or either of those values and $(1-\alpha)$.

Since in compartmental analysis individualization of the different compartments is important, we present in Table II the mean transit times for the different extravascular compartments.

From this table it appears that individualization of the compartments is impossible. Although this is in apparent contradiction with Dobson's analysis, it was to be ex-

Table II

Experiment #		3	4	5	6	9	10	11	12
	$\bar{t}_1$	4	24	9	9	15	41	49	12
Comp.1	f_1	.001	.109	.045	.204	.271	.377	.921	.412
	V_1/V	.000	.075	.014	.026	.217	.017	.769	.136
	$\bar{t}_2$	26	36	24	18	16	80	150	34
Comp.2	f_2	.989	.049	.129	.108	.499	.009	.033	.376
	V_2/V	.982	.050	.098	.027	.430	.008	.084	.333
	$\bar{t}_3$	48	70	34	105	28	151	190	97
Comp.3	f_3	.010	.843	.826	.687	.230	.614	.046	.212
	V_3/V	.018	.875	.888	.947	.352	.975	.146	.531

In this table the compartment pairs for the tissue perfusion components are numbered in increasing order of transit times. $\bar{t}_1$ is the mean transit time in each compartment pair (in minutes), f_1 the fraction of the flow going to each parallel set, and V_1/V the fraction of the total volume in each of the sets.

pected.

Although Dobson perceives shift in fractional flow, the field of the detector is mainly muscle, and in this way he detects only part of the system we do. Within the muscle, which is what he mainly sees, the number of compartments may be smaller, and better individualized than through the whole limb.

However, in our case, as in the final analysis in his, the choice of the number of compartments is empirical. Allowing for some model bias, the good fit may be fortuitous. It is indeed not difficult to see how

$$\sum_{1}^{N} A_i \, e^{-a_i t} \quad \text{may be satisfactorily fitted by}$$

$$\sum_{1}^{M} B_i \, e^{-b_i t} \quad \text{where } M < N$$

in cases where random error may cover the bias (see Appendix A).

Macroscopic heterogeneity was demonstrated already. Considering Olson's experiments where closing and opening of capillary beds was strongly suggested, microscopic heterogeneity is very likely.

At this point the model should then be re-examined. Although there are reasons to be reluctant about using compartmental analysis, the use of the fitting functions

$$n(t) = \sum_{1}^{3} A_i \, (e^{-a_i t} - e^{-b_i t})$$

and

$$d(t) = \sum_{1}^{3} \gamma_i A_i (e^{-a_i t} - e^{-b_i t}) + \sum_{4}^{6} A_i (e^{-a_i t} - e^{-b_i t})$$

assumes the following:

(1) Although microscopic heterogeneity does exist the intravascular pools behave as three parallel pairs of two compartments in series.

None of those compartments is specifically localized either in the paw or the muscle. When adrenalin is infused, there is redistribution of flow between the compartments, but also redistribution of the compartments between paw (skin, bone) and muscle.

(2) Each of those compartment pairs represents in part a fraction of the bypass circuit.

(3) Using the equations from Chapter II, one expects the same fitting equation for the nutritive flow, whether the tissue compartments are in series with, or simply an enlargement of the intravascular pools.

The way the data were fitted, the six components (3 pairs in parallel of two compartments in series) may be allocated in different fractions to the different intravascular pools.

(4) However, although no specific location within the organ is given to any of the extravascular compartments, evidence was presented suggesting that slow turnover rates were preferentially situated in the muscle.

CONCLUSION

In this work we were able to present a method allowing one to determine the density function of transit times for intraarterially injected tracers. Methodologically the main problems were the recirculation correction and the geometry factor. We did show how one can, by locating the detector over the efferent vein collect data which are not influenced by time dependent geometrical redistribution within the studied organ. The double injection method for recirculation correction, using an empirical smoothing function on the arterial injection data, gave satisfactory results.

We were able to derive theoretically the conditions needed to describe the density fractions of transit times for diffusable and non-diffusable tracers, in a manner allowing one to determine the necessary circulation parameters without undue reliance on any unique circulation model.

Our "generalized" model allowed us to define the circulation in terms of bypass and tissue perfusion parameters.

The values obtained for those parameters before and during "treatment" were consistent with observations made in other experiments.

However, the globality of the method, vs the marked heterogeneity of the limb, led to a relatively poor sensitivity to changes. Although we were able to see changes during treatment, the changes we did see were smaller than the changes expected at different places at the local level. This is due to the fact that the global changes are the alge-

braic weighted sum of local changes.

Increasing the spatial resolution of the detecting device solves this problem to some extent. In previous work (Goris, 1969; DeRoo, 1968, 1969) that approach was taken for other physiological systems.

However, information about the bypass is gathered during a short time immediately after injection. At that time local detection, even with high spatial resolution, does not allow one to distinguish the fraction of tracer which is being carried to and from distal tissue elements, from the fraction of flow proper to the small region one detects.

However, when one considers how the output function, $d(t)$, is exclusively due to tissue perfusion, $d_2(t)$, only from about five minutes after injection, an improvement of the method suggests itself.

Since, at the time, when most of the activity in the organ is due to tracers present in the tissue pools, the changes as a function of time are low, some information could be gained using high spatial resolution, and low time resolution detection, as one would have with the gamma camera.

To conclude then, we did achieve the aims of this study. The method has features allowing us to determine parameters of the peripheral circulation which cannot easily be determined by any other method. The geometry independency, the recirculation correction independent of paired organs, allows us to apply it in extreme pathological cases, and to unpaired organs.

Acknowledgment

We wish to thank Mrs. Linda McColgan, who typed the different drafts, as well as the final version.

This work was partially supported by the Bay Area Heart Research Committee, by the Belgian National Foundation for Scientific Investigation (N.F.W.O.), and the Belgian American Educational Foundation, and the U.S. Atomic Energy Commission.

Appendix A

The selection of a model and the effect of noise on parameter estimation

The use and definition of models was systematically reviewed by Berman (1963): If the aim of the model is simply to be descriptive, all one needs is a mathematical function which adequately predicts the observed values. In this "mathematical" model non-uniqueness of the parameter values does not matter.

A special kind of mathematical model is the "transfer function" model. Usually both input and output are specified or observed, and the transfer function is derived. The criterion for success is not uniqueness, but the possibility of deconvoluting the transfer function from the input and output functions.

The "physical" models are defined as follows: If the functions used are the solution of a set of differential equations, the coefficients of those equations represent physical entities of the system under study. This model is solved to the extent that the solution is unique for all the individual parameters. The problem is, in general, not only uniqueness but consistency or lack of model bias. The choice of the model may be based on independent observations, or on the data themselves.

Finally, there is the type of model, which may be of the mathematical or the physical kind, but is so chosen that "treatment" consistently influences a restricted number of

parameters.

In the body of this work the different types of models were used. Manifestly the smoothing and recirculation correction operations are an application of the "mathematical" model of the "transfer function" kind.

Hence, although good fit is a prerequisite, uniqueness is not. The problem one faces is not to determine the individual parameter values, but to estimate at which point the function fits the data well and fitting to noise starts. In this kind of problem the noise cannot be fitted, since, unlike the data without noise, it has no real convolution factor.

The analysis on the corrected data, derived from the preceding, has different aspects. If the only parameter defined is the mean transit time ($\bar{t}$), on data collected over the entire time interval of h(t), one could with minimal error determine $\bar{t}$ numerically, or from a smoothing function, even if its individual parameters are not unique. The fitting would then have been strictly mathematical, and the mean transit time is in essence a directly observed physical entity.

In practice, however, since one did not collect data over the whole time interval in which h(t) exists (and is not zero), the functional form used to fit h(t) influences the extrapolation which is implicitly performed outside of the empirical time interval.

The choice of one type of a function (in our case a sum

of exponentials) is influenced by physical characteristics assumed or independently observed, about the system.

In our case we can assume that the diffusable tracer will be well mixed by the end of the experiment, and that from then on the amount leaving the system will be simply related to the amount present.

Therefore even the most global definition of a mean transit time from a "well fitted" function is to some extent physical modeling.

But in the integral approach the physical assumptions are kept to a minimum. The number of parameters related to physical entities are restricted. They are the bypass fraction and the mean transit times for both tracers in both pathways.

Except for the extrapolation those parameters could be derived from any functional form for a fitting function, with the understanding that some additional assumption had to be made regarding the splitting of $n(t)$ into $n_1(t)$ and $n_2(t)$. (In our data however $n_1(t)$ represented most of the activity at the early times, and little error of consequence can be made in its estimation).

Besides that, this restricted number of parameters was found to change under "treatment" in a fashion expected from independent measurements and models.

One cannot, however, feel very confident about the implicit extrapolation present in the integral method in view of Strehlow's (1971) observations on the fitting by different

functional forms. He shows, i.e. how $y_1 = e^{-t} + ye^{-t/2}$ and $y_2 = 4.89\ e^{-t/1.699} + 0.094$ do overlap up to at least t = 5, but then start to diverge.

The integral approach has an error which is more influenced by the curtailing of the data collection than by error in the individual data points (Zierler 1964). But if the fitting function is a sum of exponentials, the error in the tail will be influenced by the error in the estimation of the smallest rate constants. The problem here is the same as in strict compartmental analysis.

Compartmental analysis should not be performed without investigating the influences of noise and data truncation on the parameter estimation error, since the compartmental model is strictly a physical model. However, it is not possible to define the order of the model solely on the basis of the data, since for any model compatible with the data there are degenerate models of higher order compatible with the data. One can of course assume that the physical model has the lowest order compatible with the data. Callahan and Pizer (1966) did use a modified Fourier transform, in the presence of noise and on data of short time duration (relative to the interval of the function). It proved to be necessary to extrapolate the data. The method works rather well when the slopes are well separated, and the noise level low. But the noise in the data provokes ripples in the spectrum which could be confused with peaks of low amplitude.

Myhill, Wadsworth and Brownell (1965) investigated the

effect of noise on the parameter estimation using a linear operator on a sum of two exponentials. In this case the model is defined before the data analysis. Still, with an error of only 2% in the data (which is a high level of precision in most biological tracer experiments) the accuracy in the rate constants determination was 15% of the true value when they differed by a factor of at least two. The same accuracy was obtained with 16% error in the data if the rate constants differed by a factor of at least six. The data cut-off had to be so that the last data point was 5% of the first one to separate rate constants differing by a factor of two with a data error of 2%.

Glass and Garreta (1967) did error analysis on biological data assumed to follow a sum of two exponentials, and found errors ranging from 5% and 13% in brain blood flow to 25% in bone formation. However in those cases model bias is not independently estimated.

The effect of data error was again investigated by Myhill (1967). The data set is of good quality, ranging from 100% at t = 0 to 5% at the end of the collection period. The model is simple: two exponentials. Parameter estimation was performed by a Gaussian iterative technique.

With a rate constant ratio of at least four, the technique converged for data errors of 5% or less. The calculated error in the rate constants ranged from 2 to 85%, and in the amplitude from 1 to 50%, for data error between 0.5 and 10%. The lesser rate constant and amplitude had the greatest

error.*

We found in our corrected data that the average data error (estimated from the least square) is 10%. In the case of the tissue perfusion fraction of the diffusable tracer, the total number of exponentials is six. However, since they are paired as $A_i(e^{-a_i t} - e^{-b_i t})$ with $b_i >> a_i$, ($-e^{-b_i t}$ is used exclusively to allow the function to rise), the mean transit times in each of the compartment series is approximately $1/a_i$. Hence in our case we are in a situation close to a three exponential fitting.

From the results it appears that in most cases the number of parallel sets of compartments assumed in the model is too large. As an example in experiment 3, 98.9% of the flow goes to a compartment series which comprehends 98.2% of the total volume. In experiment 4, we find respectively 83.4% and 87.5%; in experiment 11, respectively 92.1% and 76.9%.

One would expect then, from the preceding, that the error in the estimation of the different parameters would be large. This is supported by the fact that the effect of the treatment cannot be estimated on the individual parameters.

*While these pages are written, Joel Swartz is finishing a Ph.D. thesis (U.C. Berkeley, Dept. of Medical Physics) in which a theory and algorithms permitting an estimation of the error bounds of the parameters as a function of the noise of the data, are presented.

To conclude then, we were well inspired not to base the method on strict compartmental analysis. Unless the noise is decreased one cannot expect to uniquely define the parameters of a complex physical system.

Appendix B

The Algorithms

The different algorithms used are shown in the following pages. Grouping and cross-talk correction is performed on the PDP-12 computer; the language is FOCAL-12. The algorithm for the recirculation correction is the same for Xenon and colloid, with the exception of the function F(Z).

Grouping and Cross-talk Correction

READ

```
01.10 E
01.20 L O,F1,F,#700,0
01.30 L O,F2,U,#0,1
01.31 L O,$3,F,#677,0
01.35 A "RUN NO- ",RN;S RN=16*(RN-1)+256;T !
01.40 A "# EPOCHS",NE,"* CHANS",NC
01.42 S F3(0)=NE;S F3(1)=NC
01.50 S X=NE*(NC+1)-1
01.60 F I=0,X;S F1(I)=F2(I+6+RN)
01.70 L C,F1;L C,F2;L C,F3
01.75 T !!!
01.80 L G,$SMOOTH,0
*
```

GROUP

```
01.05 E
01.07 L O,F3,F,#677,0
01.10 A "CHANNEL",CH,"MAX TICKS",TM,"MAX CTS",CM
01.12 S NE=F3(0);S NC=F3(1);S F3(3)=CM
01.15 S NE=NE-1;S NN=NC+1
01.20 S Z=0;S EP=0;S T=0;S C=0
01.22 F I=1,NC;S XX(I)=0
01.24 L O,F1,F,#700,0
01.26 L O,F2,F,#700,1
01.30 S T=T+F1(NN*EP)
01.32 F I=1,NC;S XX(I)=XX(I +)1(NN*EP+I)
01.40 S C=C+F1(NN*EP+CH)
01.50 S EP=EP+1
01.60 I (C-10) 1.3,1.3;
01.70 S TB=0;S CB=0;S RT=C/T;S SQ=FSQT(C)/T
01.72 S TB=TB+F1(NN*EP);S CB=CB+F1(NN*EP+CH)
01.73 F I=1,NC;S XX(I)=XX(I +F1(NN*EP+I)
01.75 I (10-CB) 1.8;S EP=EP+1;G 1.72
01.80 S RB=CB/TB

02.10 I (4*SQ-FABS(RB-RT)) 3.1;
02.20 I (TM-T) 3.1;I (CM-C  3.1;
02.30 S T=T+TB;S C=C+CB
02.50 I (NE-EP+-.5) 3.05,3.05;S EP=EP+1;G 1.7

03.05 D 3.08;S Z=Z+1;G 3.6
03.10 F I=1,NC;S XX(I)=XX(I -F1(NN*EP+I)
03.20 S F2(NN*Z)=T;F I=1,NC;S F2(NN*Z+I)=XX(I);S XX(I)=F1(NN*EP+I)
03.30 S T=TB;S C=CB;S Z=Z+1
03.40 I (NE-EP+-.5) 3.5;S EP=EP+1;G 1.7
03.50 D 3.8;S Z=Z+1
03.60 S F3(2)=Z
03.70 L C,F1;L C,F8;L C,F3
03.90 T !!,"Z IS ",Z
03.95 L G,$PRINT,0
*
```

PRINT

```
01.05 E
01.10 L O,F1,F,#700,0
01.11 L O,F8,F,#700,1
01.12 L O,F3,F,#677,0
01.20 S Z=F3(2);S CH=F3(3);S NC=F3(1)
01.30 S NN=NC+1

04.10 S T=0;T !!
04.19 T " MINUTES CTS/MIN +/- 1 S.D."
04.20 F I=0,Z-1;D 5
04.21 A !!,"MORE OUTPUT ?";PL;I (PL-28) 4.22;A I,"CHANNEL",CH;G 4.1
04.22 L C,F1;L C,F2;L C,F3
04.24 A !!!," PLOTS ??",PL;I (PL-29) 4.25;L G,$PLOT,0
04.25 T !!!!Q

05.10 S T=T+F2(NN*I)/2
05.20 S RT=F2(NN*I+CH)/F2(NN*I)
05.30 T !,26.4,T/3000,RT*3000
05.31 T " +/-",3000*FSQT(F2(NN*I+CH))/F2(NN*I)
05.40 S T=T+F2(NN*I)/2
*
```

$(X)^{-1}.(O)=(E)$

```
01.05 E
01.08 A "TIMELENGTH",P
01.09 T "INVERSE",!
01.11 F I=1,4,13;T !;F N=0,3;A A(I+N)
01.12 T !,"BKG"
01.13 F I=1,4;A B(I)
01.15 T !,"MAX"
01.16 F I=1,4;A C(I)
01.17 T !,"#EPOCHS";A Z;S T=0
01.18 S Z=Z*5
01.19 O C

02.10 L O,F1,F,#700,1
02.20 F I=0,5,Z-2;DO 8.8
02.30 L C,F1
02.40 Q

06.10 F N=1,4;S X(N)=F1(I+N
06.20 F N=1,4;S Y(N)=0
06.21 S J=-4
06.30 F K=1,4;S J=J+4;F L=1,4;S Y(K)=Y(K)+(X(L)-B(L)*F1(I)/3000)*A(J+L)
06.40 S T=T+F1(I)/3000
06.45 F K=1,4;S Y(K)=Y(K)+3000*1000/(F1(I)*C(K))
06.50 T !,"      ",T;F K=1,4;T Y(K)
06.55 S D=T*1.38/P;F K=1,4;S J=Y(K)/1000;S H=FDIS(D,J)
06.60 R
*
```

Recirculation Determination-Correction

```
      PROGRAM STEP(INPUT,OUTPUT,TAPE3=OUTPUT,TAPE9=101,PLOT,TAPE7=PLOT
     4)
      COMMON X(100),N,IP,TZ(300),TLAG,TNORT,EXPO,PARA(6),COEF(20)
     6,PLIMIT,ISTART,ISTOP,XX(100),ITRY,RET
     6,RSLOPE,XNO
      DIMENSION          R(100),YEXP(300),TITLE(6),XLAB(3),YLAB(3)
     6,BLANK(3),CURV(6),XEXP(300),ZEXP(300)

C     X = ARRAY OF VARIABLES
C     N = NUMBER OF X VARIABLES
C     IP = NUMBER OF EXPERIMENTAL POINTS TAKEN ALONG EACH SPECTRUM
C     IT = NUMBER OF ITERATIONS
C     L = DISTANCE BETWEEN THE POINTS OF LAGRANGIAN INTERPOLATION
C                                        X(1)=NORMALISING FACTOR
C                          X(2) TO X(10) ARE COEFICIENTS
C                          X(11) TO X(19) ARE EXPONENTS
C                          X(20) SCALING RECIRCULATION
C                          X(21) RECIRC. SLOPE CORRECTION
C                          X(22) RECIRCULATION INTERCEPT CORRECTION
C

      CURV(6)=0.
      BLANK(3)=0.
      TITLE(6)=0.
      XLAB(3)=0.
      YLAB(3)=0.
      FLIP=0.5
      FLOP=2.
      READ 314, (TITLE(K),K=1,6)
      READ 314, (CURV(K),K=1,6)
      READ 313, (BLANK(K),K=1,2)
      READ 313, (XLAB(K),K=1,2)
      READ 313, (YLAB(K),K=1,2)
      READ 330, NR
      READ 330, NREX
      READ 330, N
      READ 330, IT
      READ 330, ISTART
      READ 330, ISTOP
      READ 316, M
C
C     READ IN SPECTRA
      READ 332, TNORT
      READ 332, EXPO
      READ 332, TLAG
      READ 332, BG
      READ 332, XNO
C
      IP=0
      DO 199 J=1,300
      IP=IP+1
      READ 333, TZ(J),Y(J),TEST
      IF (TEST-9.1)200,200,201
  200 CONTINUE
  199 CONTINUE
  201 CONTINUE
      PRINT 1111
      PRINT 1001, NR,NREX
      IP=IP-1
      DO 202 J=1,IP
      TZ(J)=TZ(J)-TLAG




      IF(TZ(J)-5.)1073,1074,1074
 1073 IART=IART+1
 1074 CONTINUE
      Y(J)=Y(J)-BG
      IF(Y(J)-1.)1071,1071,1072
 1071 Y(J)=0.1
 1072 PRINT 308, TZ(J),Y(J)
  202 CONTINUE
C
C
      READ 331, (PARA(K),K=1,6)
      READ 331, (X(I),I=1,6)
      READ 331, (X(I),I=7,12)
      READ 331, (X(I),I=13,18)
      READ 331, (X(I),I=19,24)
      READ 331, (X(I),I=25,30)
      READ 331, (X(I),I=31,36)
      READ 331, (X(I),I=37,42)
      PLIMIT=PARA(5)
C
C
C     PRINT INIT DATA
      PRINT 1002, IFOM
C
      PRINT 305, (PARA(I),I=1,6)
      PRINT 304
      PRINT 305, (X(I), I = 1,N)
      PRINT 1111
  100 FORMAT (I5)
  101 FORMAT (6F12.7)
  302 FORMAT(F7.3)
  303 FORMAT(3F7.3)
  304 FORMAT (20) ESTIMATED VALUES OF X0)
  305 FORMAT (8 0, 8E14.7)
  306 FORMAT (20) COMPUTED VALUES0)
  307 FORMAT (1X, 8 U ES      )0)
  308 FORMAT (2F20.3)
  309 FORMAT(6F20.3)
  311 FORMAT (20 INITIAL FUNCTION VALUE 00 E20.10)
```

Recirculation

(cont.1)

```
 114 FORMAT(2A10)
 115 FORMAT(5A10)
 116 FORMAT(F6.3)
1111 FORMAT(1H1)
1001 FORMAT('RAW DATA DOG NR=',I6,'EXPERIMENT NR=',I6)
1002 FORMAT('NR OF ITERATIONS=',I6,'STEPWIDTH=',F6.1)
1003 FORMAT('THIS ARE THE FINAL VALUES')
1004 FORMAT('NORMALISING FACTOR          ',F12.6)
1005 FORMAT('COEFFICIENTS                ',3F12.7)
1006 FORMAT('SLOPES                      ',3F12.7)
1007 FORMAT('   RAPID FRACTION           ',F12.6)
1008 FORMAT('RECIRCULATION CORRECTION ',3F12.7)
1009 FORMAT('PASSAGE NR=',I6)
1011 FORMAT('CENTRAL CIRCULATION TIME            ',F10.5,'MINUTES')
1011 FORMAT('ADAPTED BACKGROUND                  ',3F12.7,'  CPM')
1012 FORMAT('RECIRCULATION PARAMETERS ',2F12.5,'ADAPTED')
1013 FORMAT('TIME AT MAXIMUM COUNTRATE           ',F10.5,'MINUTES')
1112 FORMAT('XXXXXXXXXXXXXXXXXXXXXXXXXXXXXXXXXXXXXXXXXXXXXXXXXXXXXXXXXXXXXXX
     6XXXXXXXXXXX')
C
C
C
      DO 21 I = 1, N
   21 XX(I) = X(I)
      ITRY=0
  400 ITRY=ITRY+1
      FO = F(Z)
      PRINT 111, FO
C
C     BEGINNING OF THE OPTIMIZATION
C
      K9 = 0
      DO 10 J = 1, IP
      K9 = K9 + 1
C
C     RANDOM DIRECTION GENERATOR
C     RANF(I)   RETURNS A RANDOM NUMBER UNIFORMLY DISTRIBUTED BETWEEN
C               ZERO AND ONE AT EACH CALL
C     R(I)   HAS A GAUSSIAN DISTRIBUTION
C
      DO 40 I = 1, N
```

Bremermann's Algoritme.

```
   10 CONTINUE
C
C
      DO 4 I=1,N
      X(I)=XX(I)
    4 CONTINUE
      PRINT 1111
      PRINT 1112
      PRINT 1001, NR,NREX
      PRINT 1009, ITRY
      DO 500 K=1,9
      COEF(K+9)=X(K+22)*X(K+31)
      COEF(K)=X(K+1)*X(K+10)
  500 CONTINUE
      DO 1 J=1,IP
      YC=0.
      DO 2 K=1,18
      IF(K-7)531,531,32
  531 LI=10
      TEST=(X(K+LI)*TZ(ISTART)-1.)/X(K+LI)
      GO TO 33
   32 LI=22
      TEST=0.
   33 CONTINUE
      YC=YC+COEF(K)*TZ(J)*EXP(10.-X(K+LI))*TZ(J)
     6-COEF(K)*TEST*EXP(10.-X(K+LI))*TZ(J))
    2 CONTINUE
      DUMMY=TZ(J)-TNORT
      IF(TZ(J)-2.)3,5,3
    3 DUMMY=DUMMY/TZ(J)
    5 REC=EXP(EXPO*DUMMY)/(1.+EXP(EXPO*DUMMY))
      DUMMY=ABS(TZ(J)-TNORT)*(0.-1.)
      XC=0.
      DO 6 K=1,2
      DO 6 L=1,18
      IF(L-9)502,502,73
  502 LI=10
      TEST=(X(L+LI)*TZ(ISTART)-1.)/X(L+LI)
      GO TO 74
   73 LI=22
      TEST=0.
   74 CONTINUE
```

Recirculation

(cont. 2)

```
      XC=XC+C(I)*COEF(I)*PARA(K)*X(2J)*PARA(K+1)*
     A(EXP(-(MM*PARA(K+1))
     6*EXP(-(MM*X(L+I)))
     6*(TEST-(X(L+I)-PARA(K+1)))*EXP(-(J)*MM*X(L+I))
     6-TEST*(X(L+I)-PARA(K+1))*EXP(-(J)*MM*PARA(K+1))
     6*EXP(-(J)*MM*X(L+I))*(J)-MM*(X(L+I)-PARA(K+1)))
     6/((X(L+I)-PARA(K+1))*(X(L+I)-PARA(K+1)))
    6 CONTINUE
      YC=YC*X(I)
      YC=YC*(J+1)
      XC=XC*RES
      YC=YC*XC
      ZEXP(J)=Y(J)+C
      PRINT 333, TZ(J),Y(J),YC,ZEXP(J)
      XEXP(J)=XC
      YEXP(J)=YC
    1 CONTINUE
      PRINT 324, (XX(I),I=1,N)



      PRINT 1112
      PRINT 1112
      PRINT 1334, X(1)
      PRINT 1335,(COEF(K),K=1,9)
      PRINT 1336, (X(K),K=10,10)
      PRINT 1338, (X(K),K=20,22)
      PRINT 1335, (COEF(K),K=17,18)
      PRINT 1336, (X(K),K=32,40)
      PRINT 1311, INORT
      PRINT 1311, NS,KNO,X(41)
      PRINT 1312, (PARA(K),K=1,6)
      PRINT 1313, TZ(ISTART)
      PRINT 1112
      PRINT 1111
      IF(ITRY-4)400,401,401
  401 CONTINUE
      CALL CCSGN
      CALL PLOT(1.,1.,2,IP,TZ,Y,XLAB,YLAB,TITLE)
      CALL PLOT (1.,2.,1,IP,TZ,YEXP,BLANK,BLANK,CURV)
      CALL PLOT (1.,2.,1,IP,TZ,XEXP,BLANK,BLANK,CURV)
      CALL CCNEXT
      PRINT 1111
      CALL PLOT (1.,1.,2,ISTART,TZ,ZEXP,BLANK,BLANK,CURV)
      CALL CCNEXT
C
C
      DO 20 J=1,IP
      Y(J)=Y(J)/X(1)
      IF(Y(J)-0.000001)23,23,24
   23 Y(J)=0.000001
   24 Y(J)=ALOG10(Y(J))
      YEXP(J)=YEXP(J)/X(1)
      IF(YEXP(J)-0.000001)25,25,22
   25 YEXP(J)=0.000001
   22 YEXP(J)=ALOG10(YEXP(J))
      XEXP(J)=XEXP(J)/X(1)
      IF(XEXP(J)-0.000001)90,90,91
   90 XEXP(J)=0.000001
   91 XEXP(J)=ALOG10(XEXP(J))
   20 CONTINUE
      CALL PLOT(1.,1.,2,IP,TZ,Y,XLAB,YLAB,TITLE)
      CALL PLOT (1.,2.,1,IP,TZ,YEXP,BLANK,BLANK,CURV)
      CALL PLOT(1.,2.,1,IP,TZ,XEXP,BLANK,BLANK,BLANK)
      CALL CCNEXT
      PRINT 1111
      DO 505 J=1,60
      IF(J-20)506,506,507
  506 TZ(J)=(J-1.)*2
      GO TO 510
  507 IF(J-30)508,508,509
  508 TZ(J)=J*1.-17.
      GO TO 510
  509 TZ(J)=J*2.-48.
  510 CONTINUE
      YC=0.
      DO 511 K=1,18
      IF(K-9)512,512,513
  512 LI=10
      TEST=(X(K+LI)*TZ(ISTART)-1.)/X(K+LI)



      GO TO 514
  513 LI=32
      TEST=0.
  514 CONTINUE
      YC=YC+COEF(K)*(TZ(J)*EXP((0.-X(K+LI)))*TZ(J))
     6-COEF(K)*TEST*EXP((0.-X(K+LI)))*TZ(J))
  511 CONTINUE
      YL(J)=YC*1000.
      PRINT 338, TZ(J),Y(J)
  505 CONTINUE
      PRINT 1111
      CALL PLOT (1.,1.,1,22,TZ,Y,XLAB,YLAB,TITLE)
      CALL CCNEXT
      CALL PLOT (1.,1.,1,45,TZ,Y,XLAB,YLAB,TITLE)
      CALL CCEND
C
C
      STOP
      END
```

Bypass .Determination

```
      PROGRAM KATE(INPUT,OUTPUT,TAPE3=OUTPUT,TAPE98=101,PLOT,TAPE99=PLOT
     A)
      COMMON X(100),N,IP,ID,TZ(300),Y(300),XX(100),PARA(12),ALFA
     6,ITALL,ITEST,SLOPE(12),PTEST
      DIMENSION R(300),TITLE(6),XLAB(3),YLAB(3),BLANK(3),CURV(6),
     6YEXP(300),XEXP(300),WEXP(300)
      DO 906 I=295,300
      Y(I)=1.
  906 CONTINUE
      ALFA=0.9
C
C     X = ARRAY OF VARIABLES
C     N = NUMBER OF VARIABLES
C     IP = NUMBER OF EXPERIMENTAL POINTS TAKEN ALONG EACH SPECTRUM
C     IT = NUMBER OF ITERATIONS
C     H  = DISTANCE BETWEEN THE POINTS OF LAGRANGIAN INTERPOLATION
C
      CURV(6)=0.
      BLANK(3)=0.
      TITLE(6)=0.
      XLAB(3)=0.
      YLAB(3)=0.
      READ 314, (TITLE(K),K=1,6)
      READ 314, (CURV(K),K=1,6)
      READ 313, (BLANK(K),K=1,3)
      READ 313, (XLAB(K),K=1,2)
      READ 313, (YLAB(K),K=1,2)
      READ 303, N
      READ 300, IT
      READ 300, NREF
      READ 316, H
      READ 302, ENORT
C
C     READ IN SPECTRA
C
      IP=0
      ID=0
      DO 199 J=1,300
      IP=IP+1
      READ 303, TZ(J),Y(J),INDEX,TEST
      IF(INDEX-1)200,200,201
  200 ID=ID+1
      GO TO 203
  201 TZ(J)=TZ(J)-ENORT
  203 CONTINUE
      IF(ITEST-3.)199,202,202
  199 CONTINUE
  202 CONTINUE
C
      READ 301, (PARA(I),I=1,6 )
      READ 301, (PARA(I),I=7,12)
C
      READ 301, (X(I) , I = 1, N)
C
      DO 91 K=7,12
      X(K)=PARA(K)
   91 CONTINUE
C     PRINT OUT DATA
C
      PRINT 304
      PRINT 305, (X(I), I = 1, N)
  300 FORMAT (I6)
  301 FORMAT (6F12.7)
  302 FORMAT(F7.3)
  303 FORMAT(2F7.3,I2,F7.3)
  304 FORMAT (*0 ESTIMATED VALUES OF X*)
  305 FORMAT (* *, 8E14.7)
  306 FORMAT (*0 COMPUTED VALUES*)
  307 FORMAT (1X, * J IS     *)
  308 FORMAT (2F20.3)
  309 FORMAT(*    *,3F10.3,*    *,2F10.3)
  311 FORMAT (*0 INITIAL FUNCTION VALUE =*, E20.10)
  313 FORMAT(2A10)
  314 FORMAT(6A10)
  316 FORMAT(F6.3)
 1111 FORMAT(1H1)
 1001 FORMAT(*BYPASS    FRACTION*,F14.6)
 1002 FORMAT(*SLOPE ADAPTOR      *,2F14.6)
 1003 FORMAT(*COEFFICIENTS       *,2F14.6)
 1004 FORMAT(*ARGUMENT FRACTION *,3F9.5)
 1005 FORMAT(*SLOPES             *,2F14.6)
 1006 FORMAT(*ADAPTED BACKGROUND        *,F12.5,*CPM*)
 1007 FORMAT(*EXPERIMENT NUMBER         *,I6)
 1008 FORMAT(*                          *,F15.6)
      SXX=0.
      SX=0.
      SY=0.
      SXY=0.
      DO 800 K=1,13
      J=IP-K+1
      SX=SX+TZ(J)
```

Bypass
(cont. 1)

```
      SY=SY+ALOG(Y(J))
      SXX=SXX+TZ(J)**2
      SXY=SXY+TZ(J)*ALOG(Y(J))
  800 CONTINUE
      X(7)          =(10.*SXY-SX*SY)/(10.*SXX-SX*SX)
      X(7)=ABS(X(7))
      SLOPE(7)=X(7)*(0.-1.)
      PTEST=X(7)
      PRINT 302, PTEST
      X(10)=X(7)*2.
      X(11)=X(7)*3.
      SXX=0.
      SX=0.
      SY=0.
      SXY=0.
      DO 801 K=1,4
      J=10-K+1
      SX=SX+TZ(J)
      SY=SY+ALOG(Y(J))
      SXX=SXX+TZ(J)**2
      SXY=SXY+TZ(J)*ALOG(Y(J))
  801 CONTINUE
      SLOPE(5)    =(4.*SXY-SX*SY)/(4.*SXX-SX*SX)
      X(5)=ABS(SLOPE(5)/PARA(5))
      DO 21 I = 1, N
   21 XX(I) = X(I)
      ITALL=0
  900 CONTINUE



      ITALL=ITALL+1
      F0 = F(Z)
      PRINT 311, F0
C
C     BEGINNING OF THE OPTIMIZATION
```

BREMERMANN'S OPTIMIZATION ALGORITME

```
      DO 28 I=1,N
      X(I)=XX(I)
   28 CONTINUE
      PRINT 1111
      PRINT 314, (TITLE(K),K=1,5)
      PRINT 1037, NREX
      DO 26 K=1,6
      SLOPE(K)=X(K)*(0.-1.) *PARA(K)
   26 CONTINUE
      DO 27 K=7,12
      SLOPE(K)=X(K)*(0.-1.)
   27 CONTINUE
      DO 1 J=1,10
      YC=0.
      XC=0.
      INDEX=11
      DO 2 K=11,15
      INDEX=INDEX-1
      KDEX =INDEX-1
      IF(J-(10-K+6))3,3,4
    3 YC=YC+X(K)*        (EXP(SLOPE(K-INDEX)*TZ(J))-EXP(SLOPE(K-KDEX)*
     6TZ(J)))
      GO TO 5
    4 YC=YC+X(K)*X(K+6)*(EXP(SLOPE(K-INDEX)*TZ(J))-EXP(SLOPE(K-KDEX)*
     6TZ(J)))
      XC=XC+X(K+3)*(EXP(SLOPE(K-INDEX+6)*TZ(J))-EXP(SLOPE(K-KDEX+6)*TZ(J
     6)))
    5 CONTINUE
    2 CONTINUE
      YC=YC+XC
      YEXP(J)=YC
      XEXP(J)=XC
      WEXP(J)=YC-XC
      PRINT 339, TZ(J),Y(J),YC,EXP(J),WEXP(J)
    1 CONTINUE
      ALFA=WEXP(1)
      PRINT 1031, ALFA
      PRINT 1032, (X(I),I= 1, 2 )
      PRINT 1032, (X(I),I= 3, 4 )
```

Bypass (cont. 2)

```
      PRINT 1002, (X(I),I= 5, 6 )
      PRINT 1002, (X(I),I= 7, 8 )
      PRINT 1002, (X(I),I= 9, 10)
      PRINT 1002, (X(I),I= 11,12)
      PRINT 1003, (X(I),I=13,18)
      PRINT 1005, (SLOPE(I),I=1,12)
      PRINT 1004, (X(I),I=19,21)
      DUMMY=0.
      INDEX=10
      DO 905 K=16,18
      INDEX=INDEX-1
      KDEX=INDEX-1
      DUMMY=DUMMY+X(K)*(SLOPE(K-INDEX)-SLOPE(K-KDEX))
     6/(SLOPE(K-KDEX)*SLOPE(K-INDEX))
  905 CONTINUE
      PRINT 1008, DUMMY
      PRINT 1111
      IF(ITALL-3)903,902,901
  902 CONTINUE
      K=5.
      GO TO 900
  901 CONTINUE
      DUMMY=1000./(ALFA*1000.+DUMMY)
      ALFA=ALFA*DUMMY
      DO 906 K=16,21
      X(K)=X(K)*DUMMY
  906 CONTINUE
      IT=IT+1
      DO 907 J=IT,IP
      Y(J)=Y(J)        *DUMMY
      YEXP(J)=YEXP(J)*DUMMY
      XEXP(J)=XEXP(J)*DUMMY
      XEXP(J)=XEXP(J)*DUMMY
  907 CONTINUE
      PRINT 1001, ALFA
      SX =0.
      SY =0.
      SXX=0.
      SXY=0.
      DUMMY=0.
      TEST=0.
      J=0
      DO 908 K=13,15
      J=J+1
      L=J*2
      SX    =SX    +X(K  )*(1./SLOPE(L-1)**2-1./SLOPE(L  )**2)
      SY    =SY    +X(K  )*(1./SLOPE(L  )   -1./SLOPE(L-1)   )
      SXX   =SXX   +X(K+3)*(1./SLOPE(L+5)**2-1./SLOPE(L+6)**2)
      SXY   =SXY   +X(K+3)*(1./SLOPE(L+6)   -1./SLOPE(L+5)   )
      DUMMY=DUMMY+X(K  )*(1./SLOPE(L-1)**2-1./SLOPE(L  )**2)*X(K+6)
      TEST =TEST +X(K  )*(1./SLOPE(L  )   -1./SLOPE(L-1)   )*X(K+6)
  908 CONTINUE
      Y(290)=SX/SY
      Y(291)=DUMMY/TEST
      Y(292)=SXX/SXY
      Y(293)=(DUMMY+SXX)/(TEST+SXY)
      PRINT 1020, Y(290)
      PRINT 1021, Y(291)
      PRINT 1022, Y(292)
      PRINT 1023, Y(293)
      PRINT 1024
      PRINT 1025
      DO 920 K=1,3
      INDEX=K
      I=K*2
      PARA(K)=ABS(SLOPE(I)+SLOPE(I-1))/(SLOPE(I)*SLOPE(I-1))
      PARA(K+3)=          X(K+12)*(SLOPE(I-1)-SLOPE(I))/(          1000.
     6*SLOPE(I-1)*SLOPE(I))
      PARA(K+6)=PARA(K)*PARA(K+3)/Y(290)
      PRINT 1026, INDEX,PARA(K),PARA(K+3),PARA(K+6)
  920 CONTINUE
      PRINT 1027
      DO 921 K=4,6
      INDEX=K-3
      I=K*2
      PARA(K)=ABS(SLOPE(I)+SLOPE(I-1))/(SLOPE(I)*SLOPE(I-1))
      PARA(K+3)=          X(K+12)*(SLOPE(I-1)-SLOPE(I))/((1.-ALFA)*1000.
     6*SLOPE(I-1)*SLOPE(I))
      PARA(K+6)=PARA(K)*PARA(K+3)/Y(292)
      PRINT 1026, INDEX,PARA(K),PARA(K+3),PARA(K+6)
```

Bypass (cont. 3)

```
921 CONTINUE
    PRINT 1028
    DO 922 K=1,3
    INDEX=K
    I=K*3
    PARA(K)=ABS(SLOPE(I)+SLOPE(I-1))/(SLOPE(I)*SLOPE(I-1))
    PARA(K+3)=X(K+18)*X(K+12)*(SLOPE(I-1)-SLOPE(I))/( ALFA*    1000.
   6*SLOPE(I-1)*SLOPE(I))
    PARA(K+6)=PARA(K)*PARA(K+3)/Y(291)
    PRINT 1026, INDEX,PARA(K),PARA(K+3),PARA(K+6)
922 CONTINUE
    PRINT 1111
1020 FORMAT(*MEAN TRANSIT TIME FOR  INTRAVASCULAR     *,F15.6,*MINUTES*)
1021 FORMAT(*MEAN TRANSIT TIME FOR  BYPASS            *,F15.6,*MINUTES*)
1022 FORMAT(*MEAN TRANSIT TIME FOR  PERFUSION         *,F15.6,*MINUTES*)
1023 FORMAT(*MEAN TRANSIT TIME FOR  TOTAL DIFF        *,F15.6,*MINUTES*)
1024 FORMAT(*          COMPARTIMENTAL ANALYSIS)*)
1025 FORMAT(*   INTRAVASCULAR*)
1026 FORMAT(*COMP NR*,I3,*MEAN TRNST T *,F10.3,*MIN  FRACT FLOW*,
   6F6.3,* FRCT VOL *,F6.3)
1027 FORMAT(*  TISSUE PERFUSION*)
1028 FORMAT(*   BYPASS *)
    X(1)=3.-5.
    X(2)=30.
    XX(1)=ALOG10(1600.)
    XX(2)=ALOG10(0.1)
    CALL PLOT(1.1.2.2.X.XX.XLAB.YLAB.TITLE)
    X(2)=0.
    XX(1)=ALOG10(1000.)
    XX(2)=ALOG10(100.)
    CALL CCRGN
    CALL PLOT(1.2.1.2.X.XX.BLANK.BLANK.BLANK)
    XX(1)=ALOG10(100.)
    XX(2)=ALOG10(10.)
    CALL PLOT(1.2.1.2.X.XX.BLANK.BLANK.BLANK)
    XX(1)=ALOG10(10.)
    XX(2)=ALOG10(1.)
    CALL PLOT(1.2.1.2.X.XX.BLANK.BLANK.BLANK)
    XX(1)=ALOG10(1.)
    XX(2)=ALOG10(.1)
    CALL PLOT(1.2.1.2.X.XX.BLANK.BLANK.BLANK)
    DO 20 J=1.IP
    IF(Y(J)-.)25.25.22
 25 Y(J)=0.0001
 22 Y(J)=ALOG10(Y(J))
    IF(YEXP(J)-.)23.23.24
 23 YEXP(J)=0.00001
 24 YEXP(J)=ALOG10(YEXP(J))
    IF(XEXP(J)-.)911.911.912
911 XEXP(J)=0.001
912 XEXP(J)=ALOG10(XEXP(J))
    IF(WEXP(J)-0.)913.913.914
913 WEXP(J)=0.001
914 WEXP(J)=ALOG10(WEXP(J))
 20 CONTINUE
    CALL PLOT(1.2.2.IP.TZ.Y.BLANK.BLANK.CURV)
    CALL PLOT(1.2.1.ID.TZ.YEXP.BLANK.BLANK.CURV)
    DO 915 J=IT.IP
    Y(J-IT+1)=YEXP(J)
    TZ(J-IT+1)=TZ(J)
915 CONTINUE
    ID=IP-IT
    CALL PLOT(1.2.1.ID.TZ.Y.BLANK.BLANK.CURV)
    DO 909 J=IT.IP
    Y(J-IT+1)=XEXP(J)
909 CONTINUE
    CALL PLOT(1.2.1.ID.TZ.Y.BLANK.BLANK.CURV)
    DO 910 J=IT.IP
    Y(J-IT+1)=WEXP(J)
910 CONTINUE
    CALL PLOT(1.2.1.ID.TZ.Y.BLANK.BLANK.CURV)
    CALL CCEND
    PRINT 924, (XX(I).I=1.N)
    STOP
    END
```

F(Z) for Xenon data

```
      FUNCTION F(Z)
      COMMON X(100),N,IP,Y(300),TZ(300),TLAG,INJRT,EXPO,PARA(6),COEF(20)
     6,PLIMIT,ISTART,ISTOP,XX(100),ITRY,RET
     6,RSLOPE,XNO
      DO 90 K=1,40
      IF(X(K)-0.)91,90,90
   91 X(K)=0.00001
   90 CONTINUE
      IF(ITRY-1)401,400,402
  402 IF(ITRY-2)406,401,405
  400 IDO=ISTOP
      IDA=IP
      DO 408 K=2,4
      X(K)=XX(K)
      X(K+9)=XX(K+9)
      X(K+21)=XX(K+21)
      X(K+30)=XX(K+30)
  408 CONTINUE
      GO TO 406
  401 IDO=1
      IDA=ISTOP
      DO 409 K=2,10
      X(K)=XX(K)
      X(K+9)=XX(K+9)
      X(K+21)=XX(K+21)
      X(K+30)=XX(K+30)
  409 CONTINUE
      GO TO 406
  405 CONTINUE
      IDO=1
      IDA=IP
  406 CONTINUE
      DO 80 K=11,19
      IF(X(K)-0.01)81,82,82
   81 X(K)=0.01
   82 IF(X(K+21)-1.)83,80,80
   83 X(K+21)=1.
   80 CONTINUE
      IF(X(40)-0.15)93,92,92
   93 X(40)=0.15
   92 CONTINUE
      IF(X(41)-XNO)86,86,87
   87 X(41)=XNO
   86 IF(X(41)-0.1)88,89,89
   88 X(41)=0.1
   89 CONTINUE
      SX    =0.
      SY    =0.
      SXY   =0.
      SXX=0.
      DO 35 I=1,10
      J=IP-1+I
      SX=SX  +TZ(J)
      SXX=TZ(J)**2     +SXX
      SY=  (ALOG(Y(J)-X(41))-ALOG(TZ(J)))    +SY
      SXY=(ALOG(Y(J)  -X(41))-ALOG(TZ(J)))*TZ(J)       +SXY
   35 CONTINUE
      X(19)=(10.*SXY-SX*SY)/(SXX*10.-SX*SX)



      X(19)=ABS(X(19))
      DO 40 K=1,N
      IF(X(K)-0.)41,41,40
   41 X(K)=0.1
   40 CONTINUE
      DO 65 K=2,4,2
      DO 36 L=11,19
      IF(X(L)-PARA(K))36,37,36
   37 X(L)=0.99*PARA(K)
   36 CONTINUE
      DO 65 L=32,40
      IF(X(L)-PARA(K))65,66,65
   66 X(L)=0.99*PARA(K)
   65 CONTINUE
      DO 23 K=22,22
      X(K)=XX(K)
   23 CONTINUE
      SUM=0.
      DO 61 K=2,10
      SUM=SUM+X(K+21)/X(K+30)
      SUM=SUM+X(K)*(2.-        X(K+9)*TZ(ISTART))/X(K+9)
   61 CONTINUE
      IF(SUM-0.178.78,68
   78 SUM=SUM*(0.-1.)
```

F(Z), Xenon (cont.)

```
   68 IF(SUM-1.)69,69,70
   70 CONTINUE
      DO 62 K=2,18
      X(K)=X(K)                    /SUM
      X(K+21)=X(K+21)/SUM
   62 CONTINUE
   69 CONTINUE
      DO 500 K=1,9
      COEF(K)=X(K+1)*X(K+10)
      COEF(K+9)=X(K+22)*X(K+31)
  500 CONTINUE
      YC=0.
      DO 42 K=1,18
      IF(K-9)24,24,25
   24 LI=10
      TEST=(X(K+LI)*TZ(ISTART)-1.)/X(K+LI)
      GO TO 26
   25 LI=22
      TEST=0.
   26 CONTINUE
      YC=YC+COEF(K)*TZ(ISTART)*EXP((0.-X(K+LI))*TZ(ISTART))
     6-COEF(K)*TEST*EXP((0.-X(K+LI))*TZ(ISTART))
   42 CONTINUE
      IF(YC-0.)27,67,27
   27 CONTINUE
      DUMMY=0.9*(Y(ISTART)-X(41))/YC
      IF(X(1)-DUMMY)43,44,44
   43 X(1)=DUMMY
   44 DUMMY=1.1*(Y(ISTART)-X(41))/YC
      IF(X(1)-DUMMY)46,46,45
   45 X(1)=DUMMY
   46 CONTINUE
   67 CONTINUE
      SUM=0.
      DO 1 I=100,100
      YC=0.
```

```
      DO 2 K=1,18
      IF(K-9)31,31,32
   31 LI=10
      TEST=(X(K+LI)*TZ(ISTART)-1.)/X(K+LI)
      GO TO 33
   32 LI=22
      TEST=0.
   33 CONTINUE
      YC=YC+COEF(K)*TZ(J)*EXP((0.-X(K+LI))*TZ(J))
     6-COEF(K)*TEST*EXP((0.-X(K+LI))*TZ(J))
    2 CONTINUE
      DUMMY=TZ(J)-TNORT
      IF(TZ(J)-0.)3,5,3
    3 DUMMY=DUMMY/TZ(J)
    5 REC=EXP(EXPO*DUMMY)/(1.+EXP(EXPO*DUMMY))
      DUMMY=ABS(TZ(J)-TNORT)*(0.-1.)
      XC=0.
      DO 6 K=1,9,2
      DO 6 L=1,18
      IF(L-9)72,72,73
   72 LI=10
      TEST=(X(L+LI)*TZ(ISTART)-1.)/X(L+LI)
      GO TO 74
   73 LI=22
      TEST=0.
   74 CONTINUE
      XC=XC+X(1)*COEF(L)*PARA(K)*X(20)*PARA(K+1)*
     6(EXP(DUMMY*PARA(K+1))
     6-EXP(DUMMY*X(L+LI)))
     6+TEST*(X(L+LI)-PARA(K+1))*EXP(DUMMY*X(L+LI))
     6-TEST*(X(L+LI)-PARA(K+1))*EXP(DUMMY*PARA(K+1))
     6+EXP(DUMMY*X(L+LI))*DUMMY*(X(L+LI)-PARA(K+1)))
     6/((X(L+LI)-PARA(K+1))*(X(L+LI)-PARA(K+1)))
    6 CONTINUE
      XC=XC*REC
      XC=XC+X(41)
      YC=YC*X(1)
      SUM=SUM+((XC+YC-Y(J))/Y(J))**2
    1 CONTINUE
      F = SUM
      RETURN
      END
```

F(Z) for Colloid data

```
      FUNCTION F(Z)
      COMMON X(100),N,IP,Y(300),TZ(300),TLAG,TNORT,EXPO,PARA(6),COEF(20)
     6,PLIMIT,ISTART,ISTOP,XX(100),ITRY,RET
     6,RSLOPE,XNO
      IF(ITRY-1)400,401,402
  402 IF(ITRY-2)405,401,405
  400 CONTINUE
      IDO=1
      IDA=IP
      GO TO 406
  401 CONTINUE
      IDO=ISTOP
      IDA=IP
      DO 407 K=2,19
      X(K)=XX(K)
      X(K+21)=XX(K+21)
  407 CONTINUE
      GO TO 406
  405 CONTINUE
      IDO=1
      IDA=IP
      DO 408 K=20,22
      X(K)=XX(K)
  408 CONTINUE
  406 CONTINUE
      IF(X(41)-XNO)86,86,87
   87 X(41)=XNO
   86 IF(X(41)-0.1)88,89,89
   88 X(41)=0.1
   89 CONTINUE
      DO 23 K=21,22
      IF(X(K)-1.25)21,21,20
   20 X(K)=1.25
   21 IF(X(K)-0.75)22,23,23
   22 X(K)=0.75
   23 CONTINUE
      DO 40 K=1,N
      IF(X(K)-0.1)41,41,40
   41 X(K)=0.1
   40 CONTINUE
      PARA(2)=X(22)*RET
      PARA(4)=X(21)*RSLOPE
      DO 90 K=32,40
      TEST=PARA(2)*1.1    **2.5
      IF(X(K)-TEST)91,93,93
   91 X(K)=TEST
   93 IF(X(K-21)-TEST)92,90,90
   92 X(K-21)=TEST
   90 CONTINUE
      DO 65 K=2,4,2
      DO 36 L=11,19
      IF(X(L)-PARA(K))36,37,36
   37 X(L)=0.9*PARA(K)
   36 CONTINUE
      DO 65 L=32,40
      IF(X(L)-PARA(K))65,66,65
   66 X(L)=0.9*PARA(K)
   65 CONTINUE
      SUM=0.




      DO 61 K=2,10
      SUM=SUM+X(K+21)/X(K+30)
      SUM=SUM+X(K)*(2.-        X(K+9)*TZ(ISTART))/X(K+9)
   61 CONTINUE
      IF(SUM-0.)78,78,68
   78 SUM=SUM*(0.-1.)
   68 CONTINUE
      DO 62 K=2,10
      X(K)=X(K)                /SUM
      X(K+21)=X(K+21)/SUM
   62 CONTINUE
      DO 500 K=1,9
      COEF(K)=X(K+1)*X(K+10)
      COEF(K+9)=X(K+22)*X(K+31)
  500 CONTINUE
      YC=0.
      DO 42 K=1,18
      IF(K-9)24,24,25
   24 LI=10
      TEST=(X(K+LI)*TZ(ISTART)-1.)/X(K+LI)
      GO TO 26
   25 LI=22
      TEST=0.
   26 CONTINUE
      YC=YC+COEF(K)*TZ(ISTART)*EXP((0.-X(K+LI))*TZ(ISTART))
     6-COEF(K)*TEST*EXP((0.-X(K+LI))*TZ(ISTART))
   42 CONTINUE
      IF(YC-0.)27,67,27
   27 CONTINUE
```

F(Z) for Colloid data (cont.)

```
      DUMMY=0.9*(Y(ISTART)-X(61))/YC
      IF(X(1)-DUMMY)43,44,44
   43 X(1)=DUMMY
   44 DUMMY=1.1*(Y(ISTART)-X(61))/YC
      IF(X(1)-DUMMY)46,46,45
   45 X(1)=DUMMY
   46 CONTINUE
   47 CONTINUE
      DUMMY=ABS(TZ(IP-1)-TNORT)*(0.-1.)
      XC=0.
      DO 52 K=1,3,2
      DO 52 L=1,19
      IF(L-9)28,28,29
   28 LI=10
      TEST=(X(L+LI)*TZ(ISTART)-1.)/X(L+LI)
      GO TO 30
   29 LI=20
      TEST=0.
   30 CONTINUE
      XC=XC+X(1)*COEF(L)*PARA(K)*PARA(K+1)*
     6                                    (EXP(DUMMY*PARA(K+1))
     6                                    -EXP(DUMMY*X(L+LI))
     6+TEST*(X(L+LI)-PARA(K+1))*EXP(DUMMY*X(L+LI))
     6-TEST*(X(L+LI)-PARA(K+1))*EXP(DUMMY*PARA(K+1))
     6                                    +EXP(DUMMY*X(L+LI))*DU44Y*
     6(X(L+LI)-
     6PARA(K+1)))/((X(L+LI)-PARA(K+1))*(X(L+LI)-PARA(K+1)))
   52 CONTINUE
      TEST=(Y(IP-2)+Y(IP-1)+Y(IP))/3.  -X(61)
      DU44Y=TEST*0.95/XC
      IF(X(20)-DUMMY)53,54,54

   53 X(20)=DU44Y
   54 DU44Y=TEST*1.05/XC
      IF(X(20)-DUMMY)56,56,55
   55 X(20)=DUMMY
   56 CONTINUE
      IF(X(20)-1.)80,80,81
   80 X(20)=1.
   81 CONTINUE
      IF(X(20)-25.)95,95,96
   96 X(20)=25.
   95 CONTINUE
      SUM=0.
      DO 1 J=100,104
      XC=0.
      DO 2 K=1,18
      IF(K-9)31,31,32
   31 LI=10
      TEST=(X(K+LI)*TZ(ISTART)-1.)/X(K+LI)
      GO TO 33
   32 LI=20
      TEST=0.
   33 CONTINUE
      XC=XC+COEF(K)*TZ(J)*EXP(0.-X(K+LI))*TZ(J))
     6-COEF(K)*TEST*EXP(0.-X(K+LI))*TZ(J))
    2 CONTINUE
      DUMMY=TZ(J)-TNORT
      IF(TZ(J)-0.)3,5,3
    3 DUMMY=DUMMY/TZ(J)
    5 REC=EXP(EXPO*DUMMY)/(1.+EXP(EXPO*DUMMY))
      DUMMY=ABS(TZ(J)-TNORT)*(0.-1.)
      XC=0.
      DO 6 K=1,3,2
      DO 6 L=1,19
      IF(L-9)72,72,73
   72 LI=10
      TEST=(X(L+LI)*TZ(ISTART)-1.)/X(L+LI)
      GO TO 74
   73 LI=20
      TEST=0.
   74 CONTINUE
      XC=XC+X(1)*COEF(L)*PARA(K)*X(20)*PARA(K+1)*
     6(EXP(DUMMY*PARA(K+1))
     6-EXP(DUMMY*X(L+LI)))
     6+TEST*(X(L+LI)-PARA(K+1))*EXP(DUMMY*X(L+LI))
     6-TEST*(X(L+LI)-PARA(K+1))*EXP(DUMMY*PARA(K+1))
     6+EXP(DUMMY*X(L+LI))*DUMMY*(X(L+LI)-PARA(K+1)))
     6/((X(L+LI)-PARA(K+1))*(X(L+LI)-PARA(K+1)))
    6 CONTINUE
      XC=XC*REC
      XC=XC+X(41)
      YC=YC*X(1)
      IF(TZ(J)-2.)61,60,59
   59 SUM=SUM+(0.1-YC)**2)/0.1
      SUM=SUM+(XC-Y(J))**2
      GO TO 1
   60 SUM=SUM+((YC+XC-Y(J))**2)*10.
    1 CONTINUE
      F = SUM
      RETURN


      END
```

F(Z) for BYPASS maximising

```
      FUNCTION F(Z)
      COMMON X(100),N,IP,ID,TZ(300),Y(300),XX(100),PARA(12),ALFA
     6,ITALL,ITEST,SLOPE(12),PTEST
      X(6)=XX(6)
      DO 53 K=7,12
      TEST=X(K)*PARA(K))*0.9
      IF(X(K)-TEST)53,53,54
   54 X(K)=TEST
   53 CONTINUE
      IF(ITALL-2)900,901,902
  900 CONTINUE
      DO 903 K=7,12
      X(K)=XX(K)
      X(K+2)=XX(K+2)
  903 CONTINUE
      GO TO 917
  901 CONTINUE
      DO 916 K=1,6
      X(K)=XX(K)
  916 CONTINUE
      DO 917 K=13,15
      X(K)=XX(K)
  917 CONTINUE
      GO TO 912
  902 CONTINUE
  912 CONTINUE
C                                 ALL VARIABLES ARE POSITIVE
      DO 8 K=1,N
      IF(X(K)-0.00001)8,8,9
    8 X(K)=0.00001
    9 CONTINUE
      DO 40 K=13,15
      IF(X(K)-10.)41,40,40
   41 X(K)=10.
   40 CONTINUE
      DO 42 K=16,18
      IF(X(K)-0.1)43,42,42
   43 X(K)=0.1
   42 CONTINUE
C                                  INIT VAL FOR SLOPES OF NO ARE WHEN TO PERC
      DO 10 K=1,4
      IF(X(K)-1.33)12,12,11
   11 X(K)=1.33
      GO TO 14
   12 IF(X(K)-.73)13,14,14
   13 X(K)=0.73
   14 CONTINUE
      SLOPE(K)=PARA(K)*X(K)*(0.-1.)
   10 CONTINUE
      SLOPE(5)=PARA(5)*X(5)*(0.-1.)
      SLOPE(6)=PARA(6)*X(6)*(0.-1.)
C                                  NEGATIVE ARGUMENT HAS LARGER SLOPE
C                                  A*(EXP(-AT)-EXP(-BT))
C                                  0.7*B * A
C                                  B IS SLOPE(K+1) A IS SLOPE(K)
      DO 15 K=1,5,2
      TEST=ABS(SLOPE(K))*1.5
      IF(ABS(SLOPE(K+1))-TEST)16,15,15
   16 X(K+1)=ABS(TEST/PARA(K+1))
      SLOPE(K+1)=PARA(K+1)*X(K+1)*(0.-1.)
   15 CONTINUE
C                                  G*(EXP(-CT)-EXP(-DT))
C                                  D*0.9*C
C                                  D * 0.3
      DO 17 K=8,12,2
      DUMMY=PTEST*(0.8+(K-8)*0.4)
      IF(X(K-1)-DUMMY)32,33,33
   32 X(K-1)=DUMMY
   33 CONTINUE
      DUMMY=8.*X(K-1)
      IF(X(K)-DUMMY)18,19,19
   18 X(K)=DUMMY
   19 CONTINUE
      SLOPE(K)  =(0.-1.)*X(K)
      SLOPE(K-1)=(0.-1.)*X(K-1)
   17 CONTINUE
      IF(ITALL-2)912,911,911
  911 CONTINUE
C                                 TAIL OF DIFF IS EXCLUSIVE TISS PERFUSION
C                                   AVERAGE TAIL VALUES
      DUMMY=0.
      TEST=0.
      DO 22 I=1,10
      DUMMY=DUMMY+TZ(IP-I)
      TEST=TEST+ALOG(Y(IP-I))
   22 CONTINUE
      DUMMY=DUMMY/10.
      TEST=TEST/10.
      TEST=EXP(TEST)
      YC=0.
      INDEX=10
      DO 23 K=16,18
```

F(Z) for BYPASS
(cont.)

```
      INDEX=INDEX-1
      KDEX=INDEX-1
      YC=YC+X(K)*(EXP(SLOPE(K-INDEX)*DUMMY)-EXP(SLOPE(K-KDEX)*DUMMY))
   23 CONTINUE
      DUMMY=TEST/YC
      Y(295)=TEST
      Y(296)=YC
      Y(297)=DUMMY
      DO 24 K=16,18
      X(K)=X(K)*DUMMY
   24 CONTINUE
C                              DEFINITION OF THE COEFFICIENTS
  912 CONTINUE
      IF(ITALL-2)915,913,915
  915 CONTINUE
      TEST=0.
      DUMMY=0.
      DO 31 I=1,4
      TEST=TEST+ALOG(Y(10-I)
      DUMMY=DUMMY+TZ(10-I)
   31 CONTINUE
      TEST=TEST/4.
      TEST=EXP(TEST)
      DUMMY=DUMMY/4.
      X(15)=TEST/(EXP(SLOPE(5)*DUMMY)-EXP(SLOPE(6)*DUMMY))
      Y(300)=X(15)*(SLOPE(5)-SLOPE(6))/(SLOPE(5)*SLOPE(6))
      DUMMY=0.




      INDEX=0-1
      KDEX=0
      DO 26 K=13,16
      INDEX=INDEX+2
      KDEX=KDEX+2
      DUMMY=DUMMY+X(K)*       (SLOPE(INDEX)-SLOPE(KDEX))
     6/(SLOPE(INDEX)*SLOPE(KDEX))
   26 CONTINUE
      Y(299)=DUMMY+Y(300)
      DO 27 K=13,16
      TEST=X(K)*(1.0-Y(299)*TZ(1))*DUMMY
      X(K)=TEST
   27 CONTINUE
      IF(ITALL-2)914,913,913
  913 CONTINUE
      DO 28 K=13,21
      IF(X(K)-1.0)34,36,39
   34 X(K)=0.
      GO TO 28
   36 IF(X(K)-0.0001)37,28,28
   37 X(K)=0.01
   28 CONTINUE
      DUMMY=0.
      INDEX=0-1
      KDEX=0
      DO 33 K=13,15
      INDEX=INDEX+2
      KDEX=KDEX+2
      DUMMY=DUMMY+X(K)*X(K+6)*(SLOPE(INDEX)-SLOPE(KDEX))
     6/(SLOPE(INDEX)*SLOPE(KDEX))
   33 CONTINUE
      Y(300)=DUMMY
      ALFA=DUMMY/100.
  914 CONTINUE
      SUM=0.
      DO 1 J=1,19
      YC=0.
      XC=0.
      INDEX=13
      DO 2 K=13,15
      INDEX=INDEX-1
      KDEX=INDEX-1
      IF(J-10)3,3,4
    3 YC=YC+X(K)*       (EXP(SLOPE(K-INDEX)*TZ(J))-EXP(SLOPE(K-KDEX)*
     ATZ(J)))
      GO TO 5
    4 YC=YC+X(K)*X(K+6)*(EXP(SLOPE(K-INDEX)*TZ(J))-EXP(SLOPE(K-KDEX)*
     6TZ(J)))
      XC=XC+X(K+9)*(EXP(SLOPE(K-INDEX+6)*TZ(J))-EXP(SLOPE(K-KDEX+6)*TZ(J
     6)))
    5 CONTINUE
    2 CONTINUE
      YC=YC+XC
      IF(ITALL-2)918,919,919
  918 IF(J-10)919,919,1
  919 CONTINUE
      SUM=SUM+((Y(J)-YC)**2)/(Y(J)+0.0001)
    1 CONTINUE
      F = SUM
      RETURN



      END
```

REFERENCES

Barlow, T.E., Haigh, A.L. and Wolder, N.D.: Evidence for Two Vascular Pathways in Skeletal Muscle. Clin.Sci. 20:367 (1961).

Bassingthwaighte, J.B.: Plasma Indicator Dispersion in Arteries of the Human Leg. Circ.Res. 19:332 (1966).

Bassingthwaighte, J.B., Ackerman, F.H. and Wood, E.H.: Applications of the Lagged Normal Density Curve as a Model for Arterial Dilution Curves. Circ.Res. 18:398 (1966).

Beer, G.: Role of Tissue Fluid in Blood Flow Regulation. Circ.Res. 18,19-Suppl.I:154 (1971).

Berman, M.: The Formulation and Testing of Models. Ann.N.Y. Acad.Sci. 108:182 (1963).

Berne, R.M.: Cardiac Nucleotides in Hypoxia: Possible Role Irregulation of Coronary Blood Flow. Amer.J.Physiol. 204:317 (1963).

Berne, R.M., Rubio, R., Dobson, J.G.,Jr. and Curnish, R.R.: Adenosine and Adenine Nucleotides as Possible Mediators of Cardiac and Skeletal Muscle Blood Flow Regulation. Circ.Res. 28,29-Suppl.I:115 (1971).

Bing, R.J.: Determination of Coronary Flow Equivalent with Coincidence Counting Technique. Circulation 29:833 (1964).

Boestroem, B. and Schoedel, W.: Uber die Durchblutung der Arterovenosen Anastomosen in der Hintern Extremitat des Hundes. Pflugers Archiv. 256:371 (1953).

Bremermann, H.J. and Siu-Bik Lam, L.: Analysis of Spectra with Nonlinear Superposition. Mathematical Biosciences 8:449 (1970).

Byron, F.B.: The Pathogenesis of Hypertensive Encephatopathy and its Relation to the Malignant Phase of Hypertension; Experimental Evidence from the Hypertensive Rat. Lancet 267:201 (1954).

Callahan, A.B. and Pizer, S.M.: The Applicability of Fourrier Transform Analysis to Biological Compartmental Models. In Natural Automata and Useful Simulations, Ed. by Potter, H.H., Edelsack, E.A., Fein, L. and Callahan, A.B., Spartan, Washington, D.C. (1966).

Coleman, T.G. and Guyton, A.C.: Hypertension Caused by Salt Loading in the Dog. III. Onset Transients of Cardiac Output and Other Circulation Variables. Circ.Res. 25: 153 (1969).

Coulam, C.M., Warner, H.R., Wood, E.H. and Bassingthwaighte, J.B.: A Transfer Function Analysis of Coronary and Renal Circulation Calculated from Upstream and Downstream Indicator-Dilution Curves. Circ.Res. 19:879 (1966).

Daugherty, R.M., Scott, J.B., Dabney, J.M. and Haddy, F.J.: Local Effects of CO_2 and O_2 on Limb, Renal and Coronary Vascular Resistance. Amer.J.Physiol. 213:1102 (1967).

DeRoo, M.J.K., Goris, M.L., Cosemans, J., Gyselen, A., Billiet, L. and Van Der Schueren, G.: Computerized Dynamic Scintigraphy of the Lungs. J.Belge de Radiologie.

51 (1968).

DeRoo, M.J.K., Goris, M.L., Van Der Schueren, G., Cosemans, J., Billiet, L. and Gyselen, A.: Computerized Dynamic Scintigraphy of the Lungs. Respiration 26:408 (1969).

Dobson, E.L.: Multiple Tracer Counting with External "in vivo" counters. Federation Proceedings 14:121 (1955).

Dobson, E.L. and Warner, G.F.: Measurement of Regional Sodium Turnover Rates and Their Application to the Estimation of Regional Blood Flow. Amer.J.Physiol. 189:269 (1957).

Duhling, B.R. and Berne, R.M.: Longitudinal Gradients in periarteriolar Oxygen: A Possible Mechanism for the Participation of Oxygen in the Local Regulation of Blood Flow. Circ.Res. 27:669 (1970).

Duhling, R.R. and Berne, R.M.: Oxygen and the Local Regulation of Blood Flow: Possible Significance of Longitudinal Gradients in Arterial Oxygen Tension. Circ.Res. 28-Suppl.I:65 (1971).

Friedman, J.J.: Single Passage Extraction of ^{86}Rubidium from the Circulation of the Skeletal Muscle. Amer.J. Physiol. 216:460 (1969).

Friedman, J.J.: Muscle Blood Flow and 86-Rb Extraction: Rb as a Capillary Flow Indicator. Amer.J.Physiol. 214:488 (1968).

Friedman, J.J.: Rb Extraction as an Indicator of Capillary Flow. Circ.Res. 27-Suppl.I: (1971).

Friedman, J.J., et al: In: Physiology, Ed. by Selkurst, E.E.

Ch. 18, Little Brown and Co., Boston (1966).

Glass, H.I. and Garreta, A.C.: Quantitative Analysis of Exponential Curve Fitting for Biological Applications. Phys.Med.Biol. 12:379 (1967).

Goresky, C.A., Ziegler, H.Z. and Bach, G.G.: Capillary Exchange Modeling: Barrier Limited and Flow Limited Distribution. Circ.Res. 27:739 (1970).

Goris, M.L., DeRoo, M.J.K. and Van Der Schueren, G.: An Approach to a Storage and Data Handling Procedure in Static and Dynamic Scintigraphy. J.Belge de Radiologie 52:168 (1969).

Guyton, A.C.: Concept of Negative Interstitial Pressure Based on Pressure in Implanted Perforated Capsules. Circ.Res. 12:399 (1963).

Guyton, A.C., Prather, J., Scheel, K. and McGehee, J.: Interstitial Fluid Pressure: IV. Its Effect on Fluid Movement Through the Capillary Wall. Circ.Res. 19:1022 (1966).

Guyton, A.C., Granger, H.J. and Coleman, T.G.: Autoregulation of the Total Systemic Circulation and its Relation to Control of Cardiac Output and Arterial Pressure. Circ.Res. 28,29-Suppl.I:93 (1971).

Haddy, F.J. and Scott, J.B.: Effect of Flow Rate, Venous Pressure, Metabolites and Oxygen upon Resistance to Blood Flow Through Dog Forelimb. Circ.Res. 14,15-Suppl. I:49 (1964).

Haddy, F.J. and Scott, J.B.: Metabolically Linked Vasoactive

Chemicals in Local Regulation of Blood Flow. Phys.Rev. 48:688 (1968).

Haddy, F.J. and Scott, J.B.: Bioassay and Other Evidence for Participation of Chemical Factors in Local Regulation of Blood Flow. Circ.Res. 28-Suppl.I:86 (1971).

Hill, G.S.: Steroid Induced Hypertension in the Rat. A Microangiographic and Histologic Study of the Pathogenesis of the Hypertensive Vascular and Glomerular Lesions. Amer.J.Path. 52:1 (1968).

Hill, G.S.: Studies on the Pathogenesis of Hypertensive Vascular Diseases. Circ.Res. 26:657 (1970).

Hilton, S.M. and Chir, B.: A New Candidate for Mediator of Functional Vasodilation in Skeletal Muscle. Circ.Res. 28:70 (1971).

Hinshaw, L.B.: Autoregulation in Normal and Pathological States Including Schock and Ischemia. Circ.Res. 23,24-Suppl.I:46 (1971).

Ingvar, D.H. and Lassen, N.A.: Regional Blood Flow of the Cerebral Cortex Determined by Krypton. Acta Physiol. Scand. 54:325 (1962).

Jones, H.B.: Respiratory Systems: Nitrogen Elimination. Medical Physics Chicago: Yearbook, Ed. by Glasser, O. Vol. 2:855 (1950).

Julius, S., Pascual, A.V., Sannerstedt, R. and Mitchell, C.: Relationship Between Cardiac Output and Peripheral Resistance in Borderline Hypertension. Circulation 43: 382 (1971).

Kety, S.S.: Measurement of Regional Circulation by the Local Clearance of Radioactive Sodium. Amer. Heart J. 38:321 (1949).

Kilburn, K.H.: Muscular Origin of Elevated Plasma Potassium During Exercise. J.Appl.Physiol. 21:675 (1966).

Kontos, H.A. and Richardson, D.W.: Blood Flow and Metabolism of Forearm Muscle in Man at Rest and During Sustained Contraction. Amer.J.Physiol. 211:869 (1966).

Kontos, H.A.: Role of Hypercapnic Acidosis in the Local Regulation of Blood Flow in Skeletal Muscle. Circ.Res. 18,19-Suppl.I:98 (1971).

Lassen, N.A., Lindberg, J. and Munck, O.: Measurement of Blood Flow Through Skeletal Muscle by Intramuscular Injection of Xenon-133. Lancet 1:686 (1964).

Lassen, N.A.: Muscle Blood Flow in Normal Man and in Patients with Intermittent Claudication, Evaluated by Simultaneous ^{133}Xe and ^{24}Na Clearances. J.Clin.Invest. 43:180 (1964).

Lewis, B.M., Sokoloff, L., Wechsler, R.L., Wentz, W.B. and Kety S.S.: A Method for the Continuous Measurement of Cerebral Blood Flow in Man by Means of Radioactive Krypton (Kr^{79}). J.Clin.Invest. 39:707 (1960).

Lopez-Mojano, V., Rhodes, B.A. and Wagner, H.N.: Arteriovenous Shunting in Extremities. J.Appl.Physiol. 27:782 (1969).

Love, W.D.: Comparison of the Distribution of Potassium and Rubidium in the Organs of the Dog Using Rubidium-84.

Circ.Res. 2:112 (1954).

Martin, De Julian P. and Yudelevich, D.L.: Theory for the Quantitation of Transcapillary Exchange by Tracer Dilution Curves. Amer.J.Physiol. 207:162 (1964).

Maseri, A.: A Technique for Continuous Detection of Two Indicators in the Circulation. J.Appl.Physiol. 22:153 (1967).

Maseri, A., Caldini, P., Permutt, S. and Zierler, K.L.: Frequency Function of Transit Times Through Dog Pulmonary Circulation. Circ.Res. 26:527 (1970).

Meier, P. and Zierler, K.L.: On the Theory of the Indicator Dilution Method for Measurement of Blood Flow and Volume. J.Appl.Physiol. 6:731 (1954).

Mellander, S. and Lundvall, J.: Role of Tissue Hyperosmolality in Exercise Hyperaemia. Circ.Res. 28-Suppl.I:39 (1971).

Myhill, J., Wadsworth, G.P. and Brownell, G.L.: Investigation of an Operator Method in the Analysis of Biological Tracer Data. Biophys.J. 5:89 (1965).

Myhill, J.: Investigation of the Effect of Data Error in the Analysis of Biological Tracer Data. Biophys.J. 7:903 (1967).

Nicolls, P.A.: Vascular Patterns and Active Vasomotion as Determiners of Flow Through Minute Vessels. Angiology 6:291 (1955).

Olson, R.M.: Instantaneous Peripheral Vascular Resistance Changes Rendered by Critical Closing Phenomenon. J.

Appl.Physiol. 26:600 (1969).

Parker, H.G. and Hippensteele, J.R.: Mathematical Models for Exchange of Substances in Regional Vascular Beds - Measurements of the Rates with In Vivo Counters. Bull. of Math.Biophysics. (In print).

Parrish, D., Hayden, D.T., Garret, W. and Huff, R.L.: Analog Computer Analysis of Flow Characteristics and Volume of the Pulmonary Vascular Bed. Circ.Res. 7:746 (1959).

Pearce, M.L., McKeever, W.P., Dow, P. and Newman, E.V.: The Influence of Injection Site Upon the Form of Dye-Dilution Curves. Circ.Res. 1:112 (1953).

Perl, W. and Chinard, F.P.: Convection Diffusion Model of Indicator Transport Through an Organ. Circ.Res. 22:273 (1968).

Piiper, J. and Schoedel, W.: Untersuchungen uber die Durchblutung der Arteriovenosen Anastomosen in der Hintern Extremitat des Hundes mit Hilfe van Kugeln Verschiedener Grose. Flugers Archiv. 258:489 (1954).

Renkin, E.M.: Effects of Blood Flow on Diffusion Kinetics in Isolated Perfused Hindlegs of Cats: a Double Circulation Hypothesis. Amer.J.Physiol. 183:125 (1955).

Renkin, E.M.: The Nutritional-Shunt-Flow Hypothesis in Skeletal Muscle Circulation. Circ.Res. 28-Suppl.I:21 (1971)

Rodbar, S.: The Burden of Resistance Vessels. Circ.Res. 28-Suppl.I:2 (1971).

Rodbar, S.: Capillary Control of Blood Flow and Fluid Ex-

change. Circ.Res. 28-Suppl.I:51 (1971).

Sapirstein, L.A.: Fractionation of the Cardiac Output of Rats with Isotopic Potassium. Circ.Res. 4:689 (1956).

Scott, J.B. and Haddy, F.J.: Role in Chemical Factors in Regulation of Flow Through Kidney, Hindlimb, Heart. Amer.J.Physiol. 208:813 (1965).

Scott, J.B., Daugherty, R.M., Overbeck, H.W. and Haddy, F.J.: Vascular Effects of Ions. Federation Proc. 27:1403 (1968).

Scott, J.B., Rudko, M., Radawski, D. and Haddy, F.J.: Role of Osmolarity, K^+, H^+, Mg^{++}, and O_2 in Local Blood Flow Regulation. Amer.J.Physiol. 218:338 (1970).

Scott, J.B. and Radawski, D.: Role of Hyperosmolarity in the Genesis of Active and Reactive Hyperaemia. Circ.Res. 28,29-Suppl.I:26 (1971).

Schmidt, C.T.: Bypass in the Hind Leg of the Dog as Detected by Microspheres. (Personal Communication).

Sejrsen, P.: Blood Flow in Cutaneous Tissues in Man Studied by Washout of Radioactive Xenon. Circ.Res. 25:215 (1969).

Shinorama, Y., Meyer, J.S., Kitamura, A., Toyida, M. and Ryu, T.: Measurement of Cerebral Hemispheric Blood Flow by Intracarotic Injection of Hydrogen Gas. Circ.Res. 25: 735 (1969).

Skinner, N.S. and Powell, W.J.: Action of Oxygen and Potassium on Vascular Resistance of Dog Skeletal Muscle. Amer.J.Physiol. 212:533 (1967).

Skinner, N.S. and Powell, W.J.: Regulation of Skeletal Muscle Blood Flow during Exercise. Circ.Res. 21-Suppl.I: 59 (1967).

Skinner, N.S. and Costin, J.C.: Interaction between Oxygen, Potassium and Osmolality in Regulation of Skeletal Muscle Blood Flow. Circ.Res. 28:Suppl.I:73 (1971).

Stainsby, W.N. and Barclay, J.K.: Effect of Infusion of Osmotically Active Substances on Muscle Blood Flow and Systemic Blood Pressure. Circ.Res. 18:Suppl.I:33 (1971)

Strehlow, H. and Jen, J.: On the Accuracy of Chemical Relaxation Measurements. Chemical Instrumentation 3:47 (1971).

Thurau, K.: Micropuncture Evaluation of Local Control of Arteriolar Resistance of Kidney and Brain. Circ.Res. 28:Suppl.I:106 (1971).

Tillich, G., Mendoza, L. and Bing, R.J.: Total and Nutritional Coronary Flow. Circ.Res. 28,29-Suppl.I:148 (1971).

Warner, G.F., Dobson, E.L., Pace, N., Johnston, M.E. and Finney, C.R.: Studies of Human Peripheral Blood Flow: The Effect of Injection Volume on the Intramuscular Radiosodium Clearance Rate. Circulation 8:732 (1953).

Yano, Y., McRae, J. and Anger, H.O.: Lung Function Studies Using Short-Lived ^{81m}Kr and the Scintillation Camera. J.Nucl.Med. 11:674 (1970).

Yudilevich, D.L., Renkin, E.M., Alvares, I.A. and Bravo, I.: Fractional Extraction and Transcapillary Exchange During

Continuous and Instantaneous Tracer Administration. Circ.Res. 23:325 (1968).

Zierler, K.L.: Theory of the Use of Arteriovenous Concentration Differences for Measuring Metabolism in Steady and Non-Steady States. J.Clin.Invest. 40:2111 (1961).

Zierler, K.L.: Theory of the Use of Indicators to Measure Blood Flow and Extracellular Volume, and Calculation of the Transcapillary Movement of Tracers. Circ.Res. 12: 464 (1963).

Zierler, K.L.: Equations for Measuring Blood Flow by External Monitoring of Radioisotopes. Circ.Res. 16:309 (1965).

Zierler, K.L.: Basic Aspects of Kinetic Theory as Applied to Tracer-Distribution Studies. In Dynamic Clinical Studies with Radioisotopes. Ed. by Kniseley, R.M. and Towne, W.N.,U.S.A.E.C. 1964, p. 55.

Zweifach, B.W.: Direct Observations of the Mesenteric Circulation in Experimental Animals. Anat.Record 120:277 (1954).

TECHNICAL INFORMATION DIVISION
LAWRENCE BERKELEY LABORATORY
UNIVERSITY OF CALIFORNIA
BERKELEY, CALIFORNIA 94720